Technische Universität München

Institut für organische Chemie und Biochemie

Lehrstuhl für Biotechnologie

Functional and structural characterization of the redox regulated chaperone Hsp33

Claudia Cremers

Vollständiger Abdruck der von der Fakultät für Chemie der Technischen Universität München zur Erlangung des akademischen Grades eines

Doktors der Naturwissenschaften (Dr. rer. nat.)

genehmigten Dissertation.

Vorsitzender:		Univ.-Prof. Dr. Aymelt Itzen
Prüfer der Dissertation:	1)	Univ.-Prof. Dr. Johannes Buchner
	2)	Prof. Dr. Ursula Jakob University of Michigan, Michigan, USA

Die Dissertation wurde am 29.06.2012 bei der Technischen Universität München eingereicht und durch die Fakultät für Chemie am 01.08.2012 angenommen.

For my family

Table of Contents

Index of Figures

Index of Tables

Abbreviation

2D	two-dimensional
aa	amino acid
AAA+	ATPase associated with various cellular activities
ADP	adenosine diphosphate
AMS	4-acetamido-4"-maleimidylstilbene-2'-disulfonate
Asp	aspartate
ATP	adenosine triphosphate
bis-ANS	3,3'-Dianilino-1,1'-binaphthyl-5,5'-disulfonic
BSA	bovine serum albumin
°C	degree Celsius
CMC	critical micelle concentration
C-terminal	carboxyl-terminal
Cys	cysteine
DNA	deoxyribonucleic acid
DTT	dithiothreitol
E. coli	*Escherichia coli*
x g	gravity
g	gram
Gdn-HCl	guanidine hydrochloride
Glu	glutamate
Grx	glutaredoxin
GSH	reduced glutathione (L-γ-glutamyl-L-cysteineglycine)
GSSG	oxidized glutathione
h	hour
HAP	hydroxyapatite
HSA	human serum albumin
Hsp	heat shock protein
HOCl	hypochloride acid
H_2O_2	hydrogen peroxide
IAM	iodoacetamide
kDa	kilo Dalton
l	liter

Lys	lysine
m	milli
M	molar
min	minute
µ	micro
n	nano
NBD	nucleotide binding domain
NO_2-	nitric oxide
N-terminal	amino-terminal
NAD(P)H	nicotinamide adenine dinucleotide (phosphate)
Na-Cho	sodium-cholate
Na-DOC	sodium-deoxycholate
O_2^-	superoxide
O_2	oxygen
OD_{600}	optical density at 600 nm
ox	oxidized
PAR	4-(2-pyridylazo) resorcinol
PCMB	para-chloromercurybenzoic acid
red	reduced
RNA	ribonucleic acid
ROS	reactive oxygen species
RT	room temperature
SBD	substrate binding domain
SDS	sodium dodecyl sulfate
TCA	Trichloroacetic acid
Trp	tryptophan
Trx	thioredoxin
v/v	volume per volume
w/v	weight per volume

Declaration

I, Claudia Cremers, hereby declare that this thesis was prepared by me independently and using only the references and resources stated. His work has not been submitted to any other audit commission. Parts of this work have been published in scientific journals.

Erklärung

Hiermit erkläre ich, Claudia Cremers, dass ich die vorliegende Arbeit selbständig verfasst und keine anderen als die angegebenen Quellen und Hilfsmittel verwendet habe. Die Arbeit wurde bisher keiner Prüfungskommission vorgelegt. Teile dieser Arbeit wurde in wissenschaftlichen Journalen veröffentlicht.

_____

Claudia Cremers

Ann Arbor, 22. Juni 2012

1 Summary

Molecular chaperones are crucial for supporting the folding of nascent polypeptide chains into their three-dimensional structure under non-stress conditions, and for preventing the aggregation of unfolding protein intermediates under stress conditions, such as increased temperatures (heat-shock), low pH, or oxidative stress. Molecular chaperone foldases like DnaK/J/E and GroEL/ES require ATP for their function. However, neither foldase system appears to be functional during severe oxidative stress conditions as ATP is rapidly depleted. Our lab found that under these stress conditions (*e.g.*, oxidative heat stress or hypochlorous acid stress), cells post-translationally activate the heat shock protein 33 (Hsp33), which functions as an ATP-independent molecular chaperone holdase that protects proteins against stress-induced aggregation. Hsp33 belongs to a rapidly expanding group of redox-regulated proteins, which use reactive oxygen species for their posttranslational modification. Under non stress conditions, in the reducing environment of the cytosol, Hsp33 is inactive. Upon exposure to oxidative stress conditions that lead to protein unfolding, Hsp33 is rapidly activated. Stress sensing occurs via Hsp33's C-terminal redox-switch domain, which consists of a zinc binding domain and an adjacent metastable linker region. Under non-stress conditions, the four highly conserved cysteines, which are arranged in a $C_{232}XC_{234}$—X_n—$C_{265}XXC_{268}$ motif, bind one zinc-ion with very high affinity. This zinc binding confers stability to the zinc binding domain and the nearby linker region. Oxidative stress in combination with protein unfolding conditions leads to formation of two disulfide-bonds between the neighboring cysteines, the unfolding of the zinc binding domain and the destabilization of the nearby linker region. Once partially unfolded, Hsp33 is highly chaperone-active. This makes Hsp33 a member of a recently discovered class of chaperones that require partial unfolding to gain their full chaperone activity.

We now showed that single mutations in the N-terminal domain of Hsp33 are sufficient to either partially (Hsp33-M172S) or completely (Hsp33-Y12E) abolish the post-translational regulation of Hsp33 chaperone function. Both mutations appear to work predominantly via the destabilization of the Hsp33's

linker region without affecting zinc coordination, redox sensitivity, or substrate binding. We found that the M172S substitution causes moderate destabilization of the Hsp33 linker region, which seems sufficient to convert the redox-regulated Hsp33 into a temperature-controlled chaperone. The Y12E mutation leads to the constitutive unfolding of the Hsp33 linker region thereby turning Hsp33 into a constitutively active chaperone. These results demonstrate that the redox-controlled unfolding of the Hsp33 linker region plays the central role in the activation process of Hsp33. *In vivo* studies confirmed that even mild overexpression of the Hsp33-Y12E mutant protein inhibits bacterial growth, providing important evidence that the tight functional regulation of Hsp33 chaperone activity plays a vital role in bacterial survival.

Our work also addressed the long-standing question in the chaperone field of how chaperones recognize their client proteins. We demonstrated that activated Hsp33 uses its own intrinsically disordered regions (*i.e.*, its linker region) to discriminate between unfolded and partially structured folding intermediates. Binding to secondary structure elements in unfolding client proteins stabilizes Hsp33's intrinsically disordered linker region. This stabilization likely contributes to the high affinity that Hsp33 exerts for early unfolding intermediates. Return to non-stress conditions reduces Hsp33's disulfide bonds in the C-terminal zinc-binding domain and leads to further refolding of Hsp33. This appears to significantly destabilize the bound client proteins. In doing so, Hsp33 apparently converts its client proteins into less-structured, folding-competent client proteins of the ATP-dependent foldase DnaK/J/E.

Previous work revealed that Hsp33 is an essential protein that protects cells against the physiological antimicrobial bleach. Here we demonstrate that Hsp33 also protects bacteria against bile salts. Bacteria encounter bile salts in the gastrointestinal tract. They are known for their ability to emulsify fatty acids and for their antimicrobial activity, which is assumed to be due to bile salt-mediated disturbance of cell membrane integrity and induction of macromolecule damage. Here we present evidence that the antimicrobial action of bile salts is caused by oxidative protein unfolding and aggregation.

We demonstrate that bile salts induce the unfolding and irreversible aggregation of a distinct, partially overlapping set of proteins both *in vitro* and *in vivo.* Presence of Hsp33 prevents the bile salt-induced protein aggregation, thus substantially increasing bacterial survival. Based on the activation mechanism of Hsp33, which is known to require oxidative stress under protein unfolding conditions, we conclude that bile salts cause substantial oxidative stress conditions and unfolding *in vivo*. These results suggest that the underlying molecular mechanism for the antimicrobial action of bile salts involves oxidative protein aggregation, a process that is effectively mitigated by the highly conserved chaperone Hsp33.

2 Introduction and Outline

2.1 Protein folding in the cell

The polypeptide sequence of proteins is encoded in base triplets in the genome of each organism. Necessary for the synthesis of proteins is the transcription of this information into messenger RNA. Ribosomal complexes within the cytosol then translate this information into linear polypeptide sequences, thus defining the protein. Large fractions of newly synthesized proteins require the assistance of molecular chaperones to adapt their folded state (Hartl, 1996). The folding of larger proteins (> 100 amino acids) occurs often via folding intermediates, which can be either on-pathway to the native state or are kinetically stable, misfolded conformations, which require substantial reorganization for effective folding (Onuchic and Wolynes, 2004). Partially folded/misfolded proteins often tend to aggregate due to the exposure of hydrophobic amino acid residues. The process of aggregation is greatly enhanced within the highly crowded environment of the cell, explaining the requirement of chaperones to assist in protein folding (Ellis and Minton, 2006).

Protein folding of newly synthesized polypeptides follows a folding landscape from the unfolded state to the thermodynamically most stable native conformation (Brockwell and Radford, 2007; Dinner et al., 2000). The first 30-60 translated amino acids are shielded by the ribosome exit tunnel before they dive into the cytosol. At this point, the polypeptide chain is either unstructured or has α-helical conformation (Malkin and Rich, 1967; Seidelt et al., 2009; Tsalkova et al., 1998). Proteins then begin to gain their tertiary structures while still connected to the ribosome (Evans et al., 2008; Frydman et al., 1999; Kosolapov and Deutsch, 2009).

Numerous molecular chaperones assist the folding of nascent polypeptides chains *in vivo* (Vabulas and Hartl, 2005). Assisted folding occurs co-translationally via the ribosome-associated chaperone trigger factor, or post-translationally via the DnaK/J/E system or GroEL/ES system. The binding of folding intermediates to chaperones reduces their concentration

and prevents aggregation. In the case of DnaK/J/E, the transient release of the client from the chaperone facilitates its folding. In contrast, GroEL/ES facilitates the folding of the client proteins in the Anfinsen cage of its protein structure (Hartl and Hayer-Hartl, 2009).

2.2 Molecular Chaperones

In 1978 the term “chaperone” was coined by Laskey et al. to describe an activity associated with nucleoplasmin in *Xenopus oocytes* (Laskey et al., 1978). But it was not until 1987 that the term molecular chaperone acquired its current meaning: that is, a class of cellular proteins that assist the folding and assembly of other polypeptide chains to oligomeric structures (Ellis, 1987). Recently, the term has begun to be used more broadly to describe the additional roles of chaperones in the regulation of conformational changes and protein trafficking through membranes and into organelles (Bukau et al., 2006; Young et al., 2004).

	Prokaryotes	**Eukaryotes**	**ATP-dependency**
Foldases	DnaK/J/E	Hsp70/Hsp40/NEF	+
	GroEL/ES	Hsp60/ Hsp10	+
	HtpG	Hsp90	+
	Trigger-Factor	RAC*/NAC*	-
	Spy		-
	HdeA/B		-
Holdases	Hsp33		-
	IbpA/IbpB	Small Hsp’s	-
Disaggregases	ClpB	Hsp104	+
	ClpA/C		+
	HslU		+

Table 1: Molecular chaperones in pro-and eukaryotes
*NAC = nascent polypeptide-associated complex, RAC = ribosome-associated complex

Foldases and disaggregases typically require cycles of ATP-binding, hydrolysis, and release to regulate client protein-binding and to facilitate their refolding (Hartl and Hayer-Hartl, 2009). The most famous members of this

group are the DnaK/J/E and the GroEL/ES system. More recently, however, two periplasmic proteins (*i.e.*, HdeA and Spy) have been found to facilitate folding of client proteins without the hydrolysis of ATP (Quan et al., 2011; Tapley et al., 2009a). These proteins appear to support folding by the controlled and slow release of folding competent client proteins, which subsequently refold. Trigger factor, another ATP-independent foldase, binds to nascent polypeptide chains on the ribosome exit tunnel, shielding the emerging protein from the crowded cytosol (Merz et al., 2008). DnaK/J/E or GroEL/ES interact with trigger factor and the nascent chain, further supporting the folding of the newly synthesized protein. Chaperone holdase systems, which function typically ATP-independent, form stable complexes with client proteins under stress conditions. Upon return to non-stress conditions, they typically interact with ATP-dependent chaperones (DnaK/J/E or GroEL/ES) to facilitate the refolding of the client proteins.

Disaggregases facilitate the removal of protein aggregates in the cytosol. One of these proteins is ClpB, which, in concert with the DnaK/J/E system, disaggregates and refolds proteins *in vivo* and *in vitro.* ClpA/C and HslU unfold aggregated client proteins for peptidase (*e.g.,* ClpP and HslV) so that the polypeptide can be transferred into the proteolytic chamber for digestion (Maurizi and Xia, 2004; Sauer et al., 2004).

The purpose of all three chaperone systems is to keep the amount of insoluble proteins inside the cell to a minimum since the accumulation of protein aggregates is cytotoxic (Campioni et al., 2010).

2.3 Regulation of *E. coli* chaperone systems - The Heat shock response

The heat shock response in *E. coli* is regulated by σ^{32} (gene: *rpoH*), and it comprises more than 80 heat shock genes encoding foldases, holdases, disaggregases and proteases (Bukau, 1993; Georgopoulos and Welch, 1993; Nonaka et al., 2006). The heat shock response is triggered by stress conditions that lead to protein unfolding (Bukau, 1993; Yura et al., 1993; Yura and Nakahigashi, 1999). The expression of σ^{32} is repressed under normal growth conditions but induced upon shifts to higher temperatures. This

temperature-mediated gene expression is facilitated by the mRNA of σ^{32}, which is very sensitive to temperature changes. Raising the temperature to 42°C leads to loss of mRNA structure around the ribosome binding site, which induces the translation of the σ^{32} mRNA (Morita et al., 1999a; Morita et al., 1999b). Furthermore, regulon members of σ^{32} control both the activity and stability of σ^{32}. A negative feedback loop constituted by DnaK/J/E and GroEL/ES regulates the stability of σ^{32}: over-expression of either chaperone leads to σ^{32} degradation, whereas depletion of the chaperones, *e.g.* during protein unfolding stress, stabilizes σ^{32} (Kanemori et al., 1994; Straus et al., 1990; Tomoyasu et al., 1998). The membrane-bound ATP-dependent protease FtsH plays a major role in the chaperone-facilitated degradation of σ^{32} (Herman et al., 1995; Tomoyasu et al., 1995). Thus, expression of chaperones is very tightly regulated: under protein unfolding stress conditions, chaperone synthesis is up-regulated. This keeps the amount of toxic protein aggregates to a minimum (Campioni et al., 2010; Stefani and Dobson, 2003).

2.4 ATP-dependent chaperones

2.4.1 The GroEL - GroES system

The GroEL/ES - system from *E. coli* belongs to the Hsp60-family of chaperonins. These are large double-ring structures, which bind non-native proteins in their central folding chamber and assist their folding to the native state (Horwich 2007). About 10 % of all newly synthesized bacterial proteins, with a pre-dominant size range between 20 and 60 kDa, transit through the GroEL/ES system (Ewalt et al., 1997; Houry et al., 1999; Kerner et al., 2005). The 14 subunits of GroEL (a' 57 kDa) are arranged in two heptameric ring structures, called the cis- (Fig. 2.1, yellow) and trans-ring (Fig. 2.1, green), which are open at both sides (Braig et al., 1994; Xu et al., 1997). GroEL's co-chaperone GroES, which is an 11 kDa protein, forms a heptameric cap-like structure (Fig. 2.1, red) (Hunt et al., 1996), which interacts with the cis-ring when a polypeptide is inside GroEL's folding cage (Horovitz and Willison, 2005; Horwich et al., 2007).

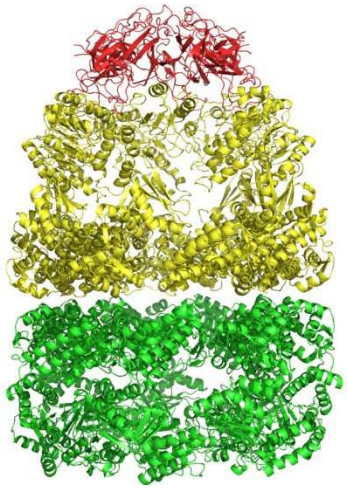

Fig. 2.1: Crystal structure of GroEL/ES
Crystal structure of the asymmetric GroEL/ES complex (PDB: 1AON) from *E. coli*. The heptameric cis-ring of GroEL is displayed in yellow, the trans-ring in green. The heptameric GroES ring is bound to GroEL's cis-ring (Xu et al., 1997).

GroEL/ES undergoes large ATP-dependent conformational changes, which are crucial for its function (Fig. 2.2) (Horovitz and Willison, 2005). Two rounds of ATP binding, hydrolysis, and release are required for the binding, folding and release of a polypeptide. The first step in the chaperone cycle involves the binding of unfolded polypeptides to the edges of the central cavity of GroEL's cis-ring. Binding of ATP to the cis-ring then induces structural changes that allow binding of GroES to the GroEL-substrate complex. This displaces the client to the interior of the cage-like structure and hence closes the GroEL-folding compartment (Sharma et al., 2008). ATP hydrolysis occurs, setting the timer for the folding of the polypeptide inside the chamber (Fenton and Horwich, 1997). ATP binding to the opposing trans-ring induces a second set of structural rearrangements leading to the release of the folded polypeptide and the dissociation of GroES from GroEL (Tang et al., 2006). If folding is not completed, the polypeptide will rebind to GroEL and another cycle occurs (reviewed in (Fenton and Horwich, 2003)).

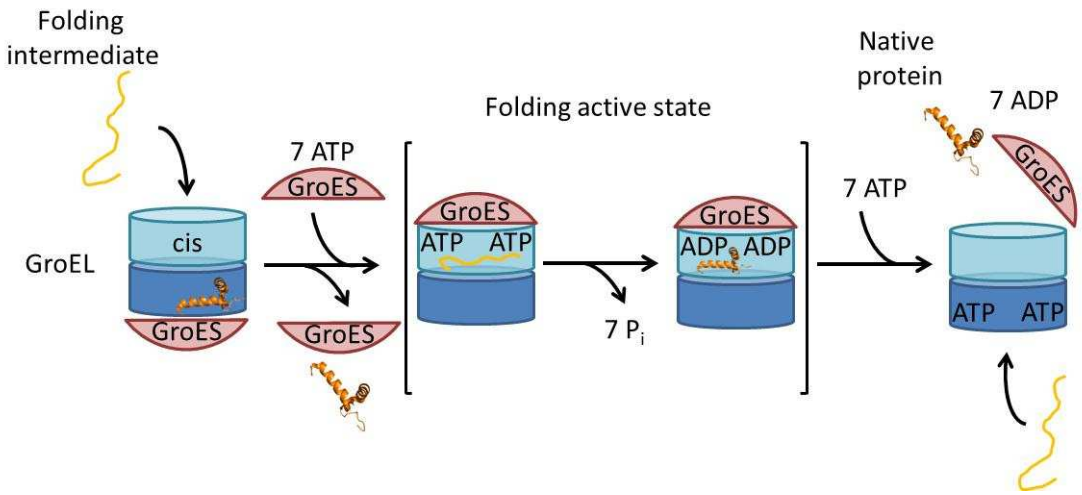

Fig. 2.2: GroEL/ES chaperone folding cycle
A client protein of GroEL/ES is captured on the cis-ring of GroEL. Binding of 7 ATP molecules to the cis-ring of GroEL induces conformational changes, which allow binding of GroES to the complex. ATP hydrolysis initiates further structural changes which facilitate the folding of the client protein. Binding of 7 ATP to GroEL's trans-ring trigger the release of the client protein. This triggers the loss of interaction between GroEL and GroES and removal of the hydrolyzed ADP. The process of binding, folding and release described here for the cis-ring proceeds staged at the trans-ring-encapsulation and consequent ATP/GroES binding on the cis-ring leads to ADP and GroES release from the trans-ring, accompanying the release of a folded substrate. (Figure modified form (Horwich et al., 2009))

2.4.2 The DnaK, DnaJ, and GrpE chaperone system

E. coli DnaK is a 70 kDa protein, which belongs to the Hsp70-class of chaperones. It has one co-chaperone, termed DnaJ (Hsp40), which is important for client binding as well as one nucleotide exchange factor, called GrpE; together, they form the DnaK/J/E system. Early studies on the induction of the heat-shock response in *Drosophila* (Ritossa, 1962, 1996) revealed that the induction of these genes is necessary to overcome heat stress, yet the studies themselves did not describe the proteins. The discovery of the respective homologous genes in bacteria goes back to the mid-1970s when genetic selections were applied to search for host genes that when mutated, block bacteriophage propagation (Georgopoulos, 1977; Saito et al., 1978; Saito and Uchida, 1977; Sunshine et al., 1977). These proteins turned out to be DnaK, DnaJ, and GrpE. In 1984, Bardwell and Craig made the breakthrough finding that *Drosophila* Hsp70 and *E. coli* DnaK are homologous proteins and execute very similar functions (Bardwell and Craig, 1984).

Hsp70 proteins have never been found to function on their own. In *E. coli*, there are three Hsp70 homologues (DnaK, HcsA and HscC), which interact with their corresponding J-domain proteins (DnaJ, CdpA, DJiA, HscB, DjiB and DjiC) and the nucleotide exchange factor GrpE. These cofactors are key for DnaK's function, as they serve to regulate the interaction with unfolded polypeptides and nucleotides. The general functions of the DnaK/J/E system include the folding of newly synthesized polypeptides at the ribosome exit (Deuerling et al., 1999; Frydman et al., 1994), interaction with mature proteins, which undergo unfolding during stress conditions (Hartl and Hayer-Hartl, 2002; Mayer and Bukau, 2005; Young et al., 2004), and the disassembly of macromolecular complexes or aggregates in cooperation with ClpB (Bukau et al., 2006).

2.4.2.1 DnaK - The main polypeptide 'folder'

Members of the Hsp70 family are characterized by a very defined domain structure. They consist of a 40 kDa N-terminal nucleotide binding domain (NBD) (Fig. 2.3, red), which is connected via a flexible hydrophobic linker to a 25 kDa substrate binding domain (SBD) (Fig. 2.3, green), followed by a short C-terminal extension (Bertelsen et al., 2009; Harrison et al., 1997; Stevens et al., 2003). In its foldases-active conformation, DnaK is monomeric. Higher oligomeric structures of DnaK have been observed recently. These structures appear to be foldase inactive but maintain DnaK's ability to bind to client proteins and hence seem to confer holdase activity to DnaK (Thompson et al., 2012). DnaK preferentially binds to short hydrophobic unstructured regions, which are presented by newly emerging polypeptides exiting the ribosome or by unfolded client proteins, which accumulate during stress conditions (Bukau and Horwich, 1998; Deuerling et al., 1999; Mayer et al., 2000; Reichmann et al., 2012; Rüdiger et al., 1997a). The SBD of DnaK can be further divided into a β-sandwich domain, which is responsible for client binding and an α-helical lid that closes over the bound client protein to trap it in the bound form (Bertelsen et al., 2009; Popp et al., 2005). The bound peptide is located in a hydrophobic cleft consisting of 4-5 residues within the β-sheets of DnaK's SBD (Rüdiger et al., 1997a; Zhu et al., 1996).

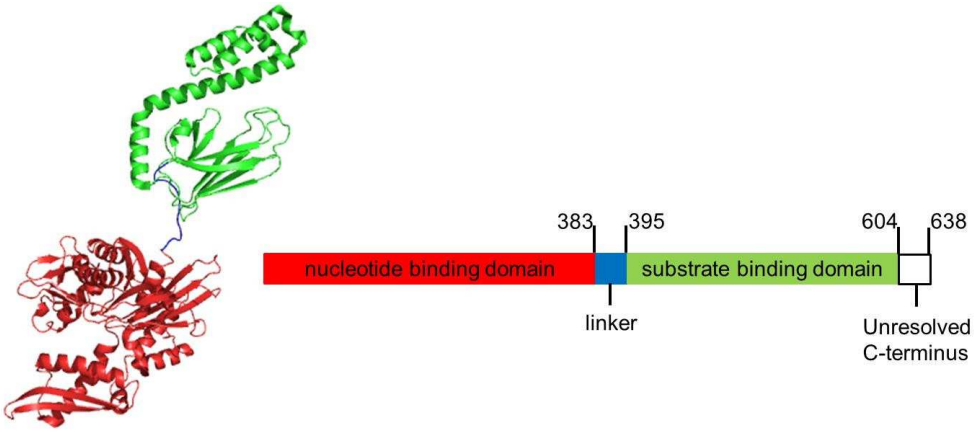

Fig. 2.3: Crystal structure and domain structure of *E. coli* DnaK
The crystal structure of *E. coli* DnaK (PDB: 2KHO) in the ADP-bound form reveals a two-domain structure. The 40 kDa N-terminal nucleotide binding domain is depicted in red. It is linked to the 25 kDa-substrate binding domain (green) via a flexible linker (blue), which is important for the allosteric regulation of the two domains. The C-terminal extension of DnaK is disordered and therefore not visible in the crystal structure (PDB: 2KHO) (Bertelsen et al., 2009).

NBD and SBD communicate allosterically via the flexible linker region (Fig. 2.3, blue), which appears to link nucleotide turnover to client protein-binding (Slepenkov and Witt, 1998). In the ATP-bound “open conformation”, DnaK exhibits very low affinity for client proteins. Upon hydrolysis of ATP, conformational changes (closed conformation) occur that convert DnaK into its high-affinity state (Fig. 2.4). This is achieved by DnaK’s interaction with DnaJ, which increases substrate affinity and reduces the substrate exchange rate (Fig. 2.4) (Palleros et al., 1995; Palleros et al., 1994). Exchange of the hydrolyzed ADP for new ATP induces the release of the client protein, and initiates a new cycle of client binding. This step is stimulated by the nucleotide exchange factor GrpE (Fig. 2.4).

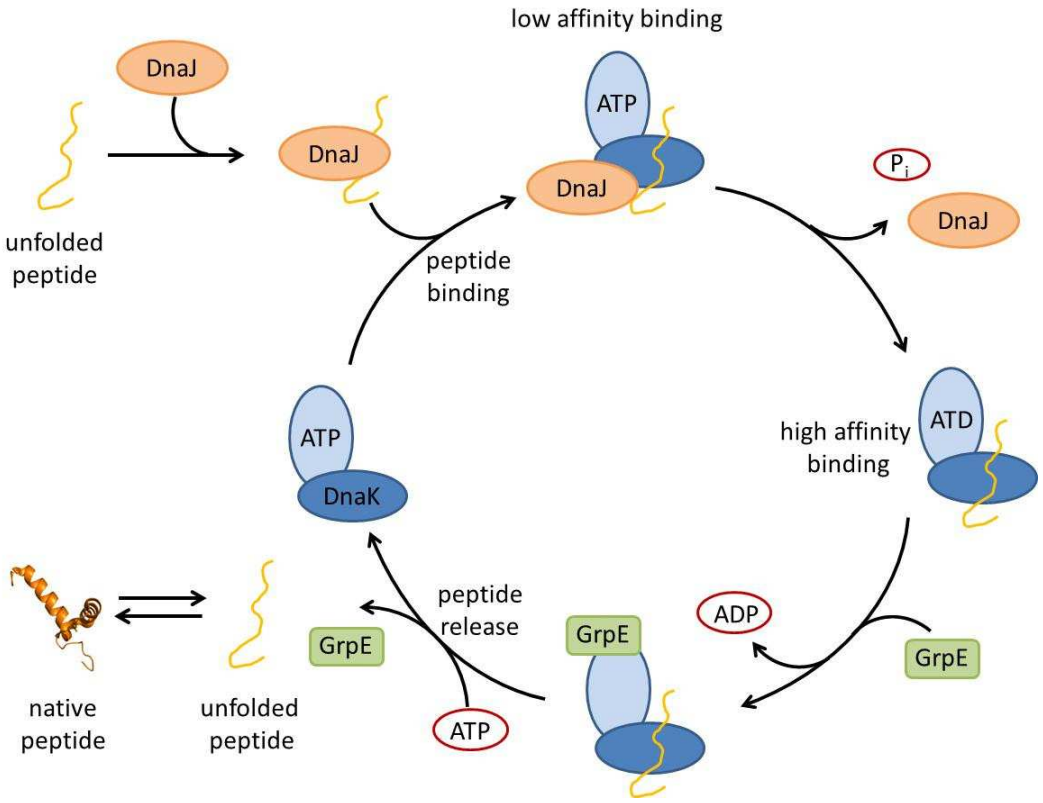

Fig. 2.4: DnaK/J/E working cycle
DnaJ, a co-chaperone of DnaK, binds initially to the unfolded client proteins and brings the client into the vicinity of DnaK. Interaction of DnaK-ATP with DnaJ-client complexes stimulates ATP-hydrolysis and converts DnaK from its low affinity binding state to its high affinity state. This, in turn, abolishes the interaction between DnaK and DnaJ. Binding of GrpE, the nucleotide exchange factor triggers the release of ADP and initiates rebinding of ATP. This returns DnaK into its low affinity state and causes release of the client. Client folding is thought to happen through several successive cycles of DnaK-binding and release.

In eukaryotes, the C-terminal domain of Hsp70 can interact with various partner proteins, like Hop and Sti1, which further affect the function of Hsp70 (Mayer and Bukau, 2005; Young et al., 2004). In prokaryotes, however, the unstructured C-terminal domain of DnaK does not appear to interact with co-chaperones but might be involved in enhancing the chaperone function of DnaK by transiently interacting with unfolded client proteins (Smock et al., 2011). This makes DnaK's C-terminal region functionally similar to the intrinsically disordered regions of small heat-shock proteins (Jaya et al., 2009) and the molecular chaperone Hsp33 (Reichmann et al., 2012), which both bind their client proteins with intrinsically disordered regions of the protein.

2.4.2.2 DnaJ transfers client proteins to DnaK

DnaJ, which belongs to the group of Hsp40 chaperones (~ 40 kDa), is a homodimer and characterized by a ~70 amino acid long J-domain, which mediates the interaction between DnaK and DnaJ (Schroder et al., 1993; Wu et al., 2005). DnaJ binds unfolded client proteins, prevents their aggregation and delivers them to DnaK for refolding (Schroder et al., 1993). Besides the conserved J-domain, Hsp40 proteins share little homology. It is thought that the C-terminal domain, which differs greatly among members of the Hsp40 family, confers client specificity (Goffin and Georgopoulos, 1998; Li et al., 2003; Lu and Cyr, 1998). The J-domain has a crucial role in stimulating DnaK's ATPase activity by binding to DnaK's N-terminal ATPase domain and threading its bound substrate into DnaK's SBD (Greene et al., 1998). This apparently converts DnaK to its high affinity binding state, and locks the peptide in DnaK's binding domain (Liberek et al., 1991). Some Hsp40 homologues, such as *E. coli* DnaJ, contain two zinc-binding domains in their C-terminal domain (Li et al., 2003; Lu and Cyr, 1998; Martinez-Yamout et al., 2000). The first zinc-binding domain of DnaJ seems to be involved in client protein recognition and binding whereas the second zinc center affects DnaJ's ability to transform DnaK into its high-affinity binding state (Linke, 2003). It is of note that the zinc binding domain of DnaJ confers some redox sensitivity to the protein. This has been shown for Hdj2, a human homologue of DnaJ, which, upon peroxide-mediated oxidation, is no longer able to transfer bound client proteins to its DnaK homologue Hsc70 for refolding *in vivo* or *in vitro* (Choi et al., 2006).

2.4.2.3 GrpE - The nucleotide exchange factor

The second co-chaperone of DnaK is GrpE, which accelerates the nucleotide exchange of DnaK (Harrison et al., 1997; Liberek et al., 1991). GrpE is a 21 kDa asymmetric homodimer, which is bent in a way that allows extensive contacts with only one DnaK monomer. Binding of GrpE to DnaK lowers DnaK's affinity to ADP by about 200-fold. This allows rebinding of ATP and transfers DnaK into its low-affinity binding state, which leads to client protein release and initiates a new chaperone cycle (Fig. 2.4) (Packschies et

al., 1997). Rebinding of ATP leads to dissociation of GrpE from DnaK (Brehmer et al., 2004; Packschies et al., 1997). At high temperatures, GrpE undergoes conformational changes that lead to changes in the interaction with DnaK. This maintains DnaK in its ADP-bound stage and hence prevents the release of client proteins under stress conditions that would otherwise lead to the aggregation of the proteins (Grimshaw et al., 2005; Siegenthaler and Christen, 2005, 2006).

2.5 ATP-independent chaperones

E. coli contains numerous ATP-independent chaperones. This class of chaperones includes the periplasmic acid-activated chaperone HdeA, the newly identified chaperone Spy, the cytosolic small heat-shock proteins (sHsp, such as *E. coli*'s IbpA and IbpB), the redox regulated chaperone Hsp33, and trigger factor. Most of these chaperones bind their client proteins under distinct stress conditions and keep them in a folding-competent state until non-stress conditions are restored (Ehrnsperger et al., 1997; Lee et al., 1997).

Under non-stress conditions, HdeA, Hsp33, and the sHsps IbpA and IbpB are chaperone-inactive. Their mode of activation involves stress-induced changes in their oligomeric structure (*i.e.* HdeA, Hsp33, IbpA and IbpB) and folding status (*i.e.* HdeA and Hsp33). The common feature for the activation of these chaperone holdases seems to be an increase in surface hydrophobicity, which accompanies their unfolding (Giese and Vierling, 2002; Graf, 2004; Raman et al., 2001; Tapley et al., 2009b; Wu et al., 2008; Yang et al., 1999). Since client binding sites on chaperones are thought to be hydrophobic in nature, these findings led to the hypothesis that local unfolding and rearrangements of the chaperones during stress conditions exposes previously buried client binding sites (Haslbeck et al., 2005; Winter and Jakob, 2004; Wu et al., 2008).

Trigger factor and Spy also function in an ATP-independent manner, yet they do not seem to use posttranslational changes in their conformation in order to become chaperone active. Trigger factor needs the association to the ribosome and interacts with the nascent polypeptide chains as they exit the

ribosome (Ferbitz et al., 2004; Rutkowska et al., 2008). Spy gets dramatically up-regulated, which appears to facilitate in its role as chaperone (Quan et al., 2011).

2.5.2 IbpA and IbpB – *E. coli*'s small heat shock proteins (sHsp)

The group of sHsp's is widely distributed in eukaryotes and prokaryotes. These proteins range in mass from 15 to 43 kDa (Narberhaus, 2002). They are classified by a conserved stretch of about 100 amino acid residues, which is arranged in a so-called α-crystallin fold. Neither the N-terminal nor the C-terminal regions of these proteins are highly conserved (Caspers et al., 1995). The chaperone-active form of sHsps varies but consists in general of large oligomeric structures, which are formed specifically under stress conditions (Buchner et al., 1998; Ehrnsperger et al., 1999; Haley et al., 2000; Haley et al., 1998; Shearstone and Baneyx, 1999).

E. coli encodes two sHsp, IbpA and IbpB (inclusion body associated protein). They were first identified as proteins associated with inclusion bodies (Allen et al., 1992) and were later shown to be present in protein aggregates formed during heat shock (Laskowska et al., 1996). High temperature induces structural rearrangements and reorganization, leading to the oligomerization of these proteins and the exposure of hydrophobic domains, which are thought to be important for client binding (Matuszewska et al., 2009; Shearstone and Baneyx, 1999). During heat stress, sHsps bind tightly to early protein-unfolding intermediates, thereby keeping their client proteins in a folding competent state (Baneyx and Mujacic, 2004). Healy recently proposed a model, where chaperone-active hetero-oligomers of IbpA and IbpB form upon heat shock treatment (Healy, 2012). Even though IbpA and IbpB are 48 % identical, their physiological role differs. IbpA alone can change the properties of aggregates formed during heat stress, while IbpB increases the efficiency of ClpB-DnaK/J/E mediated disaggregation and refolding (Ratajczak et al., 2010). Once the stress situation passes, client proteins are disaggregated and refolded by ClpB and the DnaK/J/E system (Mogk et al., 2003a; Mogk et al., 2003b).

2.5.3 The periplasmic chaperones HdeA and Spy

Periplasmic chaperones have to deal with a harsh environment. The outer membrane of *E. coli* is porous and allows the free transfer of small molecules up to a size of about 600 Da, subjecting the contents of the periplasm to an environment of low pH or small molecules like alcohols and indoles, which lead to protein unfolding and aggregation (Koebnik et al., 2000). The periplasm is free of ATP implying that the refolding of chaperone-bound, unfolded client proteins needs to be achieved without the energy source of ATP hydrolysis.

2.5.3.1 Spy (Spheroblast protein y) - A newly identified chaperone

Spy is under the control of the Bae and Cpx periplasmic stress-response systems, and is massively induced during protein unfolding stress in the periplasm (Bury-Mone et al., 2009; MacRitchie et al., 2008; Raffa and Raivio, 2002). Spy expression is induced by copper (Yamamoto and Ishihama, 2005), zinc, tannic acid and indole (Garbe et al., 2000; Yamamoto et al., 2008; Zoetendal et al., 2008) as well as butanol, which is known to have unfolding capacity (Brynildsen and Liao, 2009; Rutherford et al., 2010).

The 18 kDa Spy protein is active as a dimer and forms a cradle-like shape. Four α-helices form an antiparallel coiled-coil in the center of Spy's structure while both C- and N-termini are disordered (Fig. 2.5) (Kwon et al., 2010; Quan et al., 2011). Quan et al. were able to demonstrate that Spy has ATP-independent chaperone function *in vitro*. Spy appears to transiently bind to both thermally unfolded and chemically denatured client proteins. Slow release of the client proteins in a folding-competent conformation seems to allow Spy to support client refolding without the need of ATP or other cofactors. *In vivo*, the chaperone function seems to be facilitated by the major up-regulation of the Spy protein (Quan et al., 2011).

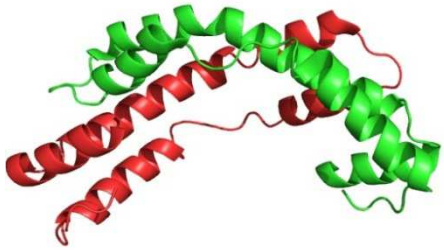

Fig. 2.5: Crystal structure of the Spy-dimer
Spy, is a chaperone, which exists as a dimeric protein in the periplasm (PDB:3OEO) (Kwon et al., 2010).

2.5.3.2 HdeA - An acid-activated chaperone

In the acidic environment of the stomach, *E. coli* is exposed to very low pH conditions. *E. coli* keeps its cytoplasmic pH neutral by using glutamate- and arginine-dependent decarboxylases (De Biase et al., 1999; Richard and Foster, 2003). By contrast, however, the periplasm rapidly gets acidified, which leads to the unfolding of proteins. Once the pH shifts back to neutral conditions, these proteins tend to aggregate (Fink et al., 1994; Tapley et al., 2009b).

HdeA is a periplasmic chaperone of 9.7 kDa, which is rapidly activated when the pH in the periplasm drops below pH <3 (Gajiwala and Burley, 2000; Hong et al., 2005). Under non-stress conditions, HdeA is a homodimer (Fig. 2.6) (Yang et al., 1998). Decrease to pH <3 causes HdeA to monomerize and to lose some of its structure. This unfolding appears to expose a hydrophobic dimer interface, which has been proposed to serve as the client protein binding interface of HdeA (Tapley et al., 2009b). The partial disorder in HdeA is thought to be crucial to HdeA's chaperone holdase function, as it allows HdeA to bind to a wide variety of different acid-unfolded periplasmic client proteins (Tapley et al., 2009b). Return to neutral pH conditions leads to the slow release of the client proteins in a folding-competent state. This slow release keeps the concentration of the client protein below the aggregation threshold and fosters their refolding as well as the refolding and dimerization of HdeA (Tapley et al., 2009a). In 2004, Tompa et al. introduced an "entropy transfer model", which states that refolding of disordered regions might provide the energy necessary to change the fold of the bound clients (Tompa and Csermely, 2004). This could be the case for HdeA, as return to neutral pH

alters the structure of the disordered regions of HdeA and therefore might be used to modulate the structure of the client proteins.

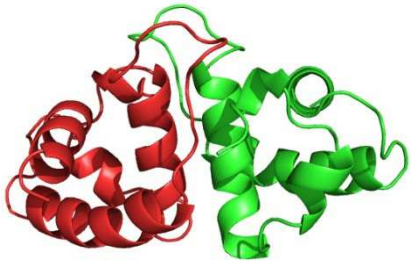

Fig. 2.6: Crystal structure of the folded HdeA dimer

HdeA crystal structure is solved at pH 7. HdeA forms a folded, inactive dimer under this condition. pH changes < 3 induce monomerization and the unfolding of the chaperone, leading to its active conformation (PDB: 1BG8) (Yang et al., 1998).

2.5.4 Hsp33 - A redox-regulated chaperone holdase

The heat shock protein Hsp33 is a highly conserved molecular chaperone in bacteria, and is also found in some eukaryotes like members of the *Trypanosomatidae* family. Hsp33 appears to act by specifically protecting bacteria against oxidative stress conditions that cause protein unfolding (Ilbert et al., 2007; Jakob, 2000; Winter et al., 2005). It has long been known that Hsp33 requires protein unfolding and oxidation conditions for its activation. Slow acting, non-denaturing oxidants such as H_2O_2 require unfolding conditions (*e.g.,* heat or detergents) to activate the chaperone (Ilbert et al., 2007; Winter et al., 2005). Recent work from our lab showed that HOCl, as a fast-acting oxidant, simultaneously induces both stress conditions in bacteria (Winter et al., 2008). Bacteria encounter these stress conditions when they are engulfed by cells of the innate immune response as they produce high levels of oxidants like hypochlorous acid (HOCl), H_2O_2 and NO to kill the invading organisms (Miller and Britigan, 1997). Furthermore HOCl is an oxidant used as general disinfectant in the household (*i.e.*, bleach).

Under oxidative stress conditions, ATP-dependent chaperone foldases, such as the DnaK/J/E system, seem to be unable to efficiently prevent protein aggregation. This is presumably due to the oxidative stress-mediated drop in cellular ATP-levels (Barrette et al., 1989; Winter et al., 2008). Moreover, Hdj2,

an eukaryotic homologue of DnaJ, is inactivated upon exposure to H_2O_2 due to the oxidation of its zinc-binding domain (Choi et al., 2006) while GrpE has been shown to lose its structure when incubated with the oxidant HOCl *in vitro* (Winter et al., 2008). These findings suggest that the activation of the ATP-independent chaperone holdase Hsp33 may serve as a compensatory mechanism to minimize protein aggregation under conditions where ATP-dependent chaperone systems are inactive.

2.5.4.1 Hsp33's domain characterization

Hsp33 (gene: *hslO*) is a 33 kDa redox-regulated chaperone (Jakob, 2000; Jakob et al., 1999). It can be structurally divided into two domains, a N-terminal domain, which stays folded under physiological conditions (Fig. 2.7, blue), and a C-terminal redox switch domain of Hsp33, which is important for sensing of oxidants and unfolding conditions (Fig. 2.8, yellow and green respectively). The mechanistic features that allow Hsp33 to sense oxidative stress conditions center around a C-terminal cysteine-rich domain (Fig. 2.7, yellow), which harbors four absolutely conserved cysteines arranged in a $C_{232}XC_{234}—X_n—C_{265}XXC_{268}$ motif. Under reducing, non-stress conditions, as found in the bacterial cytosol, all four cysteines are engaged in the tetrahedral coordination of one Zn^{2+} ion (Fig. 2.8, red sphere), whose high-affinity binding provides significant stability to Hsp33's C-terminus (Graf, 2004). This zinc-binding domain connects to Hsp33's N-terminal domain via a highly flexible ~52 amino acid linker region (Fig. 2.7, green). In the crystal structure of reduced, inactive Hsp33, the linker region is compactly folded in three α-helices. It makes extensive contacts with a largely hydrophobic, four-stranded β-sheet platform of Hsp33's N-terminal domain (Janda et al., 2004; Vijayalakshmi et al., 2001).

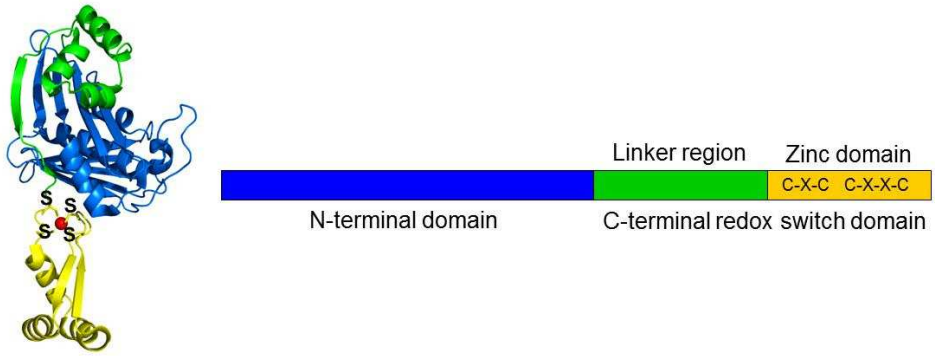

Fig. 2.7: Hsp33 is a two-domain protein

This is a model of Hsp33 in its inactive form, as a tightly folded monomer. All crystal structures of Hsp33 show Hsp33 as a dimeric protein, although solution studies revealed that reduced Hsp33 is monomeric. Hsp33 consists of two domains, a N-terminal domain (blue), which is formed by a β-sheet sandwich and a C-terminal redox switch domain (green and yellow). Hsp33's linker region (green) is part of the redox switch domain. Being adjacent to the N-terminal domain, it is important for sensing of unfolding conditions. Under non-stress conditions, the three helices of Hsp33's linker region are folded on top of Hsp33's N-terminal domain. The C-terminal zinc-binding domain (yellow) harbors 4 highly conserved cysteines, which are important for sensing changes in the cytosolic redox status. In the reduced form these cysteines are in a tetrahedral conformation, harboring a zinc ion (red sphere) (structure adapted from (Cremers et al., 2010).

2.5.4.2 Activation of Hsp33

Hsp33's chaperone function is activated by the oxidative unfolding of its own C-terminal redox switch domain. Once activated, Hsp33 protects cells against oxidative stress-induced protein unfolding and aggregation (Ilbert et al., 2007; Winter and Jakob, 2004; Winter et al., 2005).

Activation of Hsp33's chaperone function is triggered by intramolecular disulfide bond formation, which leads to the release of Zn^{2+}-ion and, concomitantly, to the unfolding of both Hsp33's zinc-binding domain and the adjacent linker region. Unfolding of the linker region has been shown to lead to the exposure of hydrophobic surface areas of Hsp33 (Graf, 2004; Ilbert et al., 2007; Raman et al., 2001; Vijayalakshmi et al., 2001). Recent studies suggested a mechanistic model for the activation of Hsp33, in which the unfolding of the linker region simultaneously depends on and controls disulfide bond formation (Ilbert et al., 2007; Winter et al., 2008). In this model, incubation of *E. coli* Hsp33 with H_2O_2 leads to the rapid formation of one disulfide bond between the distal cysteines Cys_{265}/Cys_{268}. This disulfide bond

formation triggers zinc release, and the unfolding of the zinc-binding domain, forming a chaperone inactive intermediate (Fig. 2.8) (Ilbert et al., 2007). Unfolding of the zinc binding domain appears to destabilize the adjacent linker region, which exists in a dynamic equilibrium between a folded and unfolded state. When folded, the second pair of active site cysteines is not accessible for oxidation by kinetically slow oxidants like H_2O_2 (Ilbert et al., 2007; Leichert et al., 2008a). H_2O_2 only induces the formation of the second disulfide bond between Cys_{232} and Cys_{234} in the presence of additional unfolding conditions *(e.g.,* heat or detergents), which shift the equilibrium of the linker region towards the unfolded conformation (Fig. 2.8) (Ilbert et al., 2007). Kinetically fast oxidants, such as HOCl however rapidly form the second disulfide bond even when no other unfolding condition is present (Winter et al., 2008). Once the second disulfide bond is formed, the linker region appears to remain in an unfolded conformation and two oxidized monomers associate to form the highly active Hsp33 dimer (Fig. 2.8).

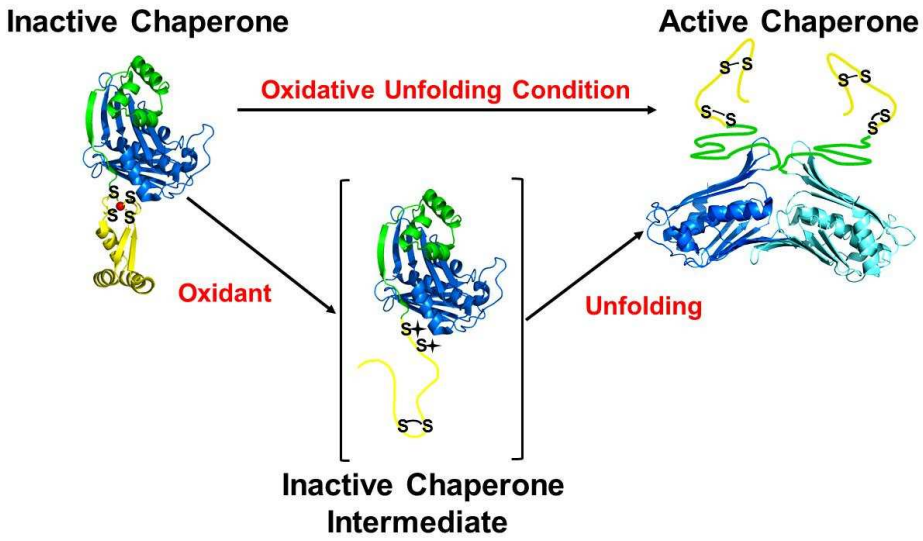

Fig. 2.8: Activation mechanism of *E. coli*'s Hsp33
Hsp33 in its reduced and inactive form is a tightly folded monomer. Sensing of oxidative stress occurs in the C-terminal zinc-binding domain. Oxidation of the two distal cysteines (Cys265/Cys268) leads to formation of a disulfide bond, zinc release and unfolding of this domain, creating an inactive chaperone intermediate. The adjacent linker region is in equilibrium between a folded and unfolded state. Slow oxidants, like H_2O_2, are not able to oxidize the two critical cysteines. Unfolding conditions, like heat or detergents, shift the linker folding state to the unfolded form, allowing the oxidation of the two critical cysteines and dimerization, linking of the protein in its active form.

The stability of Hsp33's linker region in the reduced form is conferred by interactions between the linker region and a ~ 3800 Å surface area of Hsp33's N-terminal domain. About ¾ of this area is of hydrophobic nature (Vijayalakshmi et al., 2001). The above described activation model of Hsp33 implies that the N-terminal hydrophobic platform serves a dual role, as an interaction site for the linker region under non-stress conditions and as a binding site for unfolded client proteins under stress conditions.

2.5.4.3 Hsp33 client protein binding and release

In 2004, Tompa et al. determined that many chaperones have intrinsically unfolded regions, and proposed that these are important for their chaperone function (Tompa and Csermely, 2004). Along the same lines, Tapley et al. 2009 reported that the monomerization and unfolding of the acid-activated chaperone HdeA is necessary for its chaperone function (Tapley et al., 2009b). Moreover, the sHsp PsHsp18-1 was found to interact with its clients via a flexible N-terminal domain (Jaya et al., 2009). DnaK's C-terminal region is likewise disordered and it has recently been shown that this extension enhances the chaperone function of DnaK due to transient client interaction (Smock et al., 2011). These results indicated that unfolding does not necessarily lead to a loss of function as previously proposed, but that intrinsically disordered regions might actually facilitate binding of the client proteins. This could also be the case for Hsp33 as it loses parts of its structure during the activation process (Graf, 2004; Ilbert et al., 2007; Winter et al., 2008), which could potentially be involved in client protein binding.

Hsp33 binds tightly to unfolding client proteins during oxidative protein unfolding conditions (Fig. 2.9). Upon return to non-stress conditions, Hsp33 gets rapidly reduced by the cellular glutaredoxin and thioredoxin systems *in vivo* (Hoffmann et al., 2004). Reduction alone, however, is not sufficient to release the client proteins. Effective release of the client from reduced Hsp33 requires the DnaK/J/E system, which subsequently supports the refolding of the client to the native state (Hoffmann et al., 2004). The DnaK/J/E system is inactive during oxidative unfolding conditions (Winter et al., 2008; Winter et al., 2005). Therefore having a two component chaperone system of a holdase

and the corresponding foldase guarantees that unfolded client proteins are only released and refolded when non-stress conditions are restored (Fig. 2.9) (Hoffmann et al., 2004; Winter et al., 2005). Important for an effective client protein transfer between the two systems is that Hsp33 and DnaK/J/E both bind the same client proteins. This was demonstrated by Hoffmann (2004) and Winter (2005), who showed extensive overlap in client recognition between the holdase and foldase *in vitro* and *in vivo* (Hoffmann et al., 2004; Winter et al., 2005). DnaK prefers to interact with unfolded client proteins or polypeptides, which fit into its discrete peptide-binding pocket, which is suited to bind to short extended polypeptides without any secondary structure (Chen et al., 2006; Rüdiger et al., 1997a).

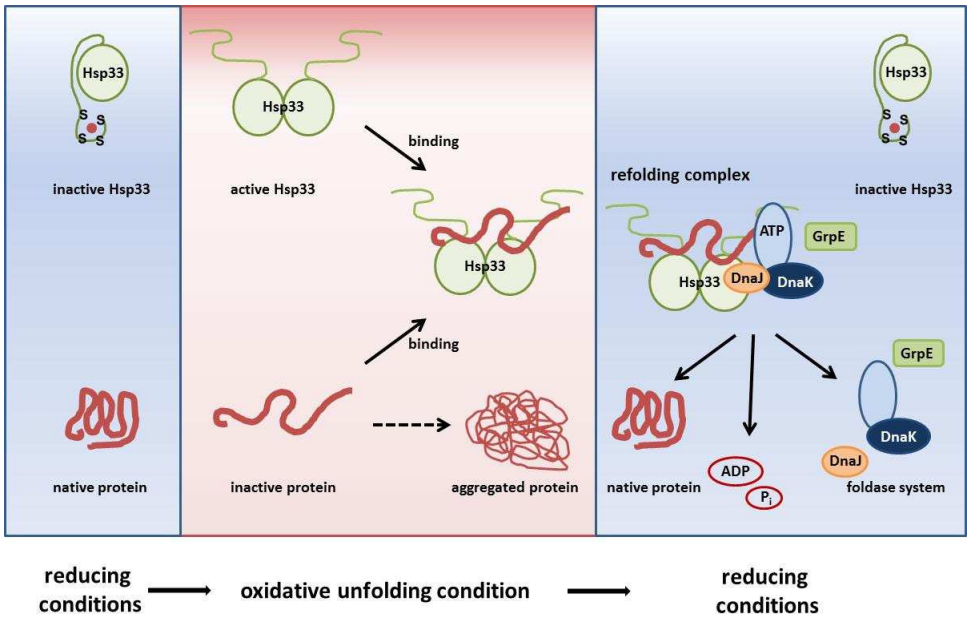

Fig. 2.9: Hsp33 substrate binding and release

Factors triggering Hsp33's activation (*e.g.*, oxidative unfolding conditions) lead to the unfolding and aggregation of Hsp33's client proteins. Hsp33 binds tightly to partially folded clients, keeping them from irreversible aggregation. Under these stress conditions, other chaperones, like the DnaK/J/E foldase system is inactive. Upon return to non-stress conditions substrate transfer from Hsp33 is triggered, by reduction of its own C-terminal domain, to the DnaK/J/E system, which is now active again (modified from Reichmann (2012) (Reichmann et al., 2012).

2.6 Physiological antimicrobials

Bacteria encounter several physiologically relevant antimicrobial while invading the mammalian host. Phagocytic cells of the innate immune-

response (*e.g.*, neutrophils, macrophages) engulf bacteria. This triggers the production of oxidants, such as peroxide and hypochlorous acid (*i.e.,* oxidative burst), which are released into the phagosomes in an effort to kill the invading microorganisms. The complex conditions encountered in the stomach and gut of mammals also presents a range of physiological challenges that microorganisms have to face while attempting to colonize the host. The host produces a plethora of antimicrobial compounds, hydrochloric acid, bile, antimicrobial peptides, as well as hydrolytic enzymes. In addition, mucosal barrier epithelia in lung, bronchia, and the intestine produce reactive oxygen species as innate response to defend against bacterial colonization. Here we will focus on reactive oxygen species as well as bile salts and their physiological functions.

2.6.1 Physiological oxidants that bacteria encounter

Aerobically grown bacteria produce constantly reactive oxygen species (ROS) as by-product of respiration and metabolic processes. When produced in excess or upon inadequate detoxification, accumulation of intracellular ROS induces oxidative stress, which leads to the modification of all macromolecules and causes damage to lipids, DNA, and proteins (Imlay, 2003; Storz and Imlay, 1999).

Physiologically relevant reactive oxygen species include superoxide ($O_2^{\cdot-}$) and hydrogen peroxide (H_2O_2). Superoxide is produced as a result of inadequate electron transfer during the electron transport chain (Messner and Imlay, 1999) when NADH dehydrogenase II auto-oxidizes and reacts with O_2 molecules. Dismutation of $O_2^{\cdot-}$ can occur spontaneously or can be catalyzed by superoxide dismutase (SOD). In either case, it leads to the production of H_2O_2, which can further react with ferrous iron to form the highly reactive hydroxylradical ($OH^{\cdot}$) by Fenton chemistry (Imlay et al., 1988).

Host enzymes are responsible for the production of antimicrobial oxidants, which are dual oxidase (DUOXI and II), NADPH oxidase (NOX1, 2, 4), nitric oxide synthase, and myeloperoxidase (MPO). NOX2, MPO, and nitric oxide synthase are found in phagocytes. NOX is responsible for the first step in

ROS production. It catalyzes the production of $O^{\cdot -}_2$, as well as dismutation of $O^{\cdot -}_2$ to H_2O_2 (Ago et al., 1999). MPO consumes about 45% of this H_2O_2 (van Dalen et al., 1997) by catalyzing Cl^- oxidation, producing HOCl in this process (Harrison and Schultz, 1976). This dramatically increases microbicidal activity (Lanza, 1998). A byproduct of this reaction is the production of $OH^{\cdot}$ (Winterbourn et al., 2006). Singlet oxygen can be produced as well when MPO reacts simultaneously with HOCl and H_2O_2 (Allen et al., 1974). MPOs are also responsible for the production of aldehydes and chloramines as secondary products.

NOX1, NOX4 and DUOXI are also found in secretory glands in mucosal surfaces of lung, bronchia, and intestine (Geiszt et al., 2003). The dual oxidase system contains one domain that is homologous to the NADPH oxidase and necessary for the generation of $O^{\cdot -}_2$ as well as a peroxidase domain, which catalyzes the production of HOCl from H_2O_2 and Cl^- (Chen et al., 2011; Ha et al., 2005; Moreno et al., 2002).

2.6.2 Oxidative stress-induced protein damage in bacteria

One of the most prevalent targets of ROS in organisms are proteins. Certain proteins are more accessible to oxidative protein damage than others. It is now clear that factors determining this sensitivity include the relative content of oxidation-sensitive amino acids, the presence of metal-binding sites, as well as the molecular conformation. Newly synthesized proteins appear to be more prone to oxidative damage than folded proteins, implying that protein folding and protein-complex formation confer oxidative stress protection (Holland et al., 2007; Medicherla and Goldberg, 2008).

Cysteines and methionines are common targets of oxidative stress. Oxidation of these sulfur-containing amino acids by peroxide can alter protein function and/or lead to irreversible damage to the protein. HOCl is a fast acting oxidant, which is able to also oxidize those residues that are just transiently accessible for oxidative modification in proteins. This can lead to widespread protein unfolding and aggregation (Winter et al., 2008). Cysteine oxidation leads to the formation of sulfenic acid, a highly reactive and unstable

oxidation intermediate, which rapidly interacts with adjacent cysteines, leading to the formation of inter- or intramolecular disulfide bonds. Alternatively, it can get further oxidized to sulfinic or sulfonic acid, modifications that are not reversible in bacteria (Stadtman and Levine, 2000). Methionine oxidation leads to the formation of methionine sulfoxide or methionine sulfone. The thioredoxin (Trx) and glutaredoxin (Grx) systems are important for the reduction of oxidized cysteines, whereas methionine oxidation is reversed by methionine sulfoxide reductase (MrsA).

Several other amino acid residues (*e.g.*, arginine, histidine, lysine, and proline) can fall victim to metal-catalyzed oxidative attacks on the amino acid side chains causing protein carbonylation, which is irreversible *in vivo* (Dalle-Donne et al., 2003) and leads to the proteasomal degradation of the carbonylated protein. In *E. coli* known carbonylated proteins include the Hsp70 and Hsp60 chaperones, the histone-like protein, H-NS, the elongation factors EF-Tu and EF-G, glutamine and glutamate synthetase, aconitase, malate dehydrogenase, as well as pyruvate kinase (Dukan and Nystrom, 1999; Tamarit et al., 1998).

2.6.3. Oxidative stress defenses in *E. coli*

Bacteria contain several different defense systems against ROS, which are required for bacterial survival. *E. coli* harbors two major oxidative stress regulons, the OxyR and the SoxRS regulon. OxyR is rapidly activated by H_2O_2, whereas SoxRS is induced by superoxide.

2.6.3.1 OxyR – Peroxide Stress Response in Bacteria

OxyR is a 34 kDa protein, which forms a homotetrameric DNA binding protein (Kullik et al., 1995). It belongs to the LysR family of regulators. It negatively regulates its own transcription and positively regulates the expression of oxyS, a small non-translated RNA as well as approximately 30 other genes (Altuvia et al., 1997; Christman et al., 1989; Tao, 1997). OxyR-dependent transcriptional regulation is activated when Cys199 is oxidized to sulfenic acid. This initial oxidation leads to disulfide bond formation with Cys208, a residue that is 17Å away from Cys199 in the reduced form. Hence,

disulfide bond formation induces significant differences in OxyR's structure, which are necessary for the cooperative binding of RNA polymerase and subsequent transcription of the target sequences (Choi et al., 2001; Tao et al., 1993; Zheng et al., 1998). OxyR is directly oxidized by H_2O_2 and reduced by both glutaredoxin and thioredoxin. Hence, deletion of genes involved in the thioredoxin and glutaredoxin pathway (*gorA trxA* or *gshA trxA*) lead to the partial activation of OxyR (Aslund et al., 1999; Hausladen et al., 1996; Zheng et al., 1998).

Genes that are up-regulated in response to OxyR activation include the peroxide scavengers alkyl hydroperoxide reductase (AhpC) and catalase (Christman et al., 1985; Gonzalez-Flecha and Demple, 1997). Other up-regulated genes are *dps*, a DNA-iron binding protein as well as members of the thioredoxin and glutaredoxin system, including *gorA* (glutathione reductase), *grxA* (glutaredoxin), *trxA* (thioredoxin) and *trxB* (thioredoxin reductase). These proteins constitute a negative feedback loop as they reduce and inactivate OxyR once the stress subsides (Zheng et al., 1998). Also *fur,* an iron-binding repressor of iron transport as well as *dsbG*, a periplasmic disulfide isomerase are upregulated in response to peroxide (Chiang and Schellhorn, 2012).

Many of the upregulated genes have clear roles in the cellular antioxidant defense. In addition, OxyR also induces the synthesis of the small non-coding RNA OxyS. OxyS indirectly regulates 30 other genes by affecting their translation efficiency and/or mRNA stability (Altuvia et al., 1997). OxyS negatively regulates the RpoS-regulon, which is important for the general stress response. It is thought that this negative regulation shuts down the translation of the less specific stress repair pathways, favoring the expression of oxidative stress-specific genes (Zhang et al., 1998).

2.6.3.2 SoxRS - transcriptional regulation during superoxide stress

The SoxRS regulon of *E. coli* is activated under superoxide stress and regulates the expression of several genes. The *soxR* and *soxS* genes in *E. coli* are adjacent but divergently transcribed via a two-stage regulatory system

(Wu and Weiss, 1991). Activated SoxR induces transcription and therefore translation of SoxS, which, in turn, activates several other genes important for superoxide stress response (Nunoshiba et al., 1992). Activation of SoxR is mainly induced $O_2^{\cdot-}$ but can also be induced by $NO^{\cdot}$ or by very high levels of H_2O_2 (Nunoshiba et al., 1993; Tsaneva and Weiss, 1990).

The 17 kDa SoxR homodimer belongs to the MerR family of transcriptional regulators, harboring two 2Fe-2S clusters. For activation oxidation by $O_2^{\cdot-}$ of the 2Fe-2S clusters occurs and induces structural changes in the protein, which allow the transcription of *soxS* by RNA polymerase (Ha, 2005; Hidalgo et al., 1995; Hidalgo and Demple, 1994). SoxR's binding to the *soxS* promoter is independent of SoxR's redox status but oxidation is required for induction of *soxS* transcription (Hidalgo and Demple, 1994)

SoxS, belongs to the AraC family of one-component transcriptional regulators, which after their translation, modulate the expression of more than 100 genes (Blanchard et al., 2007). Several of the SoxRS-regulated genes are important in the oxidative stress response. The transcription of manganese superoxide dismutase (*sodA*), for instance, is strongly up-regulated in response to superoxide, and important for the dismutation of $O_2^{\cdot-}$ to H_2O_2.

Other upregulated genes include endonuclease IV (*nfo*), which is involved in oxidative stress-induced DNA repair, as well as several enzyme involved in glucose metabolism, including fumarase (*fumC*), aconitase (*acnA*) and glucose-6-phosphate dehydrogenase (*zwf*). Latter increases the availability of NADPH, which is important for the reduction of oxidized glutathione and thioredoxin and, therefore, for maintaining the reduced status of proteins. Iron uptake is reduced due to higher expression of the Fur repressor (*fur*), which reduces the amount of hydroxyl radicals produced. Also, the membrane composition changes through the upregulation of *tolC* (outer membrane protein), *acrAB* (drug efflux pump) as well as *micF*, an antisense RNA that represses OmpF translation (Storz and Imlay, 1999). Upon return to non-stress conditions, SoxR returns to its reduced state via a reducing system, which is encoded by *rseC* and a member of the *rsxABCDGE* regulon, maybe

by the products of *rsxBC* (Koo et al., 2003). SoxS on the other hand is rapidly degraded (Griffith et al., 2004).

2.6.3.3 The glutaredoxin and thioredoxin system

Catalase, alkyl hydroperoxide reductase, and superoxide dismutases directly react with H_2O_2 or $O_2^{\cdot-}$ and detoxify the oxidants, thereby partially reducing the damage caused. *E. coli* has evolved two other systems, which are important to maintain the reducing character of the cytosol; the thioredoxin (Trx) and the glutaredoxin (Grx) system. The thioredoxin system is comprised of two thioredoxins (*trxA/C*) and one thioredoxin reductase (*trxB*), whereas the glutaredoxin system has three glutaredoxin (*grxA/B/C*), one glutathione oxidoreductase (*gorA*), and the tripeptide glutathione (GSH, L-γ-glutamyl-L-cysteineglycine).

The family of thioredoxins and glutaredoxins share little similarity in the amino acid sequence, despite their similarity in structure and function (Dyson et al., 1989; Martin, 1995; Xia et al., 1992). They are characterized by a special thioredoxin/glutaredoxin fold, which consists of three α-helices and four β-sheets. Two redox active cysteines separated by a pair of amino acids (CxxC -motif) are embedded in this fold (Martin, 1995).

The major function of Trxs and Grxs is the reduction of sulfenic acids, disulfide bonds, S-nitrosylations or S-glutathionylations in cytosolic proteins (Holmgren, 1989b). There is certain specificity in the systems but in general both systems can reduce oxidized cysteines. Protein glutathionylation needs to be resolved by the Grx-system.

Reduction of the oxidized target proteins by Trx/Grx takes place in two steps: first the N-terminal cysteine in the CxxC motif of Trx/Grx, which is more nucleophilic, attacks the disulfide bond of the target protein, introducing a mixed disulfide between the target and Trx/Grx. Subsequently, the second more C-terminal cysteine in Trx/Grx attacks the mixed disulfide, resulting in the release of the reduced target protein and the oxidized Trx/Grx (Brandes et al., 1993). One difference between the Trxs and Grxs is the mode of reduction: while Grxs are reduced non-enzymatically by reduced glutathione,

Trxs are reduced enzymatically by the NADPH-dependent thioredoxin reductase (Fig. 2.10) (Williams, 1995).

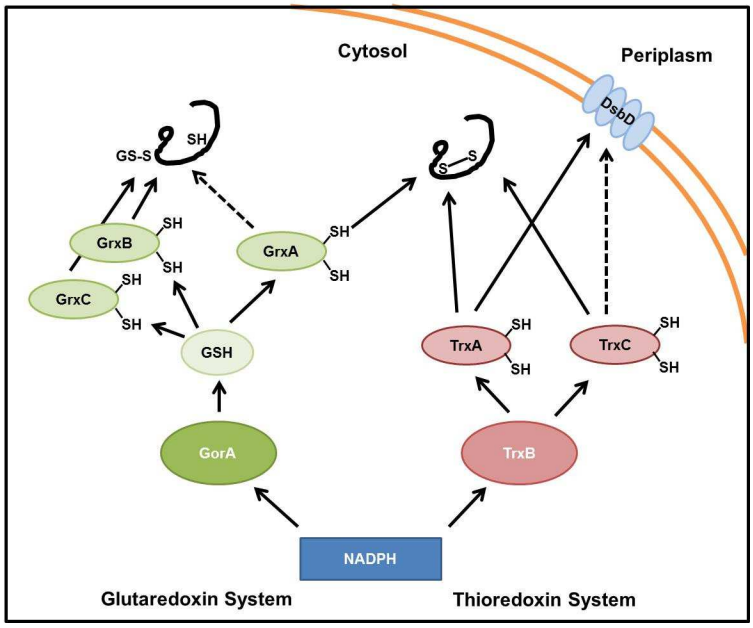

Fig. 2.10: Reduction of oxidized proteins by the Grx/Trx systems
The reduction equivalent necessary to reduce oxidized proteins with the Grx or Trx system comes from NADPH. In the Trx system, which is important for protein reduction and transfer of reducing equivalents to the periplasm, thioredoxin reductase directly reduces the thioredoxins. In the Grx system the glutathione oxidoreductase transfers the reducing equivalents to glutathione, which subsequently reduces oxidized Grx by nucleophilic attacks. The Grx reduces oxidized cysteines or proteins that are glutathionylated. Reducing equivalents for the periplasm are transferred from Trx to DsbD, which maintains periplasmic disulfide isomerases in the reduced state (Figure modified from: (Ritz and Beckwith, 2001).

Grx, while generally less efficient in reducing protein disulfide bonds, is more efficient in reducing glutathione-mixed disulfides, which form upon a nucleophilic attack of GSH on other disulfide bonds in proteins (target-GS). Grx targets this conformation and reduces the protein - forming Grx-GS. The mixed Grx-GS disulfide is subsequently reduced by a second GSH generating reduced Grx and oxidized glutathione (GSSG) (Fig. 2.12) (Aslund et al., 1994; Bushweller et al., 1992). Glutathione is kept in the reduced state by glutathione oxidoreductase (*gorA*), which is a member of the dimeric FAD-containing thiol reductase family. Reducing equivalents are used from the oxidation of NAD(P)H. *E. coli* might have other, as yet to be identified GSH reductases since the ratio between reduced and oxidized GSH : GSSG ratio

does not significantly change in a *gorA* deletion strain (Tuggle and Fuchs, 1985).

2.6.4 Bile salts

As mentioned previously, bacteria encounter numerous challenges when in the gastrointestinal tract. The first line of defense is the low pH in the stomach, followed by low oxygen level, elevated osmolality and bile in the adjacent duodenum (Chowdhury et al., 1996). Bile salts are one of the major components in bile besides ions, cholesterol, and phospholipids. Its concentrations reaches approximately 40 mmol/l in the small intestine and its composition varies from individual to individual depending on the diet (Bouchier 1982). Bile salts can form simple or mixed micelles. They facilitate the rupture and transportation of lipo-soluble molecules. The biological activity of bile salts is expressed as the critical micelle concentration (CMC) and is defined as the solute concentration at which micelles first appear (Carey and Small, 1972; Coleman, 1987). The amount of bile salts needed to reach the CMC depends not only on the type of bile salt but also on external factors such as salt content, solvent, temperature, and pH (Reis et al., 2004).

2.6.4.1 Bile salt synthesis

Bile salts are amphipathic cholesterol metabolites, which are produced in the liver by a multi-enzyme and multi-organelle process. The primary bile salts synthesized are cholic acid (salt: cholate; from here on Na-Cho) or chenodeoxycholic acid (salt: chenodeoxycholate) (Hofmann, 1999) (Fig 2.11). After synthesis, bile salts are conjugated either with glycine or taurine in order to lower the pK_a of the terminal acid group. This increases their solubility at neutral pH (Hofmann and Mysels, 1992; Hofmann and Roda, 1984). After secretion from hepatocytes, bile salts are either concentrated 5 - 10-fold in the gall bladder (bile salt concentration up to 300 mM) and stored, or they will bypass the gallbladder and are released directly in the duodenum. Bile stored in the gallbladder is released into the small intestine to conduct its physiological function upon food intake. 95% of bile salts entering the small intestine are then reabsorbed (enterohepatic circulation) (Hofmann, 1994). Further modifications of bile salts happen in the colon where bacterial

enzymes transform cholate and chenodeoxycholate into secondary bile salts (Fig. 2.11) (Christiaens et al., 1992; Desmet et al., 1995). One of these events is dehydroxylation, which converts cholic acid to deoxycholic acid (salt: deoxycholate, from here on Na-DOC), one of the most prevalent bile salts in humans (Wells and Hylemon, 2000). The terms “bile salt” and “bile acid” are often used interchangeably, since bile salts are simply bile acids compounded with a cation, usually sodium.

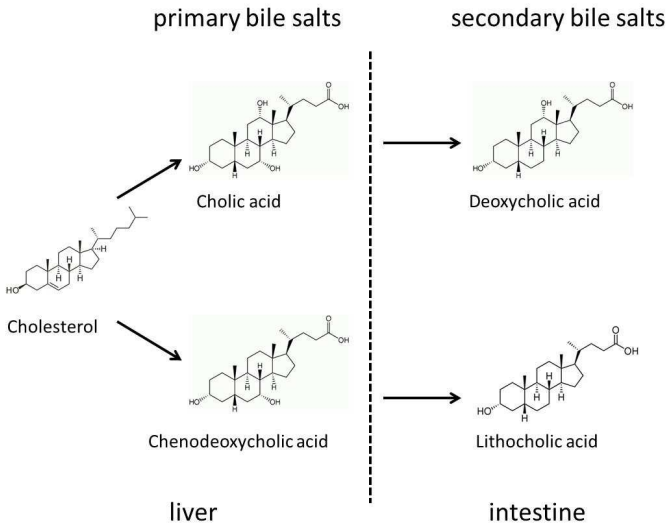

Fig. 2.11: Bile salt synthesis
The primary bile salts cholic acid and chenodeoxycholic acid are synthesized from cholesterol in the liver in a multi-enzymatic process. Upon synthesis, they are conjugated with taurine or glycine, which increases the solubility at neutral pH. Storage and concentration of bile salts follows in the gall bladder. Upon food intake, bile salts are released into the duodenum. During the circulation in the intestine, bile salts are enzymatically modified by bacteria, forming secondary bile salts.

2.6.4.2 Physiological function of bile salts

The physiological function of bile salts in the intestine is to act as a biological detergent, responsible for emulsification and solubilization of fatty acids. Their amphipathic character allows bile salts to break down fat globules into microscopic droplets, which then can be further metabolized by lipases (Hofmann, 1994, 1999). Bile salts are also responsible for the absorption of lipids, lipid soluble vitamins and cholesterol (Russell, 2003). In addition to their role in the digestion of food and absorption of macromolecules, bile salts have been shown to have antimicrobial function, particularly towards gram positive bacteria (Begley et al., 2005a). Furthermore, it has been reported that bile

salts are regulatory molecules in mammals, serving as ligands of the farnesoid X receptor-α (FXR-α), inducing numerous genes in the liver and intestine (Makishima et al., 1999; Wang et al., 1999), and playing a role in the activation of protein kinase C (PKC) (Craven et al., 1987; Rao et al., 1997).

2.6.4.3 The antimicrobial function of bile salts

The small intestine, in which the concentration of bile salts is high, harbors relatively few bacteria (Inagaki, 2006). Reduction of bile salt concentrations, which occurs as a result of liver cirrhosis or malnutrition, can lead to an overgrowth of bacteria in the small intestine (Ding et al., 1993). Elevated concentration of bile salts can also have negative effects on health. For instance, hydrophobic bile salts are known to be involved in cancer development (Pazzi et al., 1997; Powell et al., 2001).

Bile salts have antimicrobial and cytotoxic effects, which depend on the hydrophobicity of the bile salts as well as on the growth rate of bacteria and the atmosphere (King et al., 2003; Sung et al., 1993). Bacteria in the stationary phase of cell growth are much more resistant to bile salt treatment than exponentially growing cells (King et al., 2003). The amphipathic character of bile salts allows their interaction with the microbial lipid bi-layer. This induces changes in membrane integrity and causes holes to form in the cell membrane. Cell lysis upon exposure to bile salts was reported in erythrocytes (Albalak et al., 1996). At this point, however, little is known how bile salts affect the membrane of bacteria. It is known that the bacteria up-regulate numerous proteins in response to bile salts, which are directly or indirectly involved in the maintenance of membrane integrity (Ruiz et al., 2009). The resistance of bacteria towards bile salt stress has been reported to require the products of the *tol* and *pal* genes, which preserve the outer membrane of gram-negative bacteria (Dubuisson et al., 2005; Prouty et al., 2002; Ray et al., 2000). Therefore, the composition and architecture of the membrane appears to be important for bile salt resistance in bacteria. Changes in charge, hydrophobicity, and lipid liquidity appear to influence the tolerance to bile salts. These factors change, depending on the growth phase that bacteria are in.

Bile salts can also easily enter the bacterial cytosol in their unconjugated form due to a flip-flop mechanism (Cabral et al., 1987). The rate of the flip-flop depends on the number of hydroxyl groups, with dihydroxy bile salts (*e.g.*, deoxycholate) entering the cytosol at a faster rate than trihydroxy bile salts (*e.g.,* cholate) (Cabral et al., 1987). One mechanism that bacteria have evolved to reduce bile salt damage in the cytoplasm are efflux systems, which transport bile salt out of the cytoplasm.

Apart from affecting membrane integrity, bile salts have been shown to introduce secondary structures in DNA, as indicated by the up-regulation of enzymes required for DNA repair in prokaryotes and eukaryotes. Bile salts appear to also introduce secondary structures (Bernstein et al., 1999; Kandell and Bernstein, 1991; Leverrier et al., 2003), and increase the frequency of nucleotide substitutions, chromosomal rearrangements, and frame-shifts (Prieto et al., 2004, 2006).

Microarray and protein expression analysis reported the up-regulation of some chaperones, including DnaK, GroEL/ES, ClpB and the protease ClpP/L. These results indicate that bile salts might cause protein unfolding conditions. Bile salts, which are classified as anionic, non-denaturing surfactants should not interfere with the folding state of proteins. In fact, due to their non-denaturing properties, bile salts are often used as surfactants during membrane protein purification, removing lipids without changing the proteins structure or function (Hjelmeland, 1980; Tofani et al., 2004). The interaction between bile salts and proteins can thus be described as cooperative, which states that more than one bile salt molecule can interact with one protein molecule at the same time (De et al., 2007; Schweitzer et al., 2006). Several labs stated that there is the possibility that bile salts also alter the structures of proteins *in vitro* but so far only some loss in α-helical structure has been reported (De et al., 2007; Pico and Houssier, 1989; Robic et al., 2011).

Bile salt-mediated up-regulation of cysteine synthase, catalase, superoxide dismutase as well as members of the thioredoxin system (TrxA and TrxB) suggests that bile salts also induce oxidative stress *in vivo* (Begley

et al., 2005a; Bernstein et al., 1999; Hamon et al., 2012; Merritt and Donaldson, 2009).

Little has been done, however, to precisely assess the extent and role of bile salt-mediated protein unfolding/aggregation as well as oxidative stress in host defense.

2.7 Outline

Hsp33 is a redox regulated chaperone holdase, which protects cell against the lethal consequences of oxidative protein aggregation. Hsp33 undergoes major structural rearrangements during its activation process, involving the oxidative unfolding of its C-terminal redox switch domain, making Hsp33 one of the few proteins known that need to unfold to get activated. While it is known that these conformational changes are necessary for Hsp33's activation, several fundamental questions are still unanswered. Hsp33's N-terminal hydrophobic platform is buried underneath the linker region in the reduced form. It has thus the possibility to serve two functions: it could serve as interaction site for the linker region under non-stress conditions and/or it could be the binding site for unfolded client proteins under stress conditions. In this thesis, we set out to investigate the role of this conserved surface in Hsp33's chaperone function and regulation (Chapter 4.1). The second question that we addressed in this thesis concerns Hsp33's client specificity. We wondered how Hsp33 discriminates between its own unfolded regions and the unfolded regions in client proteins. We hence investigated the peptide binding specificity and analyzed how the client transfer from Hsp33 to the DnaK/J/E system is regulated (Chapter 4.2). The last question that we investigated concerns Hsp33's physiological role. We decided to use Hsp33's activation requirements for oxidative stress and unfolding conditions to investigate the physiological effects of bile salt treatment on bacteria. Our results suggest that the underlying molecular mechanism for the antimicrobial action of bile salts involves oxidative protein unfolding and aggregation (Chapter 4.3)

3 Experimental Procedures

Chemicals used for buffer preparation are obtained from Sigma Aldrich, Fisher Scientific, or Molecular Probes. Vendors for all other probes are marked in the text. Use of equipment is universally described or stated within the text.

3.1 Strains and plasmids

E. coli Bl21 DE3	F- *ompT gal dcm lon hsdS$_B$(r$_B^-$ m$_B^-$) λ(DE3 [lacI lacUV5- 7 gene 1 ind1 sam7 nin5])*
E. coli MC4100	F- *[araD139]$_{B/r}$ Δ(argF-lac)169* &lambda$^-$ e14- flhD5301 Δ(fruK-yeiR)725 (fruA25)‡ relA1 rpsL150(strR) rbsR22 Δ(fimB-fimE) 632(::IS1)deoC1*
E. coli DHB4	F′ *lac-pro lacI^Q/Δ(ara-leu)7697 araD139 ΔlacX74 galE galK rpsL phoR Δ(phoA)*PvuII *ΔmalF3 thi*

3.1.1 Strains

Bl21 DE3 *hslO*::Km	JH13
MC4100 *hslO*::Km	CC59
DHB4 *oxyR*::Km	LL09
DHB4 *rpoH*::tet	kind gift of Jon Beckwith
DHB4 Δ*trxA*	kind gift of Jon Beckwith
DHB4 *trxB*::Km	kind gift of Jon Beckwith
DHB4 *gorA::*Cm	kind gift of Jon Beckwith
DHB4 *grxA*::Km	kind gift of Jon Beckwith
DHB4 *grxC*::Cm	kind gift of Jon Beckwith
Bl21 DE3 pET11a hslO	UJ80
Bl21 DE3 hslO- pet11a hslO M172S	JHa21
Bl21 DE3 hslO- pet11a hslO Y12E	CC4
Bl21 DE3 hslO- pet11a hslO F187W W212F	HJ4
MG1655 pBB535	JW124

C600*dnaKa756* pWKG20	KL22
WM3110 pUHE21	KL5

3.1.2 Plasmids

pET11a	Novagen
pET11a *hslO*	pUJ30
pET11a *hslO*-M172S	pJHa1
pET11a *hslO*-Y12E	pCC2
pet11a *hslO*-F187W W212F	lab collection
pWKG20 (GrpE over expression)	lab collection
pBB535 (DnaK over expression)	kind gift of Bernd Bukau
pUHE21 (DnaJ over expression)	kind gift of Bernd Bukau

3.2 Generation of Hsp33 mutants

The Hsp33-M172S and Hsp33-Y12E mutants were generated by introducing single site mutations into the wild-type Hsp33 gene (*hslO*) using pUJ30 (pET11a-*hslO*) (Jakob, 2000) as a template. For mutagenesis a single site mutation kit was used (Startagene), following manufactures instruction. After cloning, introduced mutations were checked by sequencing. The plasmids were transformed with a heat shock method into JH13 (BL21 *hslO*-), generating the expression strains JHa21 (JH13, pET11a-*hslO*-M172S) and CC4 (JH13, pET11a-*hslO*-Y12E).

3.3 Protein purification

Proteins were either manually purified using a P1- pump (Pharmacia LKB) or with an Äkta-FPLC system (GE Healthcare).

3.3.1 Purification of wild-type and Hsp33 mutant proteins

Cultivation of the Hsp33 overexpressing strains for protein purification was conducted as previously described (Graumann et al., 2001). For the induction of the Hsp33-M172S and Hsp33-F187W W212F mutant, the protocol for wild-type Hsp33 was followed (Jakob et al., 1999). To overexpress large amounts

of soluble Hsp33-Y12E protein, cells were grown to an OD_{600} of 0.6-0.8 at 37°C and then shifted to 18°C. Once the temperature was reached, Hsp33-Y12E expression was induced with 1 mM IPTG for 24h. Afterward, the standard protocol for the Hsp33 purification was followed, in short the following protocol was followed:

Cells were harvested by centrifugation (5000 x g, 30 min, 4°C), resuspended in lysis buffer A (40 mM Hepes, 200 mM KCl, pH 7.5) and lysed by French press (3x 1300 psi). After the lysis, centrifugation (45000 x g, 45 min 4°C) was conducted to remove cell debris. The supernatan was loaded on an anion exchange column (Q-sepharose HP, GE Healthcare) equilibrated in buffer A. After a washing step with buffer A, bound protein was eluted with a gradient to 700 mM KCl in buffer A. Fractions containing Hsp33 were pooled, concentrated and dialyzed overnight into buffer B (5 mM KH_2PO_4, pH 6.8). Proteins were subsequently loaded on a HAP-column (Hydroxyapatite BioGel, BioRad), equilibrated with buffer B, and after washing with the same buffer the bound proteins were eluted with a gradient to 70mM KH_2PO_4, pH 6.8. Fractions containing Hsp33 were pooled and concentrated. The last column used was a Superdex 75 (HiLoad 16/600, GE Healthcare) equilibrated in 40 mM KH_2PO_4, 200mM KCl, pH 7.5. The concentrated protein was loaded and eluted with the same buffer. After pooling fractions containing Hsp33, the protein was concentrated and the buffer was exchanged to 40 mM KH_2PO_4, pH 7.5. Hsp33 was aliquoted, and stored at −20°C.

3.3.2 Purification of DnaK

Growth of DnaK overexpressing strains (JW124) and purification of DnaK was conducted as previous described (Buchberger et al., 1994). In short: cell cultures are grown at 30°C for 16 h. Cells were harvested by centrifugation (5000 x g, 30 min, 4°C) and resuspended in lysis buffer containing buffer A (20 mM Tris, 2 mM EDTA, 10% sucrose, 2 mM DTT, pH 7.2) supplemented with: 30 mM spermidine, 200 mM KCl, 5 mM EDTA and lysed by a French press (3x 1300 psi). Centrifugation (45000 x g, 45 min 4°C) to remove cell debris from lysis was conducted before proteins were ammonium precipitation by a final concentration of 60% $(NH_4)_2SO_4$. Precipitated proteins were collected by

centrifugation (45000 x g, 60 min 4°C) and dialyzed overnight against buffer A. Dialyzed protein was centrifuged and the supernatant loaded on Q-Sephaprose HP columns for anion exchange (GE Healthcare), after washing with buffer A supplemented with 50 mM KCl, proteins were eluted with a gradient to buffer A + 400 mM KCl. Fractions containing DnaK were pooled, concentrated and dialyzed against buffer B (20 mM Hepes, 10 mM $MgSO_4$, 10% sucrose, 1 mM EDTA, 2 mM DTT, pH 7.2). Dialyzed protein was loaded on an ATP-agarose column equilibrated with buffer B and washed with the same buffer containing 500 mM KCl. After washing, DnaK was eluted with a gradient of buffer B containing 4 mM ATP. Fractions containing DnaK were pooled and dialyzed into storage buffer containing 20 mM Tris, 10% sucrose, 100 mM NaCl, 40 mM KCl, pH 7.2, and subsequently aliquoted and stored at -80°C.

3.3.3 Purification of DnaJ

Cultivation of the DnaJ overexpressing strain (KL5) for protein purification was conducted as previously described (Buchberger et al., 1994; Linke, 2003). In short, cells were grown to an OD600 ~ 0.7 and protein expression was induced with 1 mM IPTG for 6 hours. Cells were harvested by centrifugation (5000 x g, 30 min, 4°C) and the pellet was resuspended in 50 mM TRIS, 5 mM DTT, 0.6 % (w/v) brij 58 pH 8.0 and subsequently lysed by French press. Cell debris was removed by centrifugation (45000 x g, 45 min 4°C) and the supernatant was 1:2 diluted with buffer A (50 mM NaH_2PO_4, 1 mM EDTA, 0.1% (w/v) brij 58, 2 mM DTT, pH 7.0). Subsequently proteins were precipitated with 60% $(NH_4)_2SO_4$ and collected by centrifugation (45000 x g, 60 min 4°C). The pellet was resuspended in buffer A containing 2 M Urea and dialyzed over night against buffer A. Aggregated proteins were removed by centrifugation (45000 x g, 30 min 4°C) and the supernatant was loaded on a cation exchange column (SP-Sepharose HP, GE Healthcare) equilibrated in buffer A. After a washing with buffer A proteins were eluted with a linear gradient to buffer A containing 1 M KCl. DnaJ containing fractions were pooled and diluted 1:2 into buffer B and subsequently precipitated with 80% $(NH_4)_2SO_4$. Precipitated proteins were collected by centrifugation (45000 x g, 60 min 4°C) and the pellet was resuspended in 50 mM Tris, 2 M urea, 0.1%

(w/v) brij 58, 2 mM DTT, 50 mM KCl, pH 7.5 and dialyzed against the same buffer. After dialysis aggregated proteins were removed by centrifugation (45000 x g, 30 min 4°C) and soluble proteins were loaded on a hydroxyapatite column equilibrated with 50 mM Tris, 2 M urea, 2 mM DTT, 1M KCl, pH 7.5 and washed with the same buffer. Proteins were eluted with a gradient from 0 - 600 mM KH_2PO_4 in the same buffer. Fractions containing DnaJ were pooled and loaded on an anion exchange column (Q-Sepharose HP, GE Healthcare) equilibrated with 50 mM Tris, 2 M urea, 2 mM DTT, 100 mM KCl, pH 9.0. DnaJ was collected in the flow through. DnaJ was subsequently concentrated and dialyzed against the storage buffer (30 mM Hepes, 120 mM KCl, 15 mM NaCl, 4% Glycerol, pH 7.5), aliquoted and stored at – 80°C.

3.3.4 Purification of GrpE

Cultivation and purification of GrpE was carried out as described by (Buchberger et al., 1994). In short, the overexpression strain KL22 was grown at 37°C to an OD600 of 0.6 and expression was induced with 1% (w/v) arabinose for 5 h. Cells were harvested by centrifugation (5000 x g, 30 min, 4°C) and resuspended in 25 ml buffer A (50 mM Tris, 5 mM DTT, pH 8.0), 1:2 supplemented with buffer B (50 mM Tris, 10 % (w/v) sucrose, pH 8.0), and then lysed by French press. Cell debris was removed by centrifugation (45000 x g, 45 min 4°C). Proteins were precipitated with 60% $(NH_4)_2SO_4$ and collected by centrifugation. The pellet was resuspended in buffer C (50 mM Tris, 1 mM EDTA, 10 % (w/v) sucrose, 10 mM ß-mercaptoethanol, pH 7.2) and subsequently dialyzed against the same buffer overnight. Soluble protein was loaded on an anion exchange column (Q-Sepharose HP, GE Healthcare), equilibrated with buffer C, washed with the same buffer and eluted with a gradient from 0-300 mM NaCl in buffer C. GrpE containing fractions were pooled, concentrated, and dialyzed overnight against buffer C. Aggregated proteins were removed by centrifugation and soluble protein was loaded on a blue sepharose column (GE Healthcare) equilibrated with buffer C. GrpE does not bind to the column and is therefore in the flow through. After concentration proteins were dialyzed against buffer D (5 mM KH_2PO_4, pH 6.8), and loaded on a HAP-column (Hydroxyapatite BioGel, BioRad) equilibrated in buffer D. After washing with buffer D GrpE was eluted with a linear gradient to 100 mM

KH_2PO_4, pH 6.8. Fractions containing GrpE are pooled, concentrated and dialyzed against 30 mM Hepes, 10 mM KCl, 5 % glycerol, pH 7.0 aliquoted, and stored at -20°C.

3.3.5 Other proteins used during this thesis

Malate dehydrogenase (Roche) was dialyzed against 40mM KH_2PO_4, pH 7.5, aliquoted and stored at -80°C.

Citrate synthase (Sigma Aldrich) was dialyzed against 50 mM Tris, 2 mM NaEDTA, pH 8, aliquoted and stored at -80°C.

Luciferase (Promega) was aliquoted and stored at -80°C.

$Hsp33_{C\text{-}terminus}$ (aa 218-287) lab stock was stored at -80°C (Purified by D. Reichmann).

Arc repressor was a kind gift from Lewis Kay, University of Toronto, stored at -80°C.

3.4 Protein concentration determination

All protein concentrations were determined spectroscopically using a Jasco spectrophotometer V-550, using the extinction coefficient (ε280) at 280 nm for the respective protein. If concentrations of protein mixtures needed to be calculated the DC Protein Assay Kit II (Bio Rad) was used according to the manufactures manual.

3.5 Preparation of Hsp33 and its variants (reduction and oxidation)

Reduced and oxidized Hsp33 and it's variants were prepared as previously reported (Graumann et al., 2001; Ilbert et al., 2007; Winter et al., 2008). Reduced, zinc reconstituted Hsp33 ($Hsp33_{red}$) was generated by incubation with 5 mM DTT (RPI) and 75% $ZnCl_2$ (of Hsp33 molarity) for 1.5 h at 37°C. Reductant and residual $ZnCl_2$ were removed using a Nap-5 column (GEHealthcare). To prepare oxidized Hsp33, 50µM $Hsp33_{red}$ was incubated with 2 mM H_2O_2 (Fisher) at either 30°C ($Hsp33_{ox\text{-}30°C}$) or 43°C ($Hsp33_{ox\text{-}43°C}$) for 3 h, or $Hsp33_{red}$ was incubated with a 10-fold molar excess of HOCl (Sigma Aldrich) at 30°C for 8 min ($Hsp33_{ox}$). Oxidants were removed with a Nap-5 column.

To investigate the influence of bile salts on Hsp33, the reduced protein was incubated with either 14 mM Na-Cholate (Na-Cho, Sigma Aldrich) or 5 mM Na-Deoxycholate (Na-DOC, Sigma Aldrich). To verify that bile salt are not inducing oxidation on their own, Hsp33 was incubated at 43°C for 3h in the presence of Na-Cho or Na-DOC and the chaperone activity was subsequently determined. To determine if bile salts have unfolding capacities, $Hsp33_{red}$ was incubated with Na-Cho or Na-DOC in the presence of 2 mM H_2O_2 at 30°C for 3 h prior determination of chaperone activity.

3.6. Chaperone activity and protein aggregation measurements

To determine the chaperone activity of wild-type Hsp33 and its variants a protocol modified from Beissinger et al. was followed (Beissinger and Buchner, 1998). Hsp33 client proteins were chemically denatured and subsequently diluted into a buffer system not containing any denaturant to induce protein aggregation. Thermal aggregation measurements were conducted at temperatures, which induce protein unfolding and aggregation. All aggregation measurements were performed on a Hitachi F4500 fluorescence spectrophotometer equipped with a temperature-controlled cuvette holder and stirrer. Light scattering was monitored at λ_{ex}/ λ_{em} of 360 nm, λ_{ex}/ λ_{em} 2.5 nm, PMT 700V.

3.6.1 Hsp33 Chaperone activity measurements

12 µM citrate synthase was denatured with 4.5 M Gdn-HCl in 40 mM HEPES-KOH (pH 7.5) overnight at room temperature. To initiate protein aggregation, denatured CS was diluted to a final concentration of 75 nM in 40 mM HEPES-KOH, pH 7.5 at 30°C under continuous stirring in the absence or presence of a 4-fold molar excess of wild-type Hsp33 or Hsp33 variants.

To assess Hsp33's ability to prevent the aggregation of thermally unfolded malate dehydrogenase or citrate synthase, MDH was diluted to a final concentration of 300 nM in 40 mM KH_2PO_4 pH 7.5 at 45°C or CS was diluted to a final concentration of 150 nM into 40 mM HEPES-KOH, pH 7.5 at 43°C. The unfolding/aggregation took place in the presence or absence of a 4-fold molar excess of Hsp33 under continuous stirring.

3.6.2 Protein unfolding or aggregation by bile salts

Malate dehydrogenase, citrate synthase or luciferase were diluted to a final concentration of 12 µM in buffer (same as aggregation buffer) containing either 14 mM Na-Cho or 5 mM Na-DOC and incubated for 1 h at either 30°C or 37°C. Light scattering was either monitored during the incubation or upon dilution into aggregation buffer. MDH was diluted to 300 nM into 40 mM KH_2PO_4, pH 7.5, citrate synthase was diluted to 500 nM into 40 mM HEPES, pH 7.5 and luciferase was diluted to 75 nM into 40 mM MOPS, 50 mM KCl, pH 7.5 at the respected temperature.

3.6.3 $Hsp33_{C\text{-}terminus}$ and α-casein competition

For competition studies, chaperones were pre-incubated with the competitors for 2 min ($Hsp33_{C\text{-}terminus}$, α-casein), before Gdn-HCl denatured citrate synthase or luciferase was added (Reichmann et al., 2012). In short, $Hsp33_{ox}$ (130 nM) or DnaK/J (130 nM and 65 nM) were pre-incubated with various amounts of α-casein (Sigma Aldrich) or oxidized $Hsp33_{C\text{-}terminus}$ (Lab stock) for 2 min at 30°C in 40 mM MOPS, 50 mM KCl, pH 7.5, before 65 nM Gdn-HCl denatured luciferase was added and aggregation was determined. Similar experiments were conducted with citrate synthase: 150 nM $Hsp33_{ox}$ or 150 nM/75 nM DnaK/J were pre-incubated with α-Casein or $Hsp33_{C\text{-}terminus}$ for 2 min at 30°C in 40 mM HEPES pH 7.5 before 75 nM Gdn-HCl denatured citrate synthase was added to initiate aggregation. Light-scattering measurements were conducted as read-out for the activity of the competitor. 0% competitor activity corresponds to CS aggregation in the presence of fully functional chaperones (*i.e.*, absence of competitor) while 100% relative competitor activity corresponds to CS aggregation in the absence of functional chaperones (*i.e.*, complete competition).

3.6.4 Arc repressor competition - concentration dependency

Citrate synthase (CS) was diluted to a final concentration of 12 µM in 4.5 M Gdn-HCl, 40 mM Hepes pH 7.5 and denatured over night at room temperature. Aggregation assays were carried out in 40 mM Hepes pH 7.5 at 30°C. The final concentration of CS was 75 nM, $Hsp33_{ox}$ 150 nM, or DnaK

187.5 nM and DnaJ 75 nM respectively, with various concentrations of Arc repressor 75 nM-1.5 µM. For competition assays between Arc and CS on Hsp33, Arc was added to Hsp33 and 10 sec later CS was added to the assay. Competition assays between Arc and CS on the DnaK/J system required 30 min pre-incubation of Arc (various concentrations) in 40 mM Hepes pH 7.5 at 30°C. Then the DnaK/J chaperones were added and 10 seconds later aggregation of CS was initiated by dilution into the buffer containing the proteins.

3.6.5 Arc repressor competition - time course

Citrate synthase (CS) was diluted to a final concentration of 12 µM in 4.5 M Gdn-HCl, 40 mM Hepes pH 7.5 and denatured over night at room temperature. Aggregation assays were carried out in 40 mM Hepes pH 7.5 at 30°C. The final concentration of CS was 75 nM, $Hsp33_{ox}$ 150nM, or DnaK 187.5 nM and DnaJ 75 nM respectively, and 750 nM Arc repressor. Arc was pre-incubated for various time points in 40 mM Hepes pH 7.5 at 30°C and then Hsp33 or DnaK/J were added respectively. CS aggregation was initiated 10 sec later by dilution into the buffer containing the protein mixture.

3.7 Tryptophan fluorescence

Trp-fluorescence measurements were conducted in a Hitachi fluorescence spectrophotometer F4500 (λ_{ex} 295 nm, λ_{em} 305 – 400 nm, λ_{ex}/ λ_{em} slits 10/5 nm, Pmt 700V). Changes in Arc's structural conformation were recorded at λ_{ex}/ λ_{em} 295/332 nm, Pmt 900 V.

3.7.1 Trp- fluorescence to monitor changes in Hsp33's structure upon oxidation and client binding interaction

Hsp33 wild type protein and the Hsp33 variant Hsp33-F187W W212F both contain one tryptophan in the linker region. Therefore Trp-fluorescence can be used to monitor conformational changes in this area.

Hsp33 or its variants in their reduced or oxidized form were diluted to a final concentration of 5 µM into 40 mM KH_2PO_4 pH 7.5 at 30°C. Trp-fluorescence spectra were recorded and buffer corrected.

Malate dehydrogenase (MDH) or $Hsp33_{C\text{-}terminus}$ do not contain any tryptophan's and can therefore be used to monitor changes in Hsp33's linker region when interaction occurs. MDH and $Hsp33_{C\text{-}terminus}$ were added in equimolar concentrations to 3 µM oxidized Hsp33 or its variant and temperature was increased to 45°C in 1°C/min steps and held at 45°C for 10 min.

3.7.2 Arc unfolding

Arc unfolding was monitored by Trp-fluorescence; the one Trp of the protein is located in the dimer interface and therefore gets exposed upon protein monomerization and unfolding. To measure structural changes induced by dilution and reduction of salt in the buffer, Arc was diluted to a final concentration of 750 nM into 40 mM Hepes pH 7.5 at 30°C.Trp-fluorescence was monitored continuously for 30 min.

3.8 Far-UV circular dichroism (CD) spectroscopy

Far-UV CD spectroscopy is used to determine changes in the secondary structure of proteins, due to the differential absorption of left and right circularly polarized light.

For Hsp33 far-UV CD spectra were recorded in 20 mM KH_2PO_4, pH 7.5 at 20°C using a Jasco-J810 spectropolarimeter as previously described (Graf, 2004). In short, Hsp33 and its variants were diluted to a final concentration of 0.2 mg/ml into 20 mM KH_2PO_4, pH 7.5 and far-UV CD spectra were cumulative recorded between 260-180 nm, buffer corrected and molar ellipticity was calculated according:

$$\text{molar ellipticity} = \frac{\theta x\ M}{c\ x\ l\ x\ 10}$$

with θ = mdeg, M = relative molecular mass, c = concentration in mg/l, and l = path length in cm and is expressed in $deg \cdot cm^2 \cdot dmole^{-1}$.

To determine the thermostability of Hsp33 and its variants, the CD signal at either 195 nm or 222 nm was continuously recorded at temperatures from 20ºC to 50°C or 20°C to 80°C, respectively. The temperature was increased at

a rate of 1ºC per minute. The temperature was controlled with a Jasco Peltier device.

To monitor changes in the secondary structure of malate dehydrogenase, citrate synthase, and luciferase due to the exposure to bile salts, proteins were diluted to 0.2 mg/ml into 20 mM KH_2PO_4, pH 7.5 in the presence or absence of 14 mM Na-Cho or 5 mM Na-DOC, and were subsequently incubated at 30°C or 37°C for 1 h. CD spectra to determine the secondary structure were subsequently acquired in the presence of the bile salt at the respected temperature. The temperature was controlled with a Jasco Peltier device. Spectra were buffer corrected and subsequently analyzed.

3.9 ANS fluorescence measurements

The fluorescence probe 3,3'-Dianilino-1,1'-binaphthyl-5,5'-disulfonic acid (bis-ANS, Molecular Probes) was used to test for the presence of hydrophobic surfaces in wild-type Hsp33 and the variants as previously described (Graf, 2004). In short, Hsp33 and bis-ANS were mixed 1:3.3 (3 µM:10 µM) in 40 mM HEPES pH 7.5 at 30°C. Emission spectra were recorded in a Hitachi fluorescence spectrophotometer F4500, λ_{ex} 370 nm, λ_{em} 400-600 nm λ_{ex}/ λ_{em} slits 2.5/5 nm, Pmt 700 V. All spectra were buffer corrected.

3.10 Zinc Determination

To determine the amount of zinc bound to reduced and oxidized wild type Hsp33 and the mutant variants, an assay was used, which is based on the formation of a bright red complex between free zinc and the dye 4-(2-pyridylazo) resorcinol (PAR, Sigma Aldrich) (ε_{500} of $PAR_2(Zn)$ = 66,000 $M^{-1}cm^{-1}$). The affinity K_a of PAR to zinc is 2 x 10^{12} M^{-1} at pH 7 (Hunt et al., 1977). To assess the amount of free or loosely bound zinc in $Hsp33_{red}$, $Hsp33_{ox\text{-}30°C}$ or $Hsp33_{ox\text{-}43°C}$ of the wild type protein and its variants 5 µM of Hsp33 was incubated with 100 µM PAR in 40 mM metal free KH_2PO_4 pH 7.5. To induce zinc release from the high affinity cysteine clusters in Hsp33, 30 µM of the mercury derivative PCMB (para-chloromercurybenzoic acid, ICN Biomedicals) were added. PCMB forms stable mercaptide bonds with Hsp33's cysteines,

leading to the release of zinc into the PAR-containing solution and the formation of PAR_2(Zn) complexes, which is monitored at 500 nm.

3.11 Malate dehydrogenase activity during bile salt exposure

The activity of malate dehydrogenase was measured during incubation with 14 mM Na-Cho or 5 mM Na-DOC. 12 µM malate dehydrogenase was incubated at 37°C in the presence or absence of the respective bile salt. Samples were withdrawn during the time course of incubation and enzymatic activity was determined. For this malate dehydrogenase was diluted to a final concentration of 125 nM in 40 mM KH_2PO_4, pH 7.5 containing 1 mM oxaloacetate (Sigma Aldrich) and 150 µM NADH (Sigma Aldrich) at 30°C. Absorbance at 340 nm was measured over a timeframe of 2 min. Malate dehydrogenase reduces oxaloacetate to malate, oxidizing one NADH per enzymatic reaction.

3.12 Luciferase activity

Luciferase converts luciferin to luciferyl adenylate, this is further converted to oxyluciferin and light, which is then detectable (chemo-luminescence). To determine luciferase activity, luciferase was diluted to a final concentration of 5 nM into assay buffer (100 mM KH_2PO_4, 25 mM glycylglycine, 2 mM NaEDTA, pH 7.5). The assay buffer was supplemented with: 70 µM luciferin, 0.5 mg/ml BSA and 2 mM MgATP. Luminescence was measured in a BMG FLUOstar Omega microplate reader (gain 3800).

3.12.1 Luciferase activity during bile salt exposure

Luciferase activity was determined to evaluate the capacity of 14 mM Na-Cho or 5 mM Na-DOC to denature the enzyme.12 µM luciferase was incubated in 40 mM MOPS, 50 mM KCl, pH 7.8 with or without the bile salt at 30°C. During the course of the experiment samples were withdrawn and activity was measured.

3.12.2 Luciferase transfer from Hsp33 to the DnaK/J/E system and subsequent refolding

12 µM luciferase was denatured in 4.5 M Gdn-HCl in 40 mM MOPS, 50

mM KCl, pH 7.8 for 90 min at RT. Unfolded luciferase was diluted into refolding buffer (40 mM MOPS, 50 mM KCl, pH 7.8, supplemented with 2mM MgATP and 0.1 mg/ml BSA) in the presence or absence of chaperones. To determine the refolding capacity of the DnaK/J/E system luciferase was diluted to a final concentration of 75 nM into refolding buffer containing 750 nM DnaK, 150 nM DnaJ, and 750 nM GrpE, in the presence or absence of DTT. To study the substrate transfer from Hsp33 to the DnaK/J/E system, luciferase was diluted into buffer containing 300 nM $Hsp33_{ox,}$ or its derivate Hsp33-Y12E in the reduced or oxidized form. Complex formation was allowed for 5 min before substrate transfer and refolding was initiated by addition of the DnaK/J/E system (750 nM, 150 nM, and 750 nM respectively). To determine the activity of luciferase samples were withdrawn and activity was measured as described above.

3.13 Protein SDS-Page gels and western blot

For separation of proteins on SDS-PAGE gels (14% Tris-Glycine (Invitrogen) or 12 % TGX-gel (BioRad)), samples were diluted to their final concentration in Laemmli buffer (final concentration: 60 mM Tris, 12.5% glycerol, 2% SDS, 0.01% bromphenol blue, +/- 125 mM β-mercaptoethanol). Samples were then boiled for 5 min if not otherwise noted, loaded on SDS-PAGE gels and electrophoresed following manufacturer's specifications in SDS running buffer (25 mM Tris, 192 mM glycine, 0.1% SDS).

Protein were either visualized on the gel by Coomassie blue staining (Wong et al., 2000) or transferred on PVDF membrane (polyvinylidene difluoride membrane, Immobilon-P, Millipore) by a semi-dry electrophoretic transfer (western blot) technique. Proteins were subsequently detected with specific antibodies: Rabbit anti-Hsp33 (Jakob lab, Alpha diagnostic Intl.)
Mouse anti-DnaK (StressGen)
Rabbit anti-DNP (Sigma Aldrich)
Goat anti-mouse (peroxidase labeled) (Sigma Aldrich)
Goat anti-rabbit (peroxidase labeled) (ThermoScientific)

In short: membranes were incubated in 5% (w/v) milk (non-fat milk powder) TBS-T (25 mM Tris, 0.05% (v/v) Tween, 137 mM NaCl, 3 mM KCl, pH

7.4) solution for 30 min at RT, or ON at 4°C to minimize unspecific antibody binding. The primary antibody was applied for 1 h at RT, unbound antibody was removed by 3 washing steps with TBS-T for 10 min before the secondary antibody was applied for 1 h at RT. Subsequent washing 3x with TBS-T removed unbound antibody before signal detection was achieved with the SuperSignal West Pico Chemiluminescent substrate (ThermoScientific) kit according to the manufacturers specifications.

3.14 2D Gel Electrophoresis, Staining of the Gels, and Image Analysis

2D gel electrophoresis and analysis were performed as described by Hiniker 2004 (Hiniker and Bardwell, 2004). In short, samples were prepared according to the protocol: 'Purification of aggregated proteins' (3.20) and the pellet was resolved in dimension sample buffer (550 µl; containing 7 M urea, 2 M thiourea, 1% (w/v) Serdolit MB-1, 1% (w/v) dithiothreitol, 4% (w/v) Chaps, and 0.5% (v/v) Pharmalyte 3-10) and spun down afterwards to remove insoluble particles. 450 µl was applied to a 24-cm IPG strip (Amersham Biosciences) containing an immobilized pH gradient (pH 3-10, nonlinear). The rehydration and first dimension separation were carried out on an Ettan IPGphor II system (Amersham Biosciences). After equilibration for the second dimension using a standard protocol from Amersham Biosciences, strips were transferred to SDS-polyacrylamide (13%) gels and electrophoresed in an Ettan DALT II system (Amersham Biosciences) in SDS running buffer. Gels were stained Coomassie blue (10% $(NH_4)_2SO_4$, 0.1% Coomassie G250, 2% phosphoric acid, 20% methanol) and destained with 5% acetic acid. Gels were scanned for analysis using an Epson scanner and subsequently analyzed using the program Delta 2D (Decodon).

3.15 TCA precipitation

To TCA precipitate proteins, the final TCA concentration in the sample should be 10%. Ice cold TCA was added to the sample, vortexed, and incubated for 30 min on ice. Precipitated proteins were spun down at 16000 x g, 4°C, 30 min. The supernatant was removed and the pellet was carefully wahsed with 200 µl 5% ice cold TCA. After removing the TCA, the pellet was shortly spun and the last TCA was removed. To ensure no residual TCA was

present, the pellet was washed with 200 µl ice cold acetone. After removal the sample was kept at RT to allow residual acetone to evaporate.

3.16 Direct AMS Trapping- *in vitro* samples

AMS (4-acetamido-4"-maleimidylstilbene-2'-disulfonate) is a reagent that covalently reacts with free thiol groups, adding a 490 Da group. This leads to a major mobility shift of the modified protein in SDS-PAGE gel (Jakob, 2000). An equal volume of 20% TCA was added to the protein sample to TCA precipitate the protein. The pellet was resuspended in 20 µl DAB (200 mM Tris, 6M urea, 50 mM EDTA, 0.5% SDS, pH 7.5) with 15 mM AMS, and incubated 1 h, 25°C, shaking (1300 rpm), in the dark. Non-reducing Laemmli buffer was added and the protein was electrophoresed in an SDS-PAGE gel, and subsequently stained and visualized.

3.17 Indirect AMS trapping – *in vivo* samples

To visualize the oxidation status of proteins *in vivo* a protocol adapted from Leichert and Jakob (Leichert and Jakob, 2004). 1.5 ml of cell suspension was harvested and subsequently proteins were TCA precipitated. The originated pellet was resuspended in 50 µl DAB containing 100 mM iodoacetamide (IAM) and incubated 1 h, 25°C, shaking (1300 rpm) to label all reduced cysteines. Samples were subsequently TCA precipitated. The pellet was resuspended in 20 µl 10 mM DTT in DAB (1 h, 25°C, shaking) to reduce all non-labeled, oxidized proteins. To remove the reducing agent proteins were once again TCA precipitated and the pellet was dissolved in 30 µl 10 mM AMS in DAB to label all previous oxidized cysteines with the 490 Da thiol reacting agent, incubated 1 h, 25°C, shaking.

Non-reducing Laemmli buffer was added to normalize the samples according to their OD_{600}

$$Vol[\text{Sample}] = \frac{OD_{600}[\text{Control}]}{OD_{600}[\text{Sample}]} \cdot Vol[\text{Control}]$$

10 µl samples were loaded on a SDS-PAGE gel and electrophoresed. Proteins were transferred onto a PVDF membrane and proteins were subsequently detected with specific antibodies.

3.18 Determination of growth rates of constitutively active mutants of Hsp33

Overnight cultures of strains expressing either wild type Hsp33 (UJ83), the two Hsp33 variants (CC4, JHa21) or no protein (CC20) from a pET11a vector in MOPS minimal media (10 x MOPS modified buffer (TEKnovo), 0.2% (w/v) glucose, 132 mM K_2HPO_4 pH 7, 20 µM thiamine) were prepared. Cell cultures were diluted 1:100 into MOPS minimal media, supplemented with no IPTG or 50 µM IPTG and cultivated at 37°C or 43°C respectively. Growth was monitored every hour with absorbance measurements at OD_{600}. After 6 h samples were withdrawn to purify aggregated proteins (3.20).

3.19 Growth experiments with bile salts

Bile salts are known to have an antimicrobial effect, due to several stresses induced in bacteria. To determine the effect bile salts have on *E. coli* several experiments were conducted to discover the effect bile salts have on bacteria.

3.19.1 Growth curves to determine the growth defect by bile salts

For growth curve experiments, overnight cultures of either wild type MC4100 or the Hsp33 deletion strain (MC4100 *hslO*-) were prepared in LB-medium (1% (w/v) tryptone, 0.5% (w/v) NaCl, 0.5% (w/v) yeast extract (Fisher Scientific)) if not otherwise stated. Cell cultures were diluted to a final OD_{600} of 0.05 and cells were cultivated at 37°C with shaking. Growth was monitored at OD_{600} and treatment with 14 mM Na-Cho or 5 mM Na-DOC was initiated in mid-log phase at an OD_{600} ~ 0.5. Growth was subsequently monitored for several hours to evaluate the recovery of the treatment.

Experiments resulting from the growth defect observations were: Purification of aggregated proteins (3.20), as well as SILAC labeling and LC-MS/MS analysis of protein aggregates (3.23), evaluations of GSH/GSSG ratios with subsequent calculations of the redox potential (3.22), and measurement of carbonylated proteins (3.21). Cells for the purification of protein aggregates, as well as to quantify protein carbonylation were grown as stated above. For the evaluation of the GSH/GSSG ratios cells were treated

with 21 mM Na-Cho and 7.5 mM Na-DOC. The SILAC labeling of proteins requires growth in MOPS minimal media, substituted with light and heavy labeled amino acids. This resulted in a slower growth of *E. coli*, requiring higher amounts of bile salts to induce a growth phenotype. This required 42 mM Na-Cho and 7.5 mM Na-DOC treatment to achieve a growth defect.

3.19.2 Spot titer experiments on LB-agar plates containing bile salts

LB-agar plates (4% (w/v) LB-agar mix (Miller)), containing various concentrations of Na-Cho or Na-DOC, were prepared fresh before use. To prepare these plates, LB-agar was autoclaved and the bile salt were added and dissolved in hot LB-agar before pouring of the plates.

For spot titer experiments, overnight cultures of either wild type *E. coli* strains (MC4100 and MC4100 *hslO-,* as well as DHB4 and its deletions) and their corresponding deletion mutants were grown in LB-medium at 30°C or 37°C. Cell cultures were diluted to a final OD_{600} of 0.05 and cells were cultivated at 30°C or 37°C, shaking. When cells reached mid-log phase the OD was normalized to OD_{600} of 0.3 and the cell suspension was 1:10 serial diluted in LB-medium before 4 µl of each cell suspension was spotted on LB-agar plates in the presence or absence of bile salts.

E. coli MC4100 strains were grown at 37°C before and after spot tittering for 18 h, whereas *E. coli* DHB4 and its deletion strains were always grown at 30°C for at least 24 h (spot titters).

3.20 Purification of aggregated proteins

A protocol to compare soluble and insoluble proteins in *E. coli* was followed (Cremers et al., 2010). 5 ml of the bacterial culture was removed from the assay and cells were harvested by centrifugation (5,000 × g, 4°C, 10 min). Cells were resuspended in 650 µl sucrose buffer (50 mM Tris-HCl pH 8.0, 25% w/v sucrose, 1 mM NaEDTA, 10 mM DTT) and homogenized by sonication (Kontes, Micro Ultrasonic cell disrupter, 2 × 10-15 sec with the output control set to 70). 5 µl lysozyme (50 mg/ml), 12.5 µl DNAse I (2 mg/ml) and 2.5 µl $MgCl_2$ (0.5 M) were added, followed by the addition of 650 µl lysis buffer (50 mM Tris-HCl pH 8.0, 1% Triton X 100, 100 mM NaCl, 0.1% (w/v)

Na-Azide, 0.1% (w/v) Na-deoxycholate, 10 mM DTT). Samples were incubated at RT for 15 min, frozen at −80°C for 20 min and thawed at 37°C for 15 min. Then 2.5 µl $MgCl_2$ (0.5 M) was added and the solution was incubated at room temperature until the viscosity decreased. 12.5 µl of 0.5 M NaEDTA was added and the lysate was centrifuged (11,000 × g, 4°C, 20 min). The supernatant was removed and the pellet was resuspended in 500 µl washing buffer A (50 mM Tris-HCl pH 8.0, 0.5% Triton X-100, 100 mM NaCl, 1 mM NaEDTA, 1 mM DTT). The solution was again homogenized by sonication as before. Protein aggregates were pelleted by centrifugation (11,000 × g, 4°C, 20 min). The supernatant was discarded and the pellet was resuspended in 500 µl washing buffer B (50 mM Tris-HCl pH 8.0, 100 mM NaCl, 1 mM NaEDTA, 1 mM DTT), and again homogenized by sonication. The washing steps were repeated 3 times. The final pellet was resuspended in 2 × reducing Laemmli buffer and boiled for 5 min. Aggregate formation was visualized by SDS-PAGE followed by Coomassie blue staining of the gels.

3.21 Protein carbonylation

Protein carbonyls can specifically react with 2,4 dinitrophenylhydrazine (DNPH) to generate protein-conjugated hydrazones (protein-DNP). The use of DNPH thus provides an index for the quantification of protein carbonyl content in protein mixtures, which can be separated by SDS-Page and are subsequently detectable with immune blotting (Yan, 2009).

1 ml cell suspension was taken before treatment with 14 mM Na-Cho and 5 mM Na-DOC, as negative control for protein carbonylation heat shock treatment was used, HOCl treatment (4 mM) was applied as positive control. During the course of the treatment 1 ml samples were withdrawn and cells were pelleted by centrifugation (16000 x g, 2 min, 4°C), cell pellets were frozen in liquid N_2 for subsequent processing.

Cell pellets were resuspended in 20 µl 40 mM MOPS, 50 mM KCl, pH 7.5 and proteins were harvested by TCA precipitation. 450 µl of 2 M HCl with 10 mM DNPH were added and proteins were incubated 1.5 h, 15°C shaking (1300 rpm) for derivatization, afterwards proteins were TCA precipitated. The pellet was washed 3 x with 500 µl of a ethyl-acetate and ethanol mix (1:1, v/v),

which needed to be vortexed and incubate 5 min at RT before subsequent centrifugation (10 min, 16000 x g, 4°C). After washing the pellet was dissolved in DAB buffer, and the protein concentration was determined. After normalization proteins were loaded on a SDS-Page and subsequently transferred on PVDF membrane for immunoblot detection with a specific antibody against DNP.

3.22 Determination of the GSH/GSSG redox-potential

Thiols are inherently oxygen sensitive and must be alkylated either before or after treatment with a reductant to determine the reduced versus total concentrations of the respective thiols. To this end, an HPLC method in which thiol containing metabolites are first alkylated with monoiodoacetic acid and then amino-labeled with 2,4-dinitrofluorobenzene allows for their photometric detection and quantitation This is used to alkalyed GSH and GSSG to determine the cellular redox potential (Reed et al., 1980).

5 ml cell suspension was harvested before and after treatment of MC4100 with 21 mM Na-Cho and 7.5 mM Na-DOC for 30 and 60 min at 37°C. The cell pellet was resuspended in 75 µl PBS (Gibco) and mixed with an equal volume of metaphosphoric acid solution (16.8 mg/ml HPO_3, 2 mg/ml EDTA and 9 mg/ml NaCl), and vortexed. The metaphosphoric acid-fixed cells were harversted by centrifugation at 13,000 x g for 10 min, 4ºC to precipitate proteins. The supernatant was transferred, thiols were alkylated with monoiodoacetic acid at a final concentration of 7 mM. The samples were vortexed and the pH was adjusted to 7-8 with saturated K_2CO_3. Then they were incubated 1 h, RT, in the dark. Finally, an equal volume of 2,4-dinitrofluorobenzene (DNFB) solution (1.5% (v/v) in absolute ethanol) was added to the mixture, vortexed and incubated for at least 4 h or overnight at RT, in the dark.

Separation of GSH GSSG derivates was performed by Victor Vitvitsky. In short: The N-dinitrophenyl derivatives of GSH and GSSG were separated by HPLC on a Waters µ Bondapak NH_2 column (300 mm x 3.9 mm, 10 µm) at a flow rate of 1 ml/min. The mobile phase consists of solvent A (4:1 methanol/water) and solvent B (154 g ammonium acetate in 122 ml of water

and 378 ml of glacial acetic acid, and adding 500 ml of the resulting solution to 1 l of solvent A). The following elution conditions were used: 0-10 min isocratic 25% solvent B, 10-30 min linear gradient 25-100% solvent B, 30-34 min 100% solvent B, 34-36 min 100-25% solvent B, 36-45 min 25% solvent B. Elution of metabolites is monitored by their absorbance at 355 nm. The concentration of individual thiols was determined by comparing the integrated peak areas with independently generated calibration curves for each compound.

3.23 SILAC and subsequent LC-MS/MS analysis

Stable isotope labeling by amino acids in cell culture (SILAC) is a straightforward approach for i*n vivo* incorporation of a labels into proteins for mass spectrometry (MS)-based quantitative proteomics, a 'light' or 'heavy' form of the amino acid (arginine) was chosen for this experiments.

MC4100 hslO^{-} was grown in MOPS minimal media supplemented with amino acids. Arginine was added either as the heavy form $^{13}C_6$ L- arginine or the light form $^{12}C_6$ L- arginine. Cells growing in $^{13}C_6$ L- arginine supplemented media were treated with 42 mM Na-Cho whereas cells growing in MOPS minimal media supplemented with $^{12}C_6$ L- arginine were treated with 7.5 mM Na-DOC when reaching mid-log phase. 30 min after the treatment a sample was withdrawn and ‘Purification of aggregated proteins’ (3.20) was conducted, final protein pellets were dissolved in DAB buffer (3.17). A small sample of aggregated proteins was run on a SDS-Page. The rest of the pelleted proteins were send to MS-Bioworks for further LC-MS/MS analysis. Equal volumes of the protein sample were loaded on a SDS-Page and electrophoresed, proteins were cut into segments and trypsin digested. Each digest was then analyzed by nano LC-MS/MS.

4 Results and Discussion

4.1 Changing Hsp33's posttranslational activation process by destabilization of the linker region

4.1.1 Site-specific mutations to alter Hsp33's linker binding interface

Hsp33 in its reduced form is a tightly folded protein. The linker region appears to be stably folded on top of a large hydrophobic four-stranded β-sheet, which has been postulated to serve as a client binding site upon linker unfolding and activation of Hsp33 (Fig. 4.1.1, A) (Graf and Jakob, 2002; Raman et al., 2001; Vijayalakshmi et al., 2001). Analysis of Hsp33's X-ray structure revealed a cluster of highly conserved hydrophobic amino acids, whose side chains face towards the linker region under reducing conditions and might therefore stabilize the folded linker conformation. Another potential function of this hydrophobic region could be its interaction with unfolded client proteins once the linker region is unfolded. To investigate the purpose of this platform, two conserved residues that map onto the hydrophobic platform, Tyr12 on β-strand 1 and Met172 on β-strand 9 (Fig. 4.1.1, B) were chosen for mutation. We predicted that alteration of these residues would affect the surface features of the four-stranded β-sheet without interfering with the stability or fold of Hsp33's N-terminal domain. To efficiently disrupt potential hydrophobic interactions, Tyr12 was replaced with glutamate (Hsp33-Y12E) while Met172 was substituted with the polar residue serine (Hsp33-M172S).

The majority of this chapter has been published in: Cremers CM, Reichmann D, Hausmann J, Ilbert M, Jakob U. **Unfolding of metastable linker region is at the core of Hsp33 activation as a redox-regulated chaperone.** : J Biol Chem. 2010 Apr 9;285(15):11243-51. Epub 2010 Feb 5. I performed all experiments presented here besides the ultracentrifugation experiments, which were obtained with the help of T. Franzmann. J. Hausmann did some of the cloning and M. Ilbert introduced me into the field of chaperone work. The manuscript was written by me and U. Jakob.

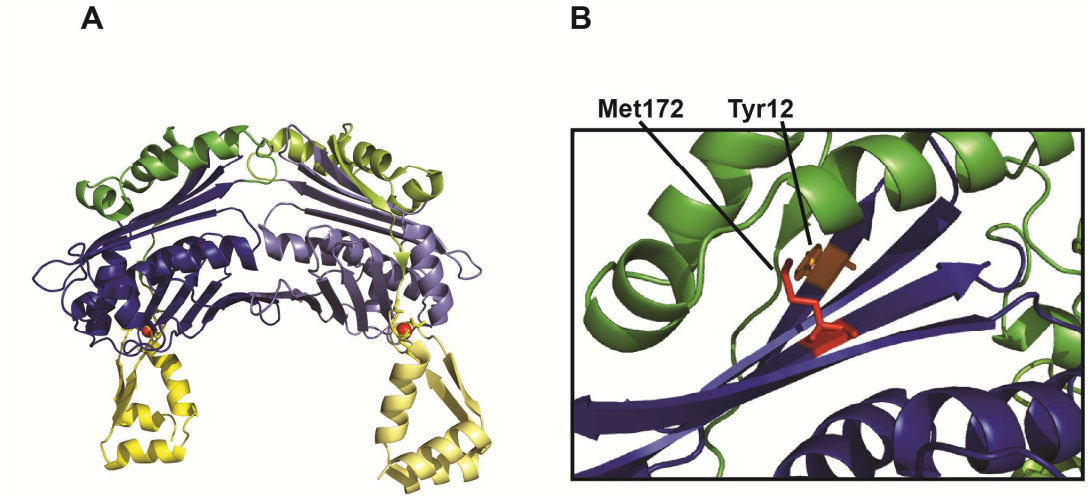

Fig. 4.1.1: Location of Hsp33's single site mutations

A. Domain structure of full-length reduced Hsp33 from *Bacillus subtilis* Hsp33 (PDB code:1VZY) (Janda et al., 2004). Hsp33 is a two-domain protein with an N-terminal domain (blue) and a C-terminal domain, composed of a highly flexible linker region (green) and a zinc binding domain (yellow) that harbors the four absolutely conserved cysteines, which coordinate one zinc ion (red sphere). Although reduced, inactive Hsp33 is monomeric in solution, it forms dimers in the crystal structure.

B. To alter the hydrophobic character of the linker-binding interface, either Tyr12 in β-sheet 1 was replaced with glutamate (Hsp33-Y12E) or Met172 in β-sheet 9 was substituted with serine (Hsp33-M172S). To illustrate the location of the targeted residues in *E. coli* Hsp33, the X-ray structure of the truncated *E. coli* $Hsp33_{1\text{-}255}$ (PDB code: 1 HW7) was used.

Both mutant proteins were overexpressed in BL21 strains lacking the endogenous Hsp33 gene (*hslO*) and solubility was determined. Hsp33-M172S behaved very similarly to Hsp33-WT. It was fully soluble upon IPTG-induced overexpression at 37°C. In contrast, the Hsp33-Y12E variant was largely insoluble under these conditions. This result indicated that the Hsp33-Y12E variant is either not folded properly and is therefore insoluble, or is constitutively exposing hydrophobic interaction site(s) that cause protein aggregation. To generate significant amounts of soluble Hsp33-Y12E protein, we changed the expression protocol and induced protein expression for 24-hours with IPTG at 18°C. This approach was sufficient to generate reasonable amounts of soluble mutant protein. We purified the two variants according to the wild-type Hsp33 protocol and prepared fully reduced, zinc-reconstituted proteins ($Hsp33\text{-}Y12E_{red}$, $Hsp33\text{-}M172S_{red}$) for subsequent functional studies (see experimental procedures).

4.1.2 Mutations in Hsp33's N-terminal domain dramatically alter Hsp33's functional regulation

Hsp33's activation by fast-acting oxidants such as HOCl occurs within the mixing time of the experiment, making evaluation of activation kinetics and determination of oxidation intermediates technically challenging (Winter et al., 2008). In contrast, H_2O_2 -mediated activation of Hsp33-WT is significantly slower ($T_{1/2}$ of ~20 min) and depends on the additional presence of unfolding conditions (*i.e.*, 43°C) (Fig. 4.1.2 B, open circles). In the absence of unfolding conditions (H_2O_2, 30°C), an oxidation intermediate of Hsp33 accumulates, which appears to lack the second disulfide bond (Leichert et al., 2008b) and is inactive as a chaperone holdase (Fig. 4.1.2 A, open circle). To determine how the introduced mutations affect the redox-regulation and chaperone function of our Hsp33 variants, we monitored their activity upon incubation in 2 mM H_2O_2 at either 30°C or 43°C.

As shown in Fig. 4.1.2 A, both variants displayed chaperone activities that were very similar to the activity of wild-type Hsp33 when incubated with H_2O_2 at 43°C for 2 hours. All three oxidized variants suppressed the aggregation of chemically denatured citrate synthase to the same extent. Similar results were observed when the activity of the proteins was tested using thermally unfolding malate dehydrogenase as an *in vitro* chaperone substrate. These results clearly indicated that the introduced mutations did not substantially affect the client binding affinity of Hsp33.

Next, we investigated both mutant variants in regards to their mechanism of activation. As described before, Hsp33-WT requires the simultaneous presence of both oxidizing and unfolding conditions for its activation. We found that the activation of Hsp33-M172S was significantly faster at 43°C and lacked the lag phase characteristic for wild-type Hsp33 (Fig. 4.1.2 B, Hsp33-M172S, closed squares and Hsp33-WT, open circles). The lag phase of Hsp33-WT has been shown to correlate to the formation of the critical second disulfide bond in Hsp33 and is thought to represent the rate-limiting step in its activation process (Leichert et al., 2008b).

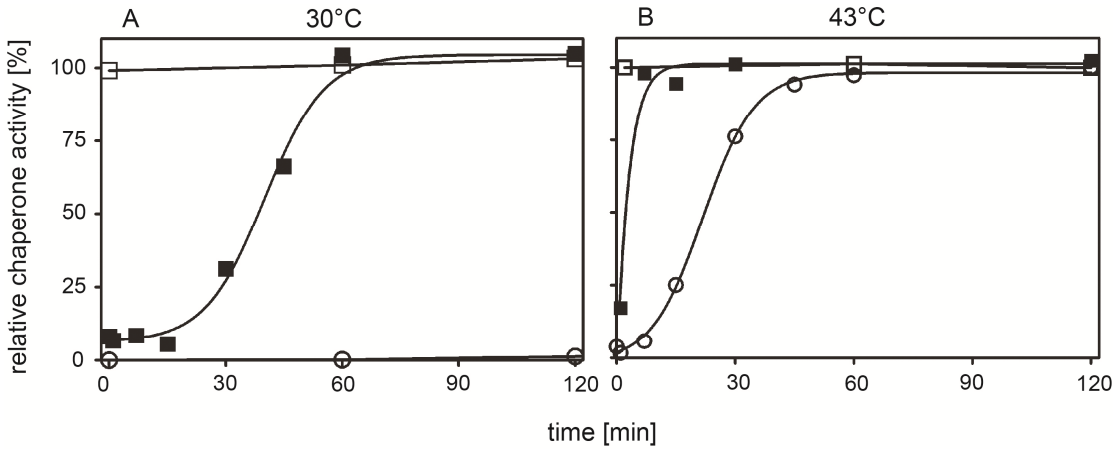

Fig. 4.1.2: Activation kinetics of wild-type Hsp33 and its mutant proteins
Reduced wild-type Hsp33 (open circles), Hsp33-M172S (closed squares), or Hsp33-Y12E (open squares) were incubated in 2 mM H_2O_2 at either 30°C (A) or at 43°C (B). At the time points indicated, aliquots of Hsp33 (final concentration 300 nM) were tested for their ability to suppress the aggregation of chemically denatured citrate synthase (final concentration 75 nM) at 30°C.

Moreover, activation of Hsp33-M172S no longer required the simultaneous presence of oxidizing and unfolding conditions. Incubation of Hsp33-M172S in 2 mM H_2O_2 at 30°C was fully sufficient for its activation (Fig. 4.1.2, A, closed squares) whereas Hsp33-WT (Fig. 4.1.2, A, open circles) remained inactive under these conditions. Likewise, simple incubation of reduced, zinc-reconstituted Hsp33-M172S at elevated temperatures (43°C) caused activation of its chaperone function (Fig. 4.1.3). Again, this is not the case for Hsp33-WT, which requires temperatures above 60°C for its oxidant-independent activation. These results suggested that the stability of Hsp33's linker region is affected by interrupting the hydrophobic interactions between the linker region and the N-terminal domain. As expected, in contrast to the oxidative activation of Hsp33, which is irreversible unless reducing agents are added, thermal activation of Hsp33-M172S is fully reversible and requires the activity tests to be performed at 43°C (Fig. 4.1.3).

While Hsp33-M172S maintained at least some requirement for posttranslational regulation, the freshly reduced and zinc-reconstituted Hsp33-Y12E mutant appeared to be fully active even without incubation in H_2O_2 or exposure to elevated temperatures (Fig. 4.1.2, A, B). Additional exposure to H_2O_2 at either 30°C or 43°C did not further increase its chaperone activity, suggesting that Hsp33-Y12E is constitutively active (Fig. 4.1.2, B, open

squares). These results indicated that altering a single residue in Hsp33's N-terminal domain is sufficient to completely abolish Hsp33's otherwise very tight regulation.

4.1.3 Zinc binding status of Hsp33's mutant variants

To exclude the possibility that high oxidation sensitivity of the active site cysteines in the two Hsp33 variants led to their uncontrolled oxidation and subsequent activation during the chaperone assays, we performed thiol trapping experiments on the reduced proteins immediately after the activity assays to assess their cysteine oxidation status (Fig. 4.1.3). We made use of the 490 Da thiol alkylating reagent 4-acetamido-4-maleimidyl-stilbene-2'-disulfonate (AMS), which irreversibly reacts with reduced cysteines and causes a distinct mass increase corresponding to the number of reduced cysteines that is easily discernible on SDS-PAGE. We found that the cysteines in both mutant proteins remain reduced during incubation and performance of chaperone assays at 43°C.

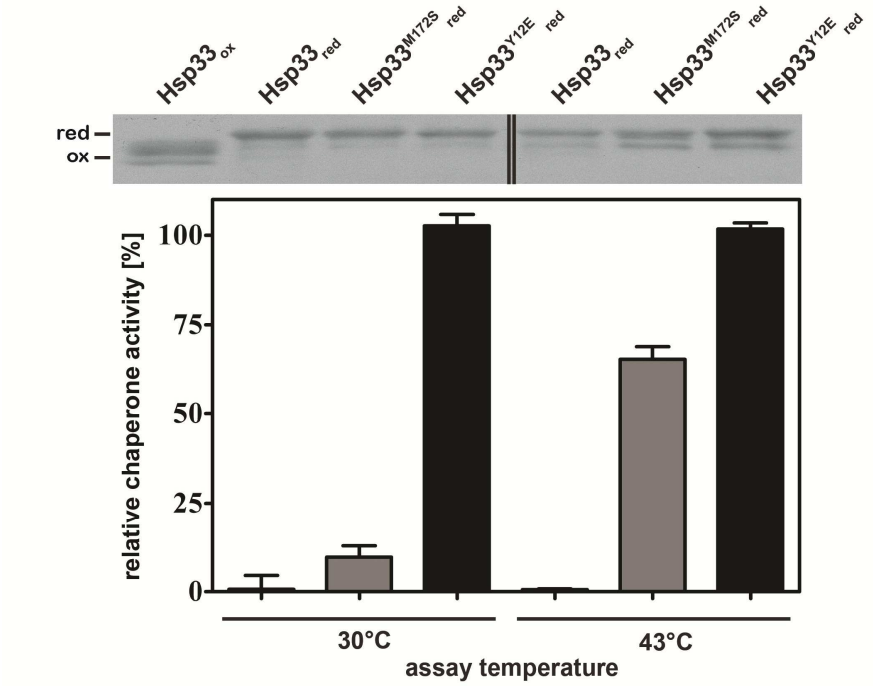

Fig.4.1.3: *In vitro* chaperone activity of Hsp33 and variants
The influence of a 4-fold molar excess of the reduced Hsp33 variants on the aggregation of chemically unfolded unfolded citrate synthase (75 nM) at 30°C or thermally unfolded citrate synthase (150 nM) at 43°C was determined. 0% activity is defined as the light scattering signal 4 min after addition of unfolded citrate synthase in the absence of Hsp33, and 100% activity corresponds to the light scattering signal

of unfolded citrate synthase in the presence of wild-type Hsp33 that had been activated for 180 min in 2 mM H_2O_2 at 43°C ($Hsp33_{ox}$). To detect any potential changes in the thiol oxidation status of wild-type Hsp33 and the variants during the activity assay, aliquots were taken immediately after the end of the activity measurement (*i.e.,* 4 min) and labeled with AMS. The change in mass can be visualized using non-reducing SDS-PAGE (top of panel). The double line (||) in the top panel indicates the position at which a second $Hsp33_{ox}$ control was removed from the image.

This result is consistent with zinc binding studies, which revealed that both mutant proteins remain fully zinc-reconstituted even in the presence of a 20-fold excess of the zinc chelator PAR ($K_\alpha = 2 \times 10^{12}\ M^{-1}$ at pH 7) (Hunt et al., 1977) (Fig. 4.1.4). This indicates that Hsp33's zinc binding is not affected by these mutations.

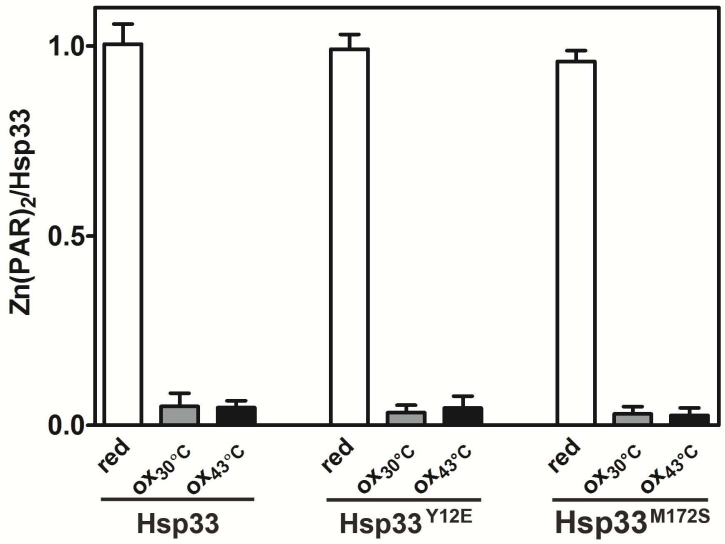

Fig. 4.1.4: Zinc coordination of wild type Hsp33 and mutant variants

5 µM freshly reduced or oxidized Hsp33-WT and mutants were incubated with 100 µM PAR. No significant zinc release was observed from reduced wild type $Hsp33_{red}$ in the presence of a 20-fold excess of PAR ($K_\alpha = 2 \times 10^{12}\ M^{-1}$ at pH 7) (Hunt et al., 1977) confirming that zinc is tightly associated with all three reduced Hsp33 variants. Only upon addition of 30 µM of the mercury derivative PCMB, release of zinc from the cysteine-coordinated zinc site was detected. The absorbance of $Zn(PAR)_2$ was monitored at 500 nm to calculate the ratio of $Zn(PAR)_2$ complexes to Hsp33. As shown in the figure, zinc binding was detected only for the reduced Hsp33 preparations. These results confirm that oxidation causes loss of zinc binding in all three Hsp33 variants.

4.1.4 Structural changes in Hsp33's linker region

Wild type Hsp33 contains one tryptophan residue, which can be used to monitor the folding status of its linker region (Ilbert et al., 2007). The

tryptophan in wild type Hsp33 is located on position 212 (W212) in α-helix 7. Hsp33 crystal structure (PDB: 1HW7) reveals that in the reduced state when the linker region is folded, W212 is exposed to the polar solvent. Previous measurements showed that activation of Hsp33 leads to changes in the environment of this tryptophan residue, which can be used as a indirect read-out of the folding status of Hsp33's linker region (Ilbert et al., 2007).

Hsp33 in its reduced form exhibits a tryptophan emission maximum of about 351 nm (Fig. 4.1.5, Hsp33-WT, solid line). Incubation of Hsp33 with 2 mM H_2O_2 at 30°C caused a slight blue shift in emission to 349 nm (Fig. 4.1.5, Hsp33-WT, dotted line), suggesting that the conformation in the linker region did not change substantially. A 9 nm blue shift to 342 nm and quenching of the signal was monitored when the protein became fully activated by incubation with H_2O_2 at 43°C (Fig. 4.1.5, Hsp33-WT, dashed line).

The emission maximum for Hsp33-M172S in the reduced form is identical to that of the wild type protein (fig. 4.1.5), and oxidation at 43°C reveals the same kind of blue shift to about 343 nm that we detected for Hsp33-WT. In contrast to wild type Hsp33, however, the emission shift in tryptophan fluorescence is already detectable when Hsp33-M172S is exposed to H_2O_2 at 30°C (Fig. 4.1.5, Hsp33-M172S, dotted line). This result suggests that the introduced mutation destabilizes the linker region, allowing H_2O_2, a slow-acting oxidant to access the two distal cysteines in Hsp33 and form the second disulfide bond even at non-stress temperatures (Ilbert et al., 2007). The quenching in fluorescence maximum is not as dramatic as it is for Hsp33-WT, which is likely due to slight differences in the protein concentrations. These results are fully consistent with the activity measurements of Hsp33-M172S, which showed that incubation in peroxide at 30°C is sufficient to fully activate the protein.

Hsp33-Y12E is constitutively active. In full agreement with this activity, we found that Hsp33-Y12E has an emission maximum around 342 nm, which is similar to the maximum of emission detectable for fully activated wild type protein (Fig. 4.1.5, Hsp33-Y12E, solid line). There are no significant differences in the tryptophan emission spectra between Hsp33-Y12E oxidized

at either 30°C or 43°. The difference between those spectra and the spectrum of the reduced protein is likely due to differences in the folding state of the zinc binding domain. If zinc is still bound and the domain is folded, it might slightly stabilize the linker region and therefore slightly affect the emission maximum.

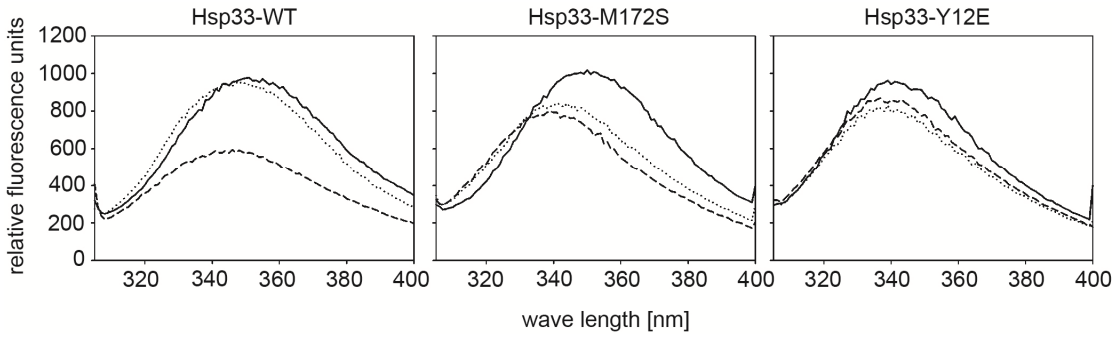

Fig. 4.1.5: Unfolding state of Hsp33's linker correlates to chaperone activity
Tryptophan fluorescence spectra of Hsp33 in its reduced form (solids line), oxidized with 2 mM H_2O_2 at 30°C (dotted line) and 43°C (dashed line) and its variants were conducted with 5 µM of protein at 30°C. Excitation at 295 nm leads to emission spectra between 305 nm and 400 nm with maxima in fluorescence between 351 nm and 343 nm depending on the folding status of Hsp33's linker region.

4.1.5 Hsp33 requires no dimerization to acquire holdase activity

To test the oligomerization status of the reduced Hsp33 variants, analytical ultracentrifugation measurements were performed with the help of Titus M. Franzmann. These measurements confirmed that both variants of Hsp33 are monomeric when they are reduced. Measurements of the S-values for reduced wild type Hsp33 and its variants were close to the calculated S-value for monomeric Hsp33 (2.7) (Akhtar et al., 2004; Graumann et al., 2001). These results are in contrast to previous studies, which suggested that dimerization of Hsp33 is required for the full activation of its chaperone function (Akhtar et al., 2004; Graf, 2004). Although our results with the Hsp33-Y12E mutant suggest that Hsp33 does not require dimerization for full chaperone function *in vitro*, we cannot eliminate the possibility that dimerization occurs upon client protein binding (Graf, 2004; Graumann et al., 2001). This aspect will require further investigation.

Results obtained with another Hsp33 mutant (Hsp33-E150R), which was designed to render Hsp33 constitutively monomeric, revealed that monomerization abolishes client protein binding. Based on our observation that monomerization does not exclude client protein binding, it is therefore conceivable that the E150R mutation not only interferes with Hsp33's dimerization but also with client binding (Graf, 2004). Nevertheless, we concluded from our results that single amino acid mutations at the linker binding interface of Hsp33's N-terminus are sufficient to generate Hsp33 variants that function as highly effective chaperone holdases despite their reduced, zinc-reconstituted and monomeric conformation.

4.1.6 Hsp33 variants show decrease in surface hydrophobicity

Our results indicated that mutations designed to alter the hydrophobic character of the N-terminal β-sheet platform affect Hsp33's regulation but not the chaperone function. To assess whether the mutations caused a detectable change in hydrophobicity, particularly in those surfaces that become exposed upon Hsp33 activation, we recorded the fluorescence spectra of reduced and oxidized wild-type and mutant Hsp33 proteins using the hydrophobic probe bis-ANS as reported in Fig. 4.1.6. As previously shown, wild-type Hsp33 undergoes substantial conformational rearrangements upon oxidative activation, which lead to the exposure of extensive hydrophobic surfaces that interact with bis-ANS (Raman et al., 2001). In the reduced form of Hsp33-WT (Fig. 4.1.6, trace a), no substantial bis-ANS interaction is detectable. Upon oxidative activation of wild type Hsp33 (2 mM H_2O_2, 43°C, 3h), however, a dramatic increase in fluorescence is visible (Fig. 4.1.6, trace a'). When both mutant proteins were exposed to the same oxidizing conditions that fully activated wild-type Hsp33, their extent of surface hydrophobicity was slightly reduced (Fig. 4.1.6, compare traces b' and c' with a'). These results confirmed that the mutations did indeed affect the hydrophobicity of surface areas that become exposed during the activation process. Furthermore, analysis of the surface hydrophobicity of the reduced, constitutively active Hsp33-Y12E mutant revealed that not all of the hydrophobic surface areas exposed upon oxidative activation of Hsp33 are necessary for its chaperone function. This mutant protein is as active as oxidized wild-type Hsp33 when reduced and

zinc-coordinated but shows significantly less overall surface hydrophobicity (Fig. 4.1.6, trace c).

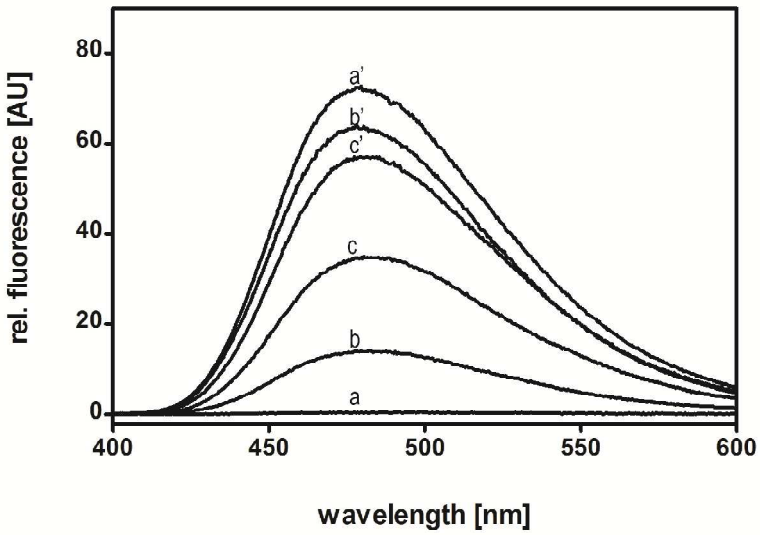

Fig. 4.1.6: Hydrophobicity of Hsp33 and variants

3 µM freshly reduced wild-type $Hsp33_{red}$ (**trace a**), Hsp33-M172S $_{red}$ (**trace b**), Hsp33-Y12E$_{red}$ (**trace c**) or active wild-type $Hsp33_{ox43°C}$ (**trace a'**), Hsp33-M172S $_{ox43°C}$ (**trace b'),** Hsp33-Y12E $_{ox43°C}$ (**trace c'**) were incubated with 10 µM of the hydrophobic probe bis-ANS in 40 mM Hepes buffer, pH 7.5. Fluorescence spectra were recorded and buffer corrected.

4.1.7 Close correlation between linker destabilization and Hsp33 activity

Based on the proposed activation model, Hsp33's chaperone function depends on the formation of the critical disulfide bond between Cys_{232} and Cys_{234}, which is both kinetically and thermodynamically linked to the folding status of the linker region (Winter et al., 2008). Mutations that destabilize the linker region should therefore enhance the rate of disulfide bond formation and activation. To investigate whether the M172S and Y12E mutations indeed altered the thermostability of the linker region in the Hsp33 variants, we performed far-UV circular dichroism (CD) spectroscopy to monitor changes in Hsp33's secondary structure as a function of temperature. As previously shown, when fully reduced and zinc-reconstituted, wild-type Hsp33 begins to irreversibly unfold at temperatures above ~50°C (Ilbert et al., 2007). When fully oxidized, zinc-depleted and activated ($Hsp33_{ox43°C}$), the linker region and zinc-binding domain of wild type Hsp33 remain unfolded at temperatures as low as 20°C (Fig. 4.1.7) and the N-terminal domain begins to unfold at a

temperature that is similar to the onset of unfolding of reduced Hsp33 (Fig. 4.1.8).

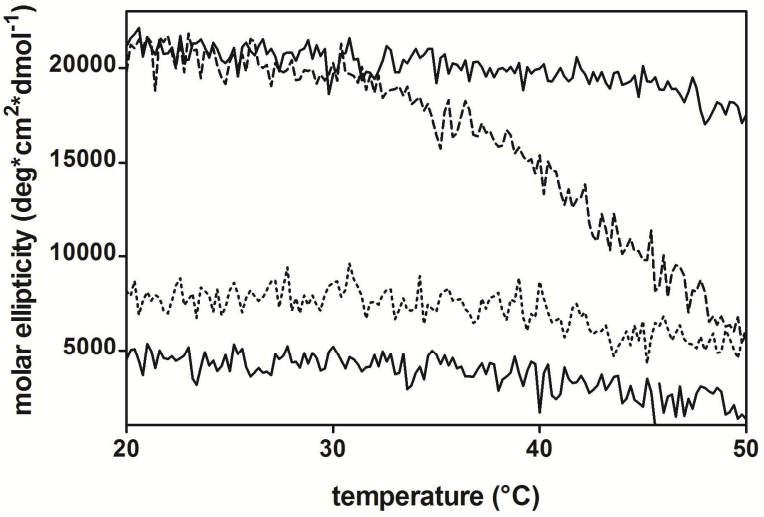

Fig. 4.1.7: Thermal stability of wild-type Hsp33 and variants (20-50°C)
Preparations of freshly reduced wild-type Hsp33 (solid line - top), Hsp33-Y12E (short dashed line), Hsp33-M172S (long dashed line), or fully active $Hsp33_{ox43°C}$ (solid line - bottom) were heated to 50°C (1°C per minute) and changes in the molar ellipticity were recorded at 195 nm using a spectropolarimeter.

This result is in stark contrast to the reduced, zinc-reconstituted Hsp33-M172S variant, which begins to unfold at temperatures as low as 30°C (Fig. 4.1.7). This unfolding (T_m ~40°C), which is fully reversible up to 50°C, is highly reminiscent of the unfolding of oxidized, inactive $Hsp33_{ox-30°C}$ intermediate which lacks zinc coordination and has a substantially destabilized linker region (T_m <43°C) (Ilbert et al., 2007). Further increase in the incubation temperature of reduced Hsp33-M172S led to the irreversible unfolding of the remaining protein with the onset of unfolding at a temperature that was again similar to reduced wild-type Hsp33 (Fig. 4.1.8). These results suggest that the M172S mutation does not globally destabilize Hsp33. Our finding that the linker region of Hsp33-M172S reversibly unfolds upon exposure to heat shock temperatures is consistent with our previous observation that the reduced Hsp33-M172S acts as a molecular chaperone when tested at 43°C but not at 30°C (Fig. 4.1.3). We concluded from these results that unfolding of the linker region is a critical element for the chaperone function of Hsp33.

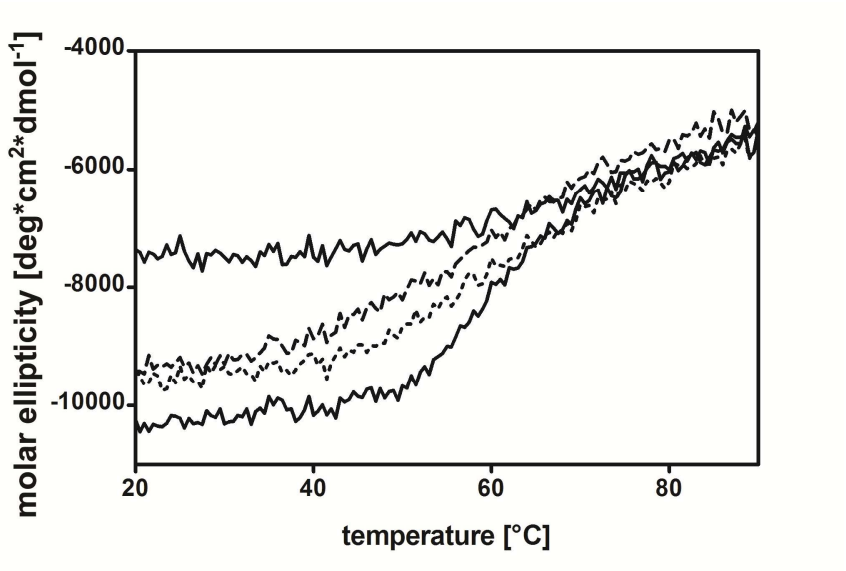

Fig. 4.1.8: Thermal stability of wild-type Hsp33 and variants (20-80°C)
Preparations of freshly reduced wild-type Hsp33 (solid line - bottom), Hsp33-Y12E (short dashed line), Hsp33-M172S (long dashed line), or fully active $Hsp33_{ox43°C}$ (solid line - top) were heated to 90°C (1°C per minute) and changes in the molar ellipticity were recorded at 222 nm using a spectropolarimeter.

This conclusion was further supported by the CD analysis of the reduced, constitutively active Hsp33-Y12E mutant, which showed dramatically decreased secondary structure content, suggestive of a constitutively unfolded linker region (Fig. 4.1.7). Subsequent incubation with H_2O_2 caused some additional loss of secondary structure as monitored by CD spectroscopy, which likely corresponds to the oxidative zinc release and the unfolding of the zinc binding domain (Fig. 4.1.9). Unfolding of the remaining protein structure started at temperatures similar to wild-type $Hsp33_{red}$ and Hsp33-$M172S_{red}$ mutant protein, suggesting that also this substitution did not globally destabilize Hsp33 (Fig. 4.1.8). Temperature scans between 20-50°C revealed the same pattern of unfolding as observed for $Hsp33_{red}$ and $Hsp33_{ox}$ (Fig. 4.1.7)

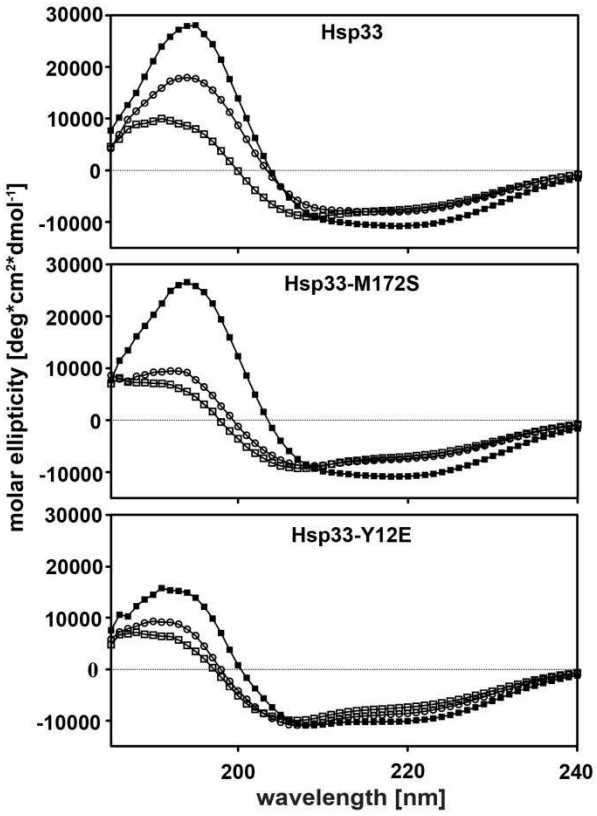

Fig. 4.1.9: Far-UV CD spectra demonstrate the loss in secondary structure
Secondary structure determination of reduced and oxidized wild type Hsp33 and mutant variants with far-UV CD spectra. Freshly reduced Hsp33 preparations ($Hsp33_{red}$) (closed squares) or preparations that were incubated with 2 mM H_2O_2 for 3 h at either 30°C (open circles; $Hsp33_{ox30°C}$) or 43°C (open squares; $Hsp33_{ox43°C}$) were recorded.

These results provide good evidence that destabilization of the linker region by single mutations in Hsp33's N-terminal linker binding domain is sufficient to eliminate Hsp33's posttranslational regulation. They further imply that the stability of the linker region plays a central role in the chaperone function of Hsp33. Hsp33's redox-sensing zinc binding domain appears to primarily serve as the molecular toggle whose redox status controls the thermostability of the linker region. This activation of Hsp33 makes physiological sense, as it confers activation of Hsp33 only upon oxidative stress conditions that lead to unfolding. Slow-acting oxidants like H_2O_2 cause cellular stress (reviewed in Oxidative stress (Storz and Imlay, 1999)) but do not lead to protein unfolding. Heat stress alone leads to protein unfolding and aggregation but it can be compensated for by other chaperone systems like the DnaK/J/E system (Baneyx and Mujacic, 2004; Winter et al., 2005). Dual

stress, *e.g.,* heat and oxidative stress, or fast acting oxidants that lead to widespread protein unfolding (HOCl) (Winter et al., 2008) require activation of the ATP-independent Hsp33 as it leads to the inactivation of ATP-dependent chaperone foldases. Hsp33 is active under these conditions and rescues unfolding protein from their fate of irreversible aggregation (Winter et al., 2008).

4.1.8 Lack of posttranslational regulation of Hsp33 affects *E. coli* growth

Our results suggested that we generated two Hsp33 mutants that lack their proper posttranslational redox regulation *in vitro*. These mutants provided us now with the unique opportunity to investigate what role the posttranslational regulation of Hsp33 plays in the cell. To investigate the effects that the expression of our mutant proteins has *in vivo*, we cultivated BL21 *hslO*- strains expressing either wild-type Hsp33 or the variants from an IPTG-inducible pET11a vector in MOPS minimal media in the presence of increasing concentrations of IPTG at 37°C (Fig. 4.1.10). We observed a significant growth defect at 37°C in strains expressing the constitutively active Hsp33-Y12E mutant at IPTG concentrations as low as 50 µM (Fig. 4.1.10 open circles). In contrast, no significant growth defect was detected in strains expressing either wild-type Hsp33 (Fig. 4.1.10 open triangles) or the temperature-controlled Hsp33-M172S (Fig. 4.1.10 open squares) mutant protein under the same growth conditions.

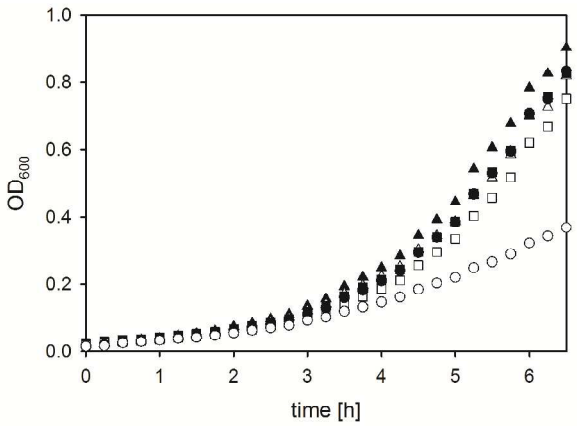

Fig. 4.1.10: Growth curves of strains expressing Hsp33 and its variants at 37°C
E. coli strains JH21 (BL21 h*slO*-) expressing (triangles) wild type Hsp33, (squares) Hsp33-M172S or (circles) Hsp33-Y12E from a pET11a plasmid were cultivated without (open symbols) IPTG or with 50 µM IPTG (closed symbols) in

MOPS minimal medium at 37°C. The OD_{600} was monitored. No growth defect was observed when cells were cultivated with 25 µM IPTG.

These results provided preliminary evidence that expression of the constitutively active Hsp33 variant might be harmful to bacteria. Analysis of the respective cell lysates five hours after IPTG-mediated protein expression was started, revealed that all three Hsp33 expressing strains contained similar steady-state levels of Hsp33 (Fig.4.1.11). The Hsp33 expression levels in the presence of 50 µM IPTG were not dramatically increased in comparison to expression level of chromosomally encoded Hsp33 under non-stress conditions. Also, no obvious change in the general protein expression pattern was observed (Fig. 4.1.11). These results argued against the possibility that the growth defect observed in Hsp33-Y12E expressing strains is due to massive overexpression of a partially unfolded protein, which would trigger the induction of the heat shock response in *E. coli*.

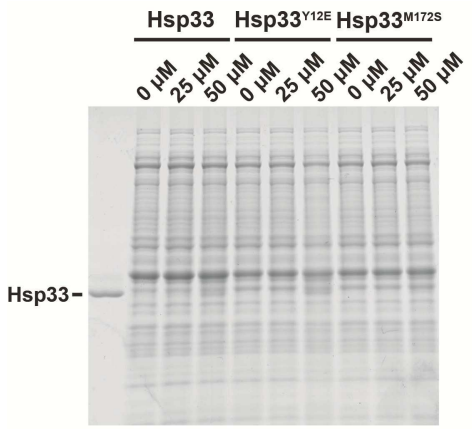

Fig. 4.1.11: Hsp33 expression level in Bl21 strains

Cells were harvested 6 hours after induction with 0, 25 or 50 µM IPTG in MOPS minimal medium at 37°C was started to check the expression levels of wild type Hsp33 and its variants. Cells were resuspended and lysed in 2 x Laemmli buffer and analyzed on reducing SDS PAGE. The amount of protein loaded was adjusted to the same cell OD_{600}.

When we analyzed and compared the soluble and insoluble protein population in these three strains, however, we detected a significant difference; a substantial proportion of Hsp33-Y12E protein was found to be insoluble and co-aggregated with a large number of different *E. coli* proteins (Fig. 4.1.12). This co-aggregation led to a small but reproducible decrease in

the overall amount of soluble *E. coli* proteins. In contrast, both wild-type Hsp33 or Hsp33-M172S proteins remained mostly soluble at 37°C and did not cause any protein aggregation.

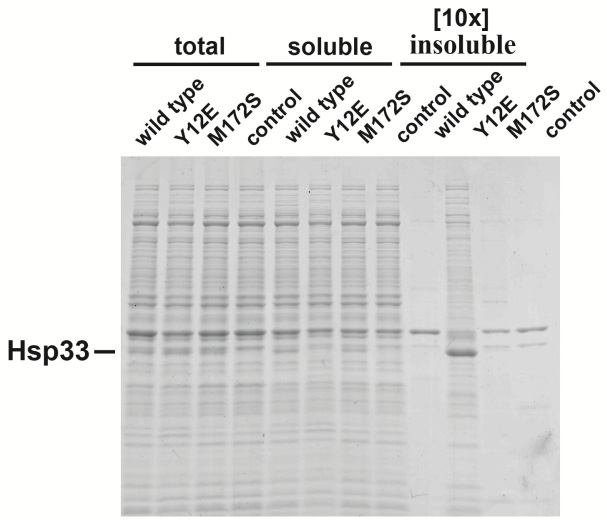

Fig. 4.1.12: Detection of aggregated proteins expressing Hsp33-Y12E at 37°C
Total cell lysates were prepared and separated into soluble proteins and insoluble aggregates 6 hours after induction with 50 µM IPTG in MOPS minimal medium at 37°C. The amount of total cell lysate and supernatant loaded was adjusted to the number of cells harvested. A 10-fold higher amount of aggregates was loaded onto the SDS-PAGE to visualize cellular proteins that aggregated.

Increasing the cultivation temperature to 43°C, which activates Hsp33-M172S *in vitro*, made expression of this protein more disadvantageous for *E. coli* as well and led to growth defects, which were significantly more pronounced than upon expression of the wild type protein (Fig. 4.1.13 A). Testing for aggregates in these strains revealed that under these temperature conditions, Hsp33-M172S also sequestered a large number of *E. coli* proteins into the insoluble protein precipitates (Fig.4.1.13 B). In contrast, very little protein was found aggregated in cells expressing wild type Hsp33.

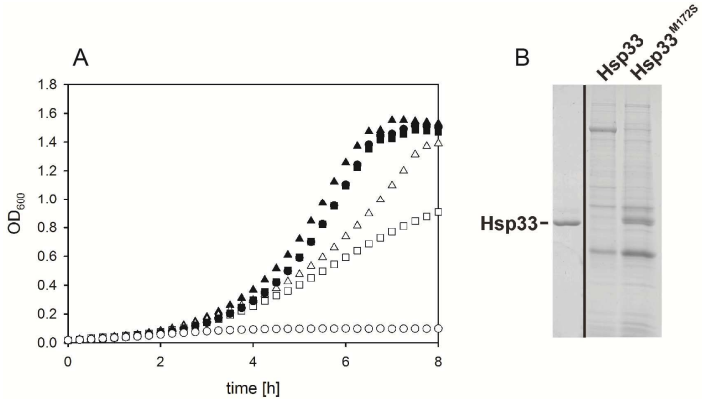

Fig. 4.1.13: Growth curves of strains expressing Hsp33 and its variants at 43°C and protein aggregation under this condition

A) *E. coli* strains JH21 (BL21, Δh*slO*) expressing (triangles) wild type Hsp33, (squares) Hsp33-M172S or (circles) Hsp33-Y12E from a pET11a plasmid were cultivated without (closed symbols) IPTG or with 50 µM IPTG (open symbols) in MOPS minimal medium at 43°C. The OD was monitored at 600 nm.

B) Comparison of aggregated proteins in *E. coli* stains expressing either Hsp33-WT or Hsp33-M172S variant at 43°C for 5 hours.

These results strongly suggest that in the absence of any posttranslational regulation, Hsp33 binds to either newly synthesized or pre-existing unfolding cellular proteins and co-aggregates with these proteins. It remains now to be determined whether the formation of aggregates *per se*, or the sequestration of specific *E. coli* proteins necessary for optimal bacterial growth is responsible for the observed growth defect. In either case, these results provide a first clue as to why chaperone holdases, such as Hsp33, require tight functional regulation.

4.1.9 Conclusion

Hsp33's crystal structures revealed the precise location of Hsp33's folding-sensitive linker in reduced, inactive Hsp33 (Janda et al., 2004). The linker region covers an extended ~3800 $Å^2$ N-terminal surface area, 75% of which is rich in hydrophobic residues (Vijayalakshmi et al., 2001). To test the model that this area serves as a linker binding surface under non-active conditions and as a client binding site upon linker unfolding and activation, we substituted two of the most centrally located hydrophobic residues with either polar (M172S) or charged (Y12E) residues. We confirmed that substitution of either one of these residues significantly decreased the hydrophobicity of those surfaces that apparently become exposed upon Hsp33's oxidative activation. We were unable, however, to detect any apparent reduction in

Hsp33's ability to prevent protein aggregation *in vitro* using different substrate proteins. These results suggest that the hydrophobic surface area directly underneath the linker binding site might not be directly involved in substrate binding. These results raise now the intriguing question as to where unfolded client proteins bind in Hsp33. Although the introduced mutations did not affect the chaperone function of Hsp33, they dramatically altered its redox regulation. Mutation of Met172 to Ser turned Hsp33 into a purely heat- or oxidative stress-regulated chaperone, whereas mutation of Tyr12 to Glu caused Hsp33 to be constitutively active. Neither mutation significantly altered the stability of Hsp33's N-terminal or zinc binding domains. However, both substantially lowered the thermostability of Hsp33's linker region, thereby apparently eradicating the thermodynamic control exerted by Hsp33's oxidation-sensitive C-terminal redox switch domain.

Our mutant studies now demonstrate that a simple mutation that destabilizes the linker region is sufficient to abrogate Hsp33 tight regulation. Our results provide the experimental evidence that the folding status of the linker region plays a central role for Hsp33's chaperone function, and they imply that Hsp33's zinc center functions primarily as a redox sensitive pivot whose oxidation status controls the thermodynamic stability of the adjacent linker region and therefore the activity of Hsp33.

This study provides the first evidence that lack of Hsp33's stringent posttranslational control becomes highly disadvantageous to *E. coli* cells. Expression of the constitutively active Hsp33-Y12E variant caused a large number of cellular proteins to co-precipitate with Hsp33. These results suggest that the ability of active Hsp33 to interact with a wide variety of proteins *in vivo* (Winter et al., 2005) generates a clear need to switch Hsp33 off under non-stress conditions. The fact that the constitutively active Hsp33-Y12E mutant can no longer regulate substrate binding and release might be sufficient to target Hsp33 with its client proteins into the insoluble aggregates. Whether it is the newly synthesized proteins that fall victim to Hsp33-Y12E's constitutive chaperone activity or mature proteins that are potentially unfolded by Hsp33, remains to be investigated.

4.2 Client recognition by Hsp33 and the DnaK/J-GrpE system

4.2.1. Client protein binding involves Hsp33's linker region

Our results from chapter 4.1 raised the intriguing question as to where unfolded client proteins bind in Hsp33. One possibility is that the linker region in Hsp33 directly participates in client binding. This would be consistent with previous suggestions that natively unfolded regions, which are, by definition highly flexible and charged (Dunker et al., 2001; Tompa, 2009; Uversky et al., 2000) would foster binding of a large variety of different substrate proteins. Their highly charged nature would increase the solubility of unfolding proteins and effectively prevent protein aggregation. Supported by the facts that disordered regions in RNA chaperones very often map with the respective RNA binding sites, and that many protein chaperones have extensive disordered regions, these observations led to the hypothesis that natively disordered regions might be directly involved in substrate interaction (Tompa and Csermely, 2004). We thus decided to directly test the idea that Hsp33's unfolded linker region might be involved in client binding. Wild type Hsp33 contains one tryptophan residue, which is conveniently located in the linker region at position 212 (W212) of α-helix 7, the last helix before the zinc-binding domain.

The first part in this chapter has been published in: Reichmann D, Xu Y, Cremers CM, Ilbert M, Mittelman R, Fitzgerald MC, Jakob U.: **Order out of disorder: working cycle of an intrinsically unfolded chaperone.** Cell 2012 Mar 2;148(5):947-57. Refolding studies described here are not published in the manuscript. The experiments described here are all performed by me. I wrote the text, which was edited by U. Jakob.

Malate dehydrogenase (MDH), a client protein of Hsp33, does not contain any tryptophan residues (Cremers et al., 2010; Reichmann et al., 2012). Hence, MDH can be used to monitor potential structural changes in Hsp33's linker region upon its binding to client proteins. If binding of MDH occurred in the vicinity of the linker region and/or affected the conformation of the linker region, changes in the Trp-fluorescence of Hsp33 would be expected. In addition, we also used another previously constructed mutant Hsp33-F187W W212F, which contains a single tryptophan at position 187 of the protein (Ilbert et al., 2007). This mutant should give us the opportunity to monitor changes in the conformation of α-helix 5, which is located at the N-terminal boundary of the linker region.

It has been previously shown that wild type Hsp33 in its reduced form ($Hsp33_{red}$) exposes W212 to the solvent, leading to a fluorescence maximum of 355 nm at 45°C (Fig. 4.2.1, Hsp33). Activation of Hsp33 by peroxide and unfolding conditions (*i.e.*, 43°C) ($Hsp33_{ox}$) causes a decrease in its fluorescence emission and a blue shift of about 9 nm, indicating conformational changes that shift W212 towards a more non-polar environment. Quenching of this signal might be due to interactions of W212 with negatively charged amino acids, which are present in its vicinity (Chen and Barkley, 1998; Vijayalakshmi et al., 2001).

When malate dehydrogenase is added to $Hsp33_{ox}$ and slowly heated to 45°C (1°C/min, held at that temperature for 10 min), it thermally unfolds and interacts with Hsp33. This interaction was found to cause a further blue shift (3 nm) and lead to a slight increase in Trp-fluorescence (Fig. 4.2.1, Hsp33, dashed line). These results suggest either direct interactions of Hsp33's α-helix 7 with malate dehydrogenase, or conformational changes induced by malate dehydrogenase binding to Hsp33.

In contrast to W212, which is solvent exposed, F187W is buried in reduced Hsp33-F187W W212F. Hence the emission maximum of this variant is at about 338 nm. Activation of Hsp33-F187W W212F causes a dramatic red shift (emission maximum at 353 nm) and a substantial decrease in fluorescence, which is consistent with the unfolding of α-helix 5 (Fig. 4.2.1) (Ilbert et al.,

2007). Incubation of MDH in this solution was found to lead to a slight blue-shift and an increase in fluorescence (Fig. 4.2.1, Hsp33-F187W W212F), which suggests that also this part of the linker region is affected by the binding of MDH. When the inactive reduced Hsp33 wild type or Hsp33-F187W W212F mutant was tested, we found that MDH aggregation caused the quenching of the tryptophan fluorescence signal without shifting the emission maximum (data not shown). These results suggest that the conformation of the unfolded linker region between Hsp33 N-terminal domain and C-terminal redox switch domain is affected client protein binding. It remains now to be determined whether this is a direct interaction or whether structural changes occur in the linker region that are conferred by client binding in other parts of the protein.

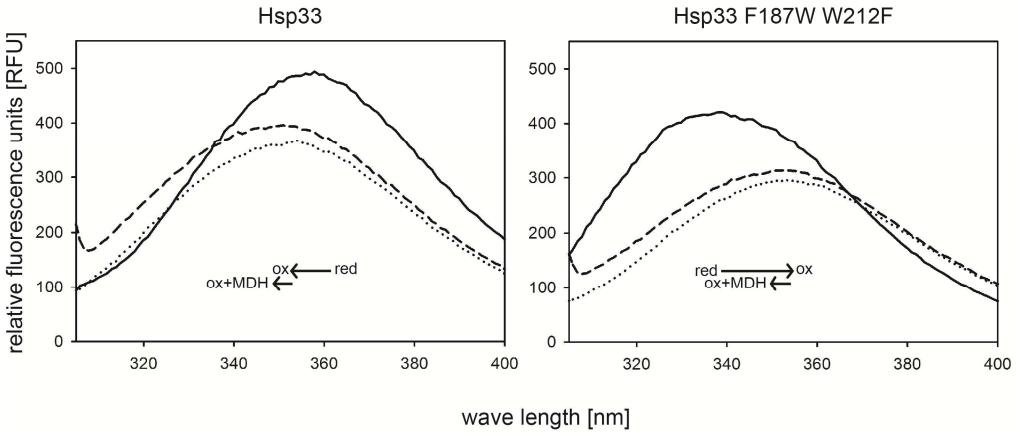

Fig. 4.2.1: Trp fluorescence of wild type Hsp33 and its variant Hsp33-F187W W212F

Trp fluorescence emission spectra of 5 µM $Hsp33_{red}$ (solid line), $Hsp33_{ox}$ (dotted line) or $Hsp33_{ox}$ + malate dehydrogenase (5 µM) (dashed line) and its variant Hsp33-F187W W212F were recorded in 40 mM phosphate buffer pH7.5 at 45°C to monitor structural rearrangements in Hsp33 linker region upon interaction with MDH.

Our results are consistent with several other experiments that demonstrated the involvement of Hsp33's linker region in client protein binding (Reichmann et al., 2012). Tryptic digest of Hsp33 coupled with LC/MS analysis, for instance, revealed a destabilization of Hsp33's linker region upon oxidative activation and a subsequent stabilization of the linker region upon client protein binding. In contrast, Hsp33's zinc-binding domain, which also loses stability upon activation, does not regain any stability upon client protein binding. These results agree with previous studies that demonstrated that the

zinc-binding domain is not involved in client binding; deletion of the C-terminal 60 amino acids does not alter the activation mechanism of Hsp33 nor does it change its client binding capacity (Ilbert et al., 2007). The N-terminal domain of Hsp33 also seems to undergo some structural rearrangements during activation (Reichmann et al., 2012). These regions include the monomer-monomer interface of Hsp33 as well as the hydrophobic linker binding surface of Hsp33 (Graumann et al., 2001; Reichmann et al., 2012).

4.2.2 Client protein recognition in Hsp33

Hsp33's activation involves the oxidative unfolding of its own C-terminal redox switch domain. This finding raised the obvious question how Hsp33 recognizes hundreds of different unfolded client proteins (Winter et al., 2008; Winter et al., 2005) while discriminating against binding to its own intrinsically disordered C-terminal redox switch domain, which is present at high local concentration.

Marianne Ilbert and Dana Reichmann in the lab performed binding experiments of Hsp33 to peptide arrays to determine the peptide binding specificity of Hsp33. Overlapping 12-mer peptides of 18 different Hsp33 and DnaK-client proteins were synthesized on a chip (3914 peptides). Incubation of the peptide chip with reduced, inactive Hsp33 ($Hsp33_{red}$) and consecutive visualization of binding by using a fluorescence labeled antibody against Hsp33 was first used to test the specificity of binding. Reduced Hsp33 did not reveal significant binding to any of the peptides. In contrast, activated, oxidized Hsp33 ($Hsp33_{ox}$) bound strongly to select numbers of overlapping peptides (Reichmann et al., 2012). Fluorescence intensities were scored from 0 to 1 and analyzed. Relative occurrence of amino acids in good binders (high score) *versus* non-binders (low score) was compared to the relative frequency of all 20 amino acids in the peptide library and showed that there were only a few amino acids slightly more abundant in good binders. In contrast, several amino acids were overrepresented in non-binders: aspartate (Asp) and glutamate (Glu), as well as tryptophan (Trp), cysteine (Cys) and lysine (Lys) (Reichmann et al., 2012). It is of note that Glu, Asp, Cys, and Lys are enriched in natively unfolded proteins (Prilusky et al., 2005), like α-casein, as well as in

Hsp33‘s own C-terminal redox switch domain, suggesting that Hsp33 might disfavor binding to completely unfolded regions in proteins. Comparison of secondary structure features agreed with this conclusion as it showed that peptides with a good Hsp33 binding score are primarily in α-helices and β-sheets, whereas the majority of non-binders are found in unstructured regions and loops (Reichmann et al., 2012).

Similar experiments have been previously performed with DnaK (Rüdiger et al., 1997b), the ATP-dependent chaperone foldases, which is responsible for refolding Hsp33’s client proteins upon return to reducing conditions (Hoffmann et al., 2004). To assess the overlap in peptide binding specificity between Hsp33 and DnaK, we compared our results with those obtained by Rüdiger et al. For DnaK, the majority of high affinity binding peptides were predicted to be in unstructured regions of client proteins (Reichmann et al., 2012; Rüdiger et al., 1997b). This result agreed with the physiological role of DnaK, which, in complex with its co-chaperones (DnaJ and GrpE), interacts with unfolded polypeptide chains as they emerge from the ribosome (Deuerling et al., 1999). These results, however, implied that while Hsp33 and the DnaK-system might share client specificity (Winter et al., 2005), they might exert different peptide binding specificity. To investigate this possibility, I compared the binding of Hsp33 or the DnaK/J/E system to several different client proteins.

To test the hypothesis that Hsp33 indeed discriminates against intrinsically disordered proteins and prefers structured folding intermediates while DnaK binds preferentially unstructured regions in client proteins, chaperone competition assays were performed. Hsp33 and the DnaK/DnaJ-complex (DnaK/J) bind tightly to chemically unfolded citrate synthase or luciferase upon dilution into refolding buffer and prevent their irreversible aggregation. We reasoned that effective competitors will compete for citrate synthase or luciferase binding to the chaperones, and displace the clients. The client proteins, in turn, will aggregate. Hence, high competitor activity would be reflected by high levels of client protein aggregation and *vice versa*.

Wild type Hsp33 was activated by oxidation with HOCl ($Hsp33_{ox}$) as described in chapter 3.5. and incubated with increasing concentrations of the intrinsically disordered fragment of Hsp33's own C-terminus (aa218-287, $Hsp33_{C\text{-}terminus}$), a natively unfolded protein. Chemically unfolded citrate synthase or luciferase was added and light scattering was monitored. As shown in figure 4.2.2, presence of a 100-fold molar excess of unfolded $Hsp33_{C\text{-}terminus}$ had no effect on the activity of $Hso33_{ox,}$ indicating that $Hsp33_{ox}$ does not bind its own C-terminal domain. In contrast, a 50-fold molar excess of the oxidized C-terminus of Hsp33 reduced the binding between DnaK/J and citrate synthase by nearly 20 % while a 100-fold molar excess reduced binding by almost 40 % (Fig. 4.2.2). This result indicates that DnaK/J is able to bind the intrinsically disordered region of Hsp33. Very similar results were obtained when luciferase was used as chaperone client protein. While presence of the oxidized $Hsp33_{C\text{-}terminus}$ (325 nM) had no effect on the binding between Hsp33 (130 nM) and luciferase (65 nM), binding of luciferase to DnaK/J (650 nM and 130 nM) was inhibited by about 50 % (Fig. 4.2.2, insert).

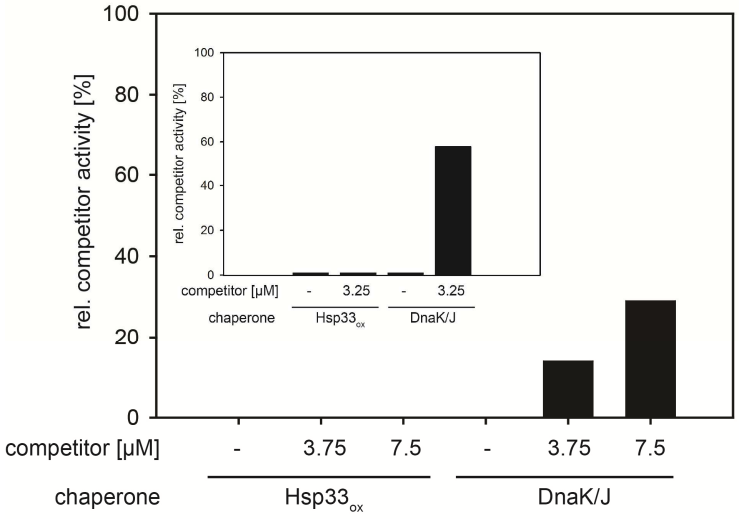

Fig. 4.2.2: Effect of oxidized Hsp33 C-terminus competing with citrate synthase or luciferase as substrate of Hsp33 or DnaK/J.

The competition of oxidized $Hsp33_{C\text{-}terminus}$ towards chemically unfolded citrate synthase (75 nM), luciferase (65 nM insert) was measured with a 2-fold molar excess of $Hsp33_{ox}$ or DnaK/J (10-, and 2-fold molar excess). Light scattering measurements were conducted at 30°C. 0 % competitor activity is defined by chaperone activity in absence of any competitor, whereas the light scattering signal of substrate in absence of any chaperone was defined as 100 % competition. Oxidized $Hsp33_{C\text{-}terminus}$ had no effect on citrate synthase or luciferase aggregation.

Like MDH, $Hsp33_{C\text{-}terminus}$ does not contain any tryptophan residues. To test whether presence of Hsp33's C-terminus affects the conformation of Hsp33's linker region, we incubated activated $Hsp33_{ox}$ with excess amounts of its own oxidized C-terminus. No changes in Trp-fluorescence were observed (Fig. 4.2.3). These results agree with our activity data and indicate that Hsp33's C-terminus has no influence on the linker conformation of Hsp33.

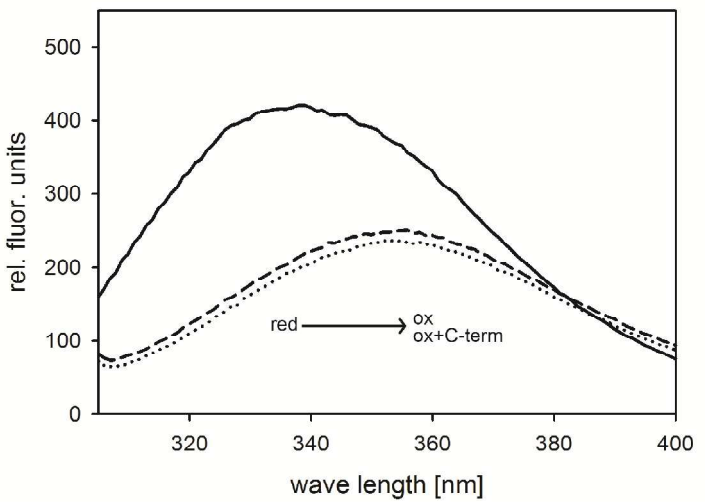

Fig. 4.2.3: Trp-fluorescence of Hsp33 using oxidized C-terminus as potential client

Trp-fluorescence emission spectra of 5 µM $Hsp33_{red}$ (solid line), $Hsp33_{ox}$ (dotted line) or $Hsp33_{ox}$ + oxidized $Hsp33_{C\text{-}terminus}$ (50 µM) (dashed line) were recorded in 40 mM phosphate buffer pH 7.5 at 30°C to monitor structural rearrangements in Hsp33 linker region.

Another model protein that we used was α-casein, which is a known intrinsically disordered protein. About 55 % of the protein is classified as unstructured with about 30 % of α-helical structure present in the remaining part of the protein (Szasz et al., 2011). While the α-helical content of α-casein would make it a potential binding partner of Hsp33, analysis of the amino acid contents revealed a clear overrepresentation of Glu, Asp, Lys, Cys, and Trp, the characteristic non-binding amino acids of Hsp33.

Competition assays confirmed α-casein's ability to interact with DnaK/J, and revealed again only a weak interaction with $Hsp33_{ox}$. One issue, which interfered with our ability to perform competition assays at higher ratios of α-casein and luciferase or citrate synthase was the fact that α-casein functions as a chaperone when added in high concentrations to our aggregation

assays. Hence, the highest concentration of α-casein that we could use was a 15-fold molar excess over client proteins. This amount of α-casein was however sufficient to cause a 50 % reduction of DnaK/J's chaperone activity (Fig. 4.2.4), whereas a less than 10 % effect was observed with Hsp33 (Fig. 4.2.4).

Aggregation of luciferase (65 nM) was suppressed at even lower concentrations of α-casein. Hence, competition assay were performed with a maximum of a 5-fold molar excess of α-casein to luciferase. This excess of α-casein, however, was able to almost completely compete for luciferase binding with DnaK/J (650 nM and 130 nM respectively), whereas no effects were observed on Hsp33's (130 nM) chaperone activity (Fig. 4.2.4, insert).

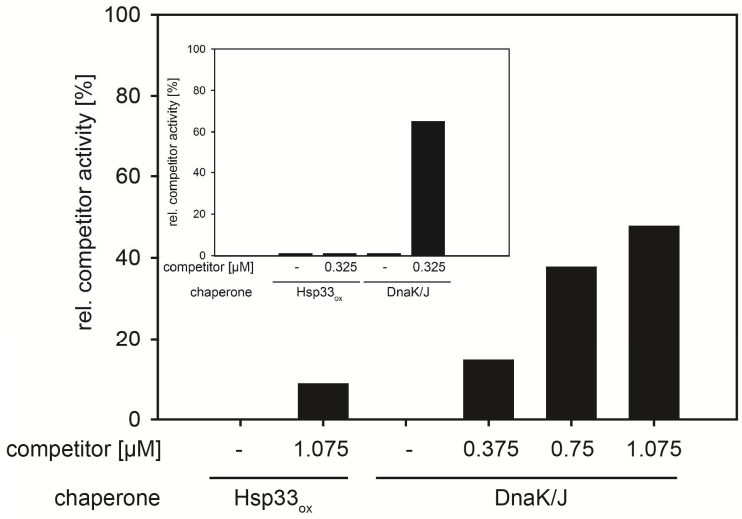

Fig. 4.2.4: Effects of α-casein competing with citrate synthase / luciferase as clients of Hsp33 and DnaK/J

The competition of α-casein binding of chemically unfolded citrate synthase (75 nM) or luciferase (65 nM, insert) to a 2-fold molar excess of $Hsp33_{ox}$ or DnaK/J (10-, and 2-fold molar excess) was measured with light scattering. A 15-fold molar excess of α-casein to citrate synthase already decreased citrate synthase aggregation to a certain extent, so for analysis citrate synthase aggregation in context with α-casein was always set as fully aggregated citrate synthase (0 % activity), whereas 100 % chaperone activity was defined by suppression of aggregation without competitor present.

These results provide experimental support for our peptide array studies, and indicated that natively unfolded proteins do not serve as client proteins of Hsp33 but interact with the DnaK/J system. The abundance of Glu, Asp, Cys, and Lys, which are enriched in intrinsically unfolded proteins and found in

Hsp33's own C-terminal redox switch domain, are disfavored in binding to Hsp33. In contrast, the DnaK/J system interacts with these unfolded polypeptides.

To test whether our conclusions for good binders was correct as well (*i.e.,* binding of $Hsp33_{ox}$ to structured folding intermediates), Dana Reichmann performed competition assays with a peptide, which was identified as a high affinity binder of Hsp33. The 25 aa peptide, derived from NADH ubiquinone oxidoreductase (Pep^{NuoC}), exhibited the highest score in the peptide array study over seven repeats. As predicted, the peptide was able to bind to $Hsp33_{ox}$ and competed well with chemically unfolded citrate synthase for binding to Hsp33. In comparison, DnaK/J only weakly interacted with Pep^{NuoC}. The highest used concentration (1.5 µM) of Pep^{NuoC} diminished the binding of $Hsp33_{ox}$ to citrate synthase by about 70 % while binding of citrate synthase to DnaK/J was barely affected (see Fig. 2a in Reichmann et al.). These results revealed that this synthesized peptide is a good interaction partner for Hsp33 but not for the DnaK/J system (Reichmann et al., 2012).

Taken together, these results show that there is profound difference in the peptide binding specificity of the two chaperones. To further test the model that activated $Hsp33_{ox}$ and the DnaK/J system have the same client proteins but recognize different structural features, we investigated the influence of Hsp33 and the DnaK/J system on Arc repressor, a common client protein of the two chaperones.

4.2.3 The transcriptional repressor Arc: A client protein for both Hsp33 and DnaK/J

Arc is a 55 amino acid protein, which is a dimer when kept at high protein and salt concentrations. Dilution of Arc into buffer that contains no salt, however, leads to its rapid dissociation and slow unfolding without the formation of insoluble aggregates (Bowie and Sauer, 1989). Based on our previous results, we reasoned that both Hsp33, which prefers more structured regions for binding, and DnaK/J, which prefers unfolded polypeptides, will bind Arc yet potentially at different time points during its unfolding. We

therefore first investigated if Arc was dissociating and unfolding under the buffer conditions that we used in our competition assays. Arc was diluted to a final concentration of 0.75 µM into 40 mM HEPES, pH 7.5 buffer at 30°C. Fluorescence of Arc's single tryptophan, which is located in the dimer interface (Fig. 4.2.5, insert) was monitored over 30 min to follow Arc's dissociation and unfolding (Fig. 4.2.5). This followed a biphasic kinetic with a fast phase that likely corresponds to the monomerization of Arc and a second slow phase, in which the protein slowly unfolds (Bowie and Sauer, 1989).

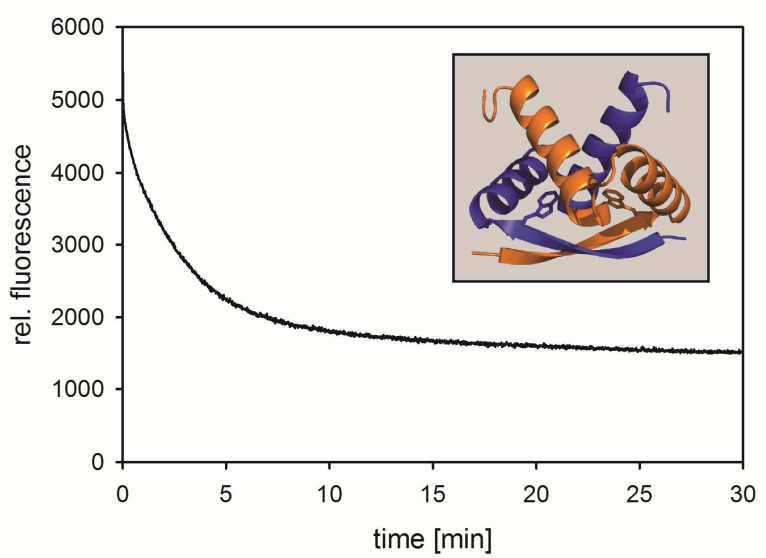

Fig. 4.2.5: Trp-fluorescence to monitor unfolding of Arc
Arc was diluted to a final concentration of 0.75 µM in 40 mM HEPES buffer, pH 7.5 and unfolding was monitored by Trp-fluorescence at 332 nm and 30°C. Insert: Structure of the transcriptional repressor Arc dimer (PDB: 1QTG) with the single Trp highlighted in the dimer interface (Schildbach et al., 1995)

To test the efficiency of Arc's competitor activity, we investigated the effects of different concentrations of Arc on $Hsp33_{ox}$'s chaperone function using freshly diluted Arc or on DnaK/J using Arc 30 min after unfolding was initiated (Fig. 4.2.6). Hence, Arc was either added to the chaperone (t = 0 min) or DnaK/J was added to unfolding Arc (t = 30 min). Complex formation was allowed for 10 sec before chemically unfolded citrate synthase was added and light scattering was monitored.

We found a very strong correlation between increased Arc concentration and its increased activity to function as competitor for both tested chaperones.

20-fold molar excess (1.5 µM) of Arc to citrate synthase (75 nM) abolished DnaK/J-binding to citrate synthase by about 75 %. For Hsp33, a very similar trend was detected, and a 15-fold molar excess (1.125 µM) of Arc reduced Hsp33's ability to prevent citrate synthase aggregation by nearly 80 % (Fig. 4.2.6).

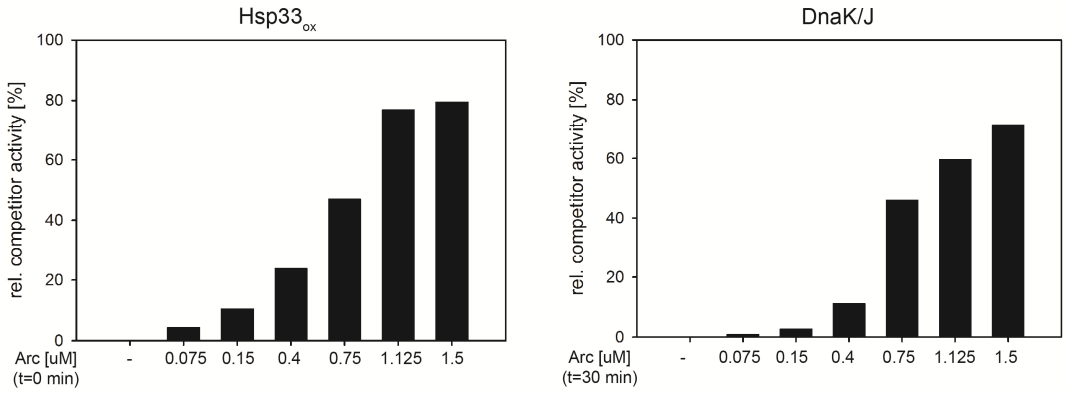

Fig. 4.2.6: Arc's relative competitor activity is concentration dependent
The ability of increasing concentrations of Arc on competing with chemically unfolded citrate synthase (75 nM) for binding to $Hsp33_{ox}$ (150 nM) 0 min after initiation of unfolding or to DnaK/J (187 nM and 75 nM) 30 min after initiation of unfolding, was tested by measurement of light scattering of citrate synthase.

These results demonstrated that Arc is indeed a client protein for both Hsp33 and the DnaK/J system. To test if there was indeed a correlation between the extent of Arc unfolding and its ability to serve as competitor for either Hsp33 or the DnaK/J system, we initiated unfolding of Arc (0.75 µM) and added Hsp33 (150 nM) or the DnaK/J (187 nM and 75 nM respectively) at distinct time points to allow complex formation between Arc and the chaperone. After 10 sec, chemically denatured CS was added and light scattering was monitored.

We predicted that if Hsp33 interacted with folding intermediates that are more structured, Arc would serve as an inhibitor at its early stages of unfolding. DnaK/J, however, which prefers unfolded polypeptide chains, should interact with Arc at later stages of Arc's unfolding process. A 10-fold molar excess of Arc (0.75 µM) towards chemically unfolded citrate synthase (75 nM) was chosen for competition assays (Fig. 4.2.7).

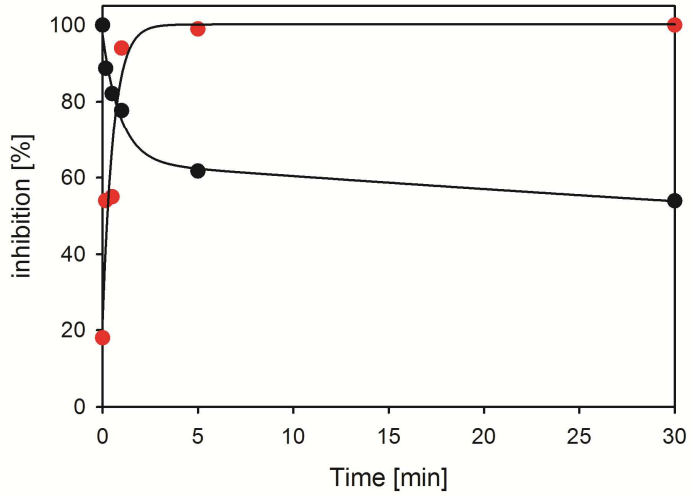

Fig. 4.2.7: Arc competitor activity depends on its folding status
At defined time points during Arcs unfolding (0.75 µM), Hsp33 (150 nM) or DnaK/J (187 nM and 75 nM) were added and complex formation was allowed for 10 seconds, followed by adding 75 nM of chemically denatured citrate synthase. Light scattering of citrate synthase was monitored.

As shown in figure 4.2.7, the ability of $Hsp33_{ox}$ to interact with Arc decreased with increasing unfolding of Arc (Fig 4.2.5), whereas DnaK/J's ability to interact with Arc increased over the course of unfolding. These results, together with the results obtained by Winter et al. strongly supported our hypothesis that Hsp33 and the DnaK/J system share the ability to bind to the same substrate protein but that they significantly differ in their folding state specificity (Hoffmann et al., 2004; Winter et al., 2005).

4.2.4 Substrate transfer from Hsp33 to the DnaK/J/E system

These results led us to the next step in Hsp33's chaperone cycle, the client protein transfer from Hsp33 to the DnaK/J/E system. Hsp33 is a chaperone holdase that keeps proteins in a folding competent state during stress conditions. Upon return to non-stress conditions, the bound clients are released. Previous studies showed that reduction of Hsp33's C-terminal redox switch domain is necessary but not sufficient for client protein release (Hoffmann et al., 2004). Reducing conditions and a functional DnaK/J/E system are both needed for the release of client proteins and their subsequent refolding to a native state.

Dana Reichmann together with Ying Xu investigated the effects that reduction had on the complex between $Hsp33_{ox}$ and citrate synthase or luciferase. By using limited proteolysis and SUPREX analysis they found that return of the Hsp33-client protein complex to reducing conditions leads to conformational changes in the client protein, consistent with increased destabilization and unfolding (Reichmann et al., 2012). This effect is not due to changes in the thiol status of the client proteins but appears to be triggered by the refolding of Hsp33's C-terminal redox switch domain after reduction of its four conserved cysteines (Reichmann et al., 2012). As outlined above, a more unfolded client protein is favored by the DnaK/J system. These results suggested that Hsp33 might change the structure of the bound client into a more unfolded conformation upon reduction, essentially converting the client protein into a suitable substrate of the DnaK/J system.

To study the client protein transfer from Hsp33 to the DnaK/J system in more detail, we conducted refolding studies of chemically unfolded luciferase in the presence of $Hsp33_{ox}$. Luciferase unfolds when incubated for 90 min in 4.5 M guanidine hydrochloride at pH 7.8. Dilution into ATP-containing refolding buffer does not lead to spontaneous refolding of the luciferase in the presence of 2 mM DTT (Fig. 4.2.8, triangles). Dilution of chemically denatured luciferase into buffer containing the DnaK/J/E system led to refolding of about 75 % of luciferase activity with a $T_{1/2}$ of 4.5 min. The presence of DTT slightly increased the refolding yield without affecting the rate of refolding (Fig. 4.2.8, open and close circles). These results nicely correlated with earlier studies conducted in the lab (Hoffmann et al., 2004).

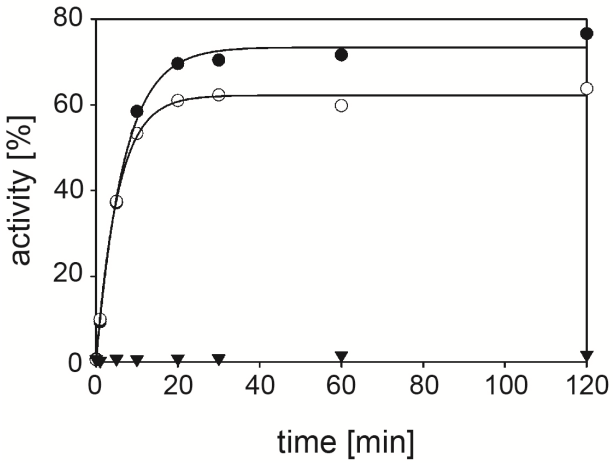

Fig. 4.2.8 Refolding of luciferase by the DnaK/J/E chaperone system
Chemical denatured luciferase (75 nM) was diluted into refolding buffer containing DnaK (750 nM), DnaJ (150 nM), and GrpE (750 nM) with (closed circle) or without 2 mM DTT (open circle) or just refolding buffer with 2 mM DTT (triangle). At indicated time points, samples were removed and luciferase activity was determined.

Hoffmann et al. also showed that Hsp33 itself does not support the refolding of luciferase. Instead, $Hsp33_{ox}$ forms very stable complexes with luciferase and does not release luciferase unless reducing conditions and the DnaK/J/E system are present (Hoffmann et al., 2004). We confirmed also these results and showed that in the presence of reducing conditions and the DanK/J/E system, luciferase regains about 55 % of its enzymatic activity. The $T_{1/2}$ of this reaction was found to be about 12.5 min and hence slightly slower than in the absence of Hsp33 (Fig. 4.2.9, left graph, closed circles compare to Fig. 4.2.8, closed circles).

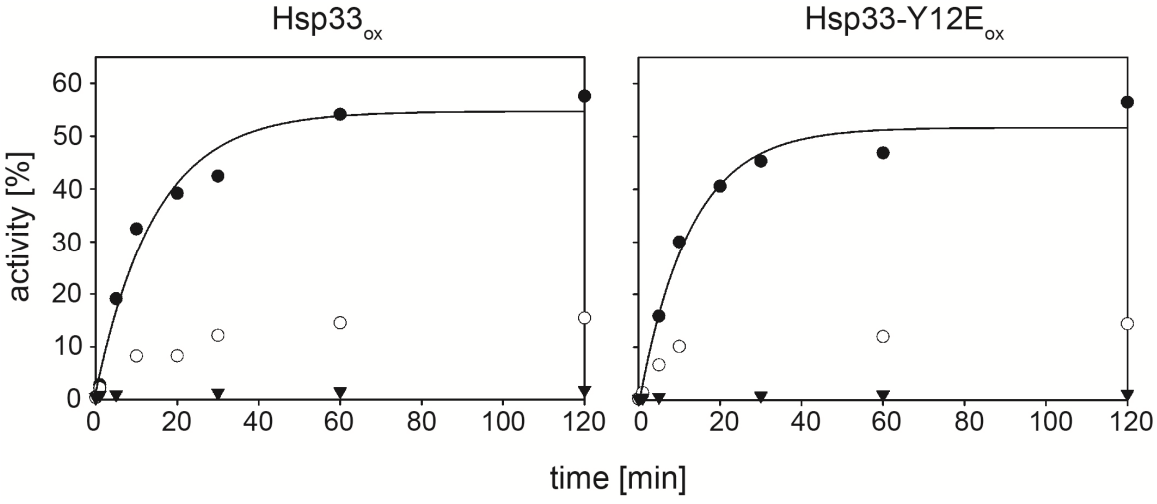

Fig. 4.2.9: Refolding of luciferase transfer from $Hsp33_{ox}$ and Hsp33-$Y12E_{ox}$ to the DnaK/J/E system

Chemical denatured luciferase (75 nM) was diluted into refolding buffer containing 300 nM $Hsp33_{ox}$ or Hsp33-$Y12E_{ox}$, complex formation was allowed for 10 min. The influence of addition of DnaK (750 nM), DnaJ (150 nM), and GrpE (750 nM) with (closed circle) or without 2 mM DTT (open circle) or just refolding buffer containing 2 mM DTT (triangle) was monitored.

In chapter 4.1, we described the Hsp33-Y12E mutant of Hsp33, which is constitutively active both *in vivo* and *in vitro* despite its reduced zinc binding domain (Cremers et al., 2010). This mutant protein provided us with the opportunity to monitor substrate transfer from a reduced chaperone-active version of Hsp33 to the DnaK/J/E system, eliminating the need of any reductant. We reasoned that if this mutant protein behaved like $Hsp33_{ox}$ upon reduction, substrate transfer should occur without the need for reductants. If, however, the mutant behaved like the oxidized protein, then addition of DTT would not cause client release or refolding. First, we confirmed that HOCl-oxidized Hsp33-$Y12E_{ox}$ behaved the same way as activated wild type $Hsp33_{ox}$ (Fig. 4.2.9, right graph). Reactivation of luciferase required both the DnaK/J/E system and reducing agents and the final yield of luciferase activity was about 55 % ($T_{1/2}$ = 12.5 min). These results showed that the introduced mutation does not alter the ability of the chaperone to transfer its substrate to the DnaK-refolding machinery.

We then went on to analyze the potential substrate transfer from the reduced, chaperone active form of Hsp33-Y12E to the DnaK/J/E system. As before, we let the complex between the two proteins form for 10 min. Then the DnaK/J/E system was added with or without 2 mM DTT and luciferase refolding was monitored. As shown in Fig. 4.2.10, we found that the DnaK/J/E system is able to refold luciferase presented by Hsp33-$Y12E_{red}$ without the need of reducing agents. It is of note that the luciferase refolding kinetic proceeded without the initial lag phase, which was characteristic for the refolding in the presence of wild type $Hsp33_{ox}$ (Fig. 4.2.9). These results suggest that disulfide bond reduction, which proceeds with a $T_{1/2}$ of about 2 min (Hoffmann et al., 2004; Winter et al., 2008) is rate limiting for the release/refolding of luciferase and likely responsible for the observed lag phase. The final refolding yield of luciferase was about 50 % of the initial

luciferase activity when DTT was present (Fig. 4.2.10, closed circle), and about 40% when no DTT was added (Fig. 4.2.10, open circle). This result is consistent with the results obtained with the DTT-dependence of the DnaK/J/E system, suggesting that this effect is due to DTT-mediated changes in DnaK's activity. The halftime of the refolding reaction was found to be about 8 min for Hsp33-Y12E$_{red}$, and about 12.5 min for Hsp33-Y12E$_{ox,}$ which again is consistent with the fact that reduction of Hsp33's cysteines affects the rate of luciferase refolding.

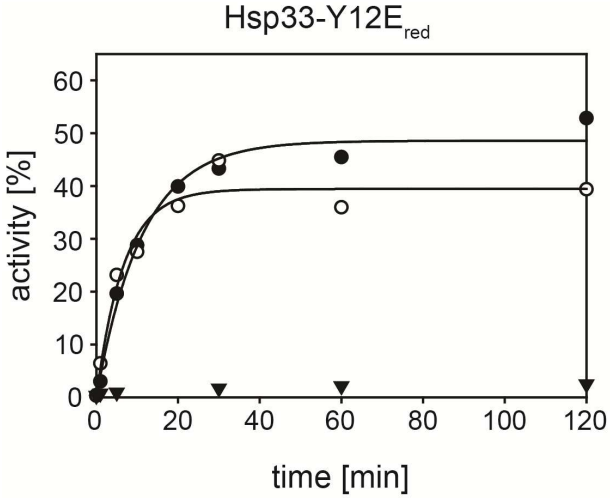

Fig. 4.2.10: Refolding of luciferase transfer from Hsp33-Y12E$_{red}$ to the DnaK/J/E chaperone system

Chemical denatured luciferase (75 nM) was diluted into refolding buffer containing 300 nM Hsp33$_{ox}$, complex formation was allowed for 10 min. The influence of addition of DnaK (750 nM), DnaJ (150 nM), and GrpE (750 nM) with (closed circle) or without 2 mM DTT (open circle) or just refolding buffer with 2 mM DTT (triangle) was monitored. At indicated time points samples were removed and luciferase activity was determined.

Reichmann et al. recently described that the re-reduction of the complex between Hsp33$_{ox}$ and the client protein leads to the further stabilization of Hsp33's zinc binding domain, which alters the conformation of the client protein and leaves it in a more unfolded form, a condition that makes the substrate more favorable for the DnaK/J/E system (Reichmann et al., 2012; Rüdiger et al., 1997b). It is now tempting to speculate that this conversion of the client protein to a more unfolded state lowers Hsp33's affinity for the client protein and hence favors client protein release. Peptide binding studies using

the Hsp33Y12E mutant variant will reveal whether the reduced form of Hsp33 has indeed lower affinity for clients or different client specificity.

4.2.5 Conclusion

A unique feature that some stress-activated chaperone holdases seem to share is their ability to convert large parts of their structure into intrinsically disordered regions after encountering a specific stress condition (Ilbert et al., 2007; Tapley et al., 2009b; Winter et al., 2008). Taking on a state of native disorder parallels their activation as chaperones. One model that was proposed suggested that hydrophobic interfaces in these chaperones might serve double duty – as stabilizing interfaces of the intrinsically disordered regions under non-stress conditions and as potential client protein binding sites when unfolding of the chaperones unmask these sites (Ilbert et al., 2007; Reichmann et al., 2012; Tapley et al., 2009b; Tyedmers et al., 2010). This model, however, implied that the unfolded regions in the chaperone remain unfolded during client binding, raising the question as to how the chaperone holdases distinguish between their own unfolded regions and the unfolded client proteins. And why are these regions not client proteins of chaperone foldases? By studying Hsp33, we were able to find answers to these fundamental questions. We showed that Hsp33 uses parts of its own intrinsically disordered region, the 55 amino acid long linker region, to bind to its unfolding client proteins. This interaction stabilizes the intrinsically unfolded part of Hsp33, and prevents the further unfolding and aggregation of the client protein. The disordered status of the linker region provides Hsp33 with the possibility to bind a wide variety of different binding partners, without requiring sequence specificity. This result fits to results obtained by Jaya et al., who showed that the small heat shock protein PsHsp18-1 binds to a wide variety of unfolded proteins with its own unfolded N-terminal arm (Jaya et al., 2009).

The experiments conducted here revealed that Hsp33 preferably binds to client proteins with residual structure, such as proteins that are early on the unfolding pathway. It has been shown that intrinsically unfolded proteins interact with structured macromolecules, such as proteins, DNA, or membranes by using these binding partners as stabilizing scaffolds that

promote the refolding of the intrinsically disordered regions (Tompa and Csermely, 2004). Reichmann et al. revealed that this is indeed the case for Hsp33; binding of partially unfolded client proteins leads to the stabilization of Hsp33's unfolded linker region (Reichmann et al., 2012).

Another notable feature in Hsp33's substrate recognition is the discrimination against amino acids that are mainly found in unstructured regions of proteins. These amino acids (Glu, Asp, Cys and Lys) are also highly abundant in Hsp33's intrinsically disordered redox switch domain (Reichmann et al., 2012). Therefore it can be argued that Hsp33's redox sensor is designed to not compete with its own client proteins.

Hsp33 as a chaperone holdase relies on foldase systems, like DnaK/J/E for client protein refolding upon return to non-stress conditions. In contrast to Hsp33, DnaK preferentially binds to short hydrophobic unstructured regions, which are presented by newly emerging polypeptides exiting the ribosome or by unfolded client proteins, which accumulate during stress conditions (Bukau and Horwich, 1998; Deuerling et al., 1999; Mayer et al., 2000; Reichmann et al., 2012; Rüdiger et al., 1997a). This difference in peptide binding specificity raised the question, however, as to how the client transfer from the holdase to the foldase system is regulated. Tompa originally proposed that refolding of intrinsically disordered regions might provide entropic energy necessary to unfold the bound client proteins (Tompa and Csermely, 2004). Hsp33's binding to client proteins and the concomitant stabilization of its own linker region does not seem to cause unfolding of the client protein, as the DnaK/J/E system is unable to release and refold clients in complex with oxidized Hsp33. Yet, it appears that reduction of Hsp33's C-terminal redox switch domain upon return to non-stress conditions might be the trigger to cause unfolding of the client proteins. It is so far still unclear whether the C-terminal domain of Hsp33 is completely refolded but it appears that zinc is reconstituted and most proteolytic sites reveal the same accessibility as in reduced Hsp33 (Reichmann et al., 2012). These results clearly suggest a more compact structure of Hsp33 compared to the oxidized form. It is possible that the refolding of Hsp33's C-terminal redox switch domain serves three purposes:

1) to unfold the client, converting it into a client protein for refolding by the DnaK/J/E system; 2) to foster interaction between Hsp33 and the DnaK/J/E system, necessary for client release; 3) to lower the affinity of Hsp33 for its client proteins, so that the transfer can happen. Detailed biochemical studies with the respective mutant variants of Hsp33 are needed to address these questions.

4.3 The antimicrobial effects of bile salts

4.3.1 Bile salts induce protein unfolding *in vitro*

Bile salts are described as ‘soft detergents’ as they are frequently used for purification of membrane proteins (Hjelmeland, 1980; Tofani et al., 2004). However, De et al. showed in 2007 that cooperative binding of bile salts, in particular Na-Cholate (Na-Cho) and Na-Deoxycholate (Na-DOC), lead to structural changes in bovine serum albumin (De et al., 2007). They concluded that protein-bile interactions lead to a loss of α-helical structure, an increase in random coil and a shift and decrease in Trp-fluorescence, all indicative for protein unfolding (De et al., 2007). Several other papers agreed with these results and described the cooperative interaction of bile salts with bovine serum albumin and human serum albumin, which altered the structure of the proteins without causing protein aggregation (Pico and Houssier, 1989; Schweitzer et al., 2006).

Here we show that Na-Cho or Na-DOC induces changes in the protein structure of malate dehydrogenase (MDH), citrate synthase (CS), and luciferase, causing a loss in enzymatic activity. The effects of Na-Cho or Na-DOC on the structure of proteins appear to depend on the thermal stability of the proteins. The more stable the protein, the less pronounced is the effect of Na-Cho or Na-DOC on the structure of the protein. Moreover, we discovered that bile salts can induce irreversible protein aggregation, which is surprising as bile salts are thought to have detergent-like character. Hsp33, which is activated by bile salts both *in vitro* and *in vivo*, protects unfolding proteins against this irreversible aggregation and enhances bacterial resistance toward bile salts.

The results described in this chapter are going to be published in a publication currently in preparation. I performed all experiments besides the HPLC runs for the GSH/GSSG ratios were done by Victor Vitvitsky. I wrote the manuscript, which was edited by U. Jakob.

4.3.1.1 Effect of Na-Cho and Na-DOC on the structure and function of malate dehydrogenase (MDH)

The critical micelle concentration (CMC) of bile salts varies and depends on pH, temperature, salt concentration, solvents, and on the technique used to determine the CMC (Reis et al., 2004). In this study, we typically used 14 mM Na-Cho or 5 mM Na-DOC, which are concentrations that are slightly above the average CMC in comparable buffer systems.

Malate dehydrogenase is an *in vitro* client protein for many chaperones as it readily unfolds at temperatures above 43°C. To test whether bile salts have any effect on this protein, we recorded far-UV CD spectra to capture potential changes in the protein's secondary structure. At 30°C, no significant changes in the secondary structure of MDH were detected (Fig. 4.3.1). Upon shift of the temperature towards 37°C, however, incubation of MDH with either Na-Cho or Na-DOC led to substantial changes in the secondary structure, corresponding to a loss of α-helices (Fig.4.3.1, dotted line). The effects of Na-Cho on the structure of malate dehydrogenase appeared to be more pronounced (Fig.4.3.1, dashed line) than the structural changes induced by Na-DOC. These studies reveal, for the first time, structural changes in proteins other than bovine serum albumin or human serum albumin.

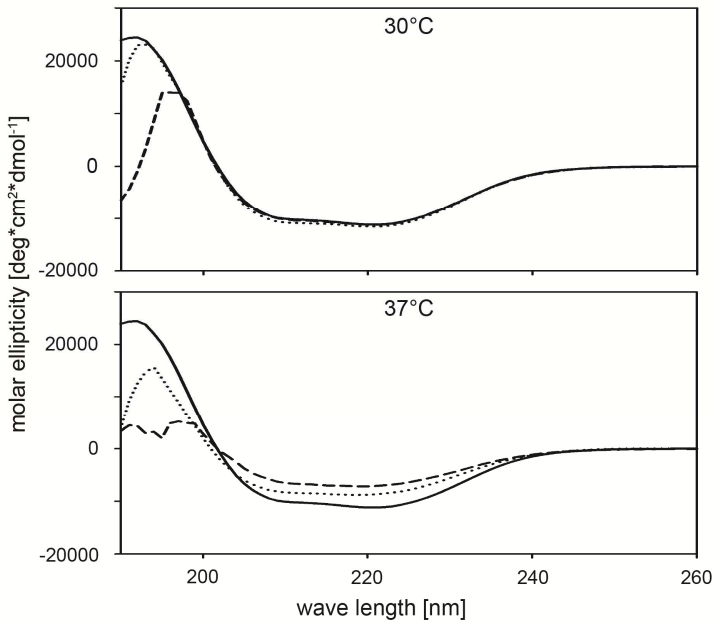

Fig. 4.3.1: Structural changes of malate dehydrogenase upon incubation in Na-Cho or Na-DOC at 30°C and 37°C

Changes in MDH's secondary structure were monitored by far-UV CD spectroscopy. 5.7 µM MDH was incubated with no detergent (solid line), 14 mM Na-Cho (dashed line), or 5 mM Na-DOC (dotted line) at 30°C or 37°C. After 1 hour incubation, far-UV CD spectra were recorded to determine the structural changes induced by the detergents.

To determine whether the changes in MDH's secondary structure have any effect on the function of the enzyme, we investigated the enzymatic activity of MDH in the absence and presence of bile salts. In the activity assay, the conversion of oxaloacetate to malate is measured by the rate of consumption of NADH, which is spectroscopically active at 340 nm. Incubation of MDH at 37°C led to a minimal (<10%) loss of enzymatic function in the absence of bile salts within the 90 min of the experiment (Fig. 4.3.2, circle). Incubation of MDH in the presence of Na-Cho (Fig. 4.3.2, squares) or Na-DOC (Fig. 4.3.2, triangle), however, led to a dramatic loss in function and the enzymatic activity dropped to about 20 %.

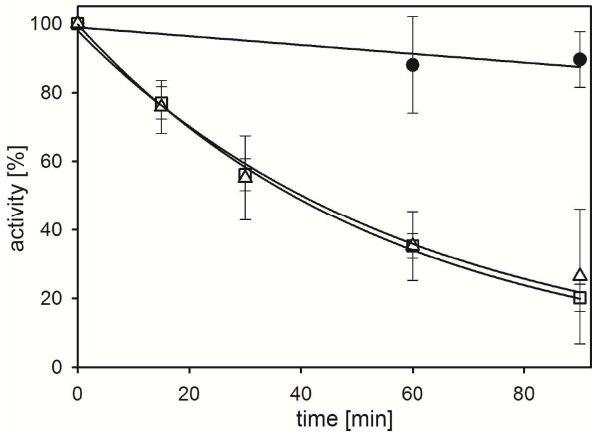

Fig. 4.3.2: Loss of enzymatic activity of malate dehydrogenase upon exposure to Na-Cho or Na-DOC at 37°C

Incubation of MDH (12 µM) in the absence of bile salts (circles) or in the presence of 14 mM Na-Cho (squares) or 5 mM Na-DOC (triangles) at 37°C. Absorbance a 340 nm was measured to determine the rate of NADH consumption by active MDH.

To assess whether the observed bile salt-induced unfolding of MDH leads also to protein aggregation, we incubated 12 µM MDH with 14 mM Na-Cho at 37°C and measured light scattering. Although bile salts are generally thought of as 'soft surfactants', which solubilize membrane proteins without affecting

their activity, we found that incubation of MDH with Na-Cho at 37°C causes significant aggregation of the enzyme (Fig. 4.3.3, insert). This was in contrast to Na-DOC, which induced structural changes (Fig. 4.3.1) but did not cause immediate MDH aggregation. Here, dilution of the Na-DOC incubated protein into bile salt-free buffer caused the rapid aggregation of MDH. These results provide first evidence that individual bile salts affect proteins differently. These are very novel findings as bile salts have not been previously reported to cause protein aggregation (De et al., 2007; Pico and Houssier, 1989; Schweitzer et al., 2006)

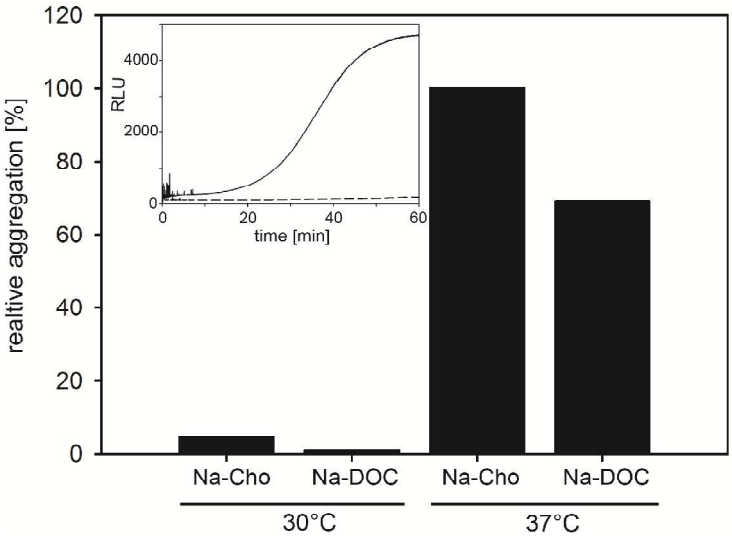

Fig. 4.3.3: Aggregation of malate dehydrogenase after removal of bile salt
12 µM malate dehydrogenase was incubated with 14 mM Na-Cho or 5 mM Na-DOC at either 30°C or 37°C. Aggregation was determined spectroscopically after 1:24 dilution into buffer containing no subsequent bile salts (final concentration 500 nM).
Insert: Aggregation of malate dehydrogenase during the exposure to Na-Cho and Na-DOC at 37°C.
12 µM malate dehydrogenase was incubated with 14 mM Na-Cho or 5 mM Na-DOC at 37°C and protein aggregation was measured spectroscopically over the time course of an hour. At 30°C no aggregation was observed (data not shown).

In agreement with our CD and activity measurements, we did not observe any significant MDH aggregation in the presence of Na-Cho or Na-DOC upon incubation at 30°C (Fig. 4.3.3). It is conceivable that bile salts and temperatures have an additive effect in destabilizing MDH. Hence, bile salt-mediated destabilization at 30°C might not be severe enough to cause detectable protein unfolding. However, upon increasing in temperature to

37°C, the additive destabilization by bile salts might affect the stability of MDH enough to cause significant unfolding and protein aggregation. Taken together we show that Na-Cho and Na-DOC, two common bile salts, affect the structure and function of malate dehydrogenase at physiological temperatures.

4.3.1.2 Interaction between Na-Cho and Na-DOC leads to the unfolding and aggregation of citrate synthase

To test whether bile salts have a general ability to unfold proteins and cause protein aggregation, we tested the influence of bile salts on citrate synthase, another commonly used chaperone client. As before, we determined the influence of Na-Cho and Na-DOC on the structure of citrate synthase by far-UV CD spectroscopy. We observed slight changes in the secondary structure content of citrate synthase upon incubation with Na-Cho at 30°C, which significantly increased upon incubation at 37°C. In contrast, we did not observe any significant changes in CS structure upon incubation in Na-DOC at 30°C and only very slight changes at 37°C (Fig. 4.3.4). Direct structural analysis using CD analysis programs was not possible because the presence of the bile salts in the solution interfered with the measurements of the CD spectra at wavelengths lower than 200 nm.

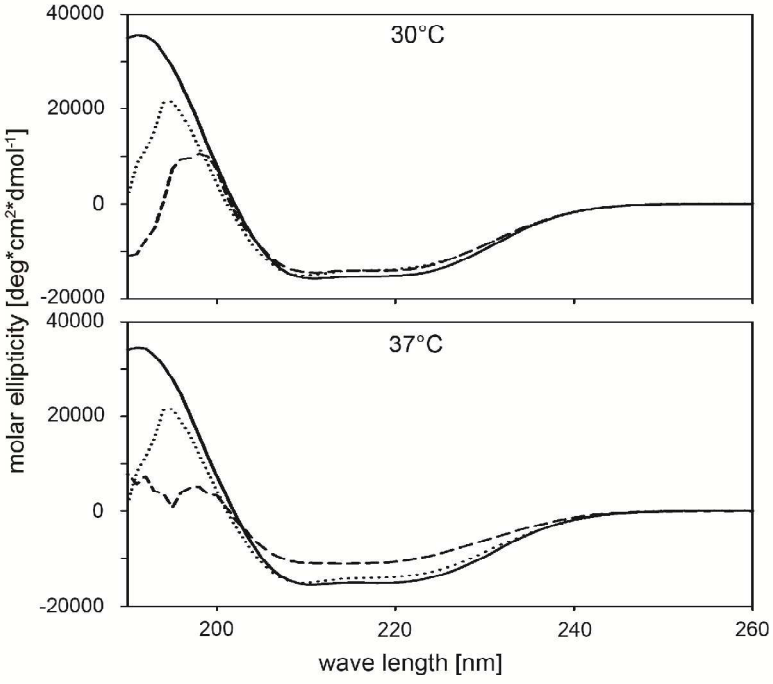

Fig. 4.3.4: Structural changes of citrate synthase when incubated with Na-Cho or Na-DOC at 30°C or 37°C

Changes in citrate synthase's secondary structure were monitored with far-UV CD spectroscopy. 4 µM protein was incubated with no detergent (solid line), 14 mM Na-Cho (dashed line), or 5 mM Na-DOC (dotted line) at 30°C or 37°C. After 1 hour far-UV CD spectra were collected at the respective temperatures to determine the structural changes induced by the detergent.

Light scattering measurements agreed well with our CD measurements and showed that incubation of citrate synthase (12 µM) with 14 mM Na-Cho at 37°C unfolds the protein to an extent that leads to a slow increase in protein aggregation in the presence of Na-Cho (Fig. 4.3.5, insert) and even higher aggregation when CS is incubated in Na-Cho for one hour and then diluted into bile salt-free buffer. As expected, the extent of aggregation was significantly lower when the incubation of citrate synthase with Na-Cho was conducted at 30°C. Incubation with Na-DOC at 30°C did not cause any aggregation while incubation at 37°C caused some aggregation when the bile salts were removed (Fig. 4.3.5).

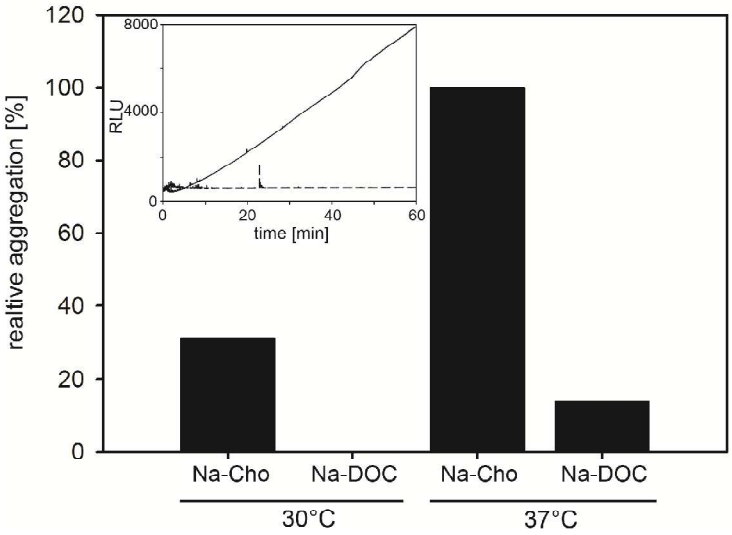

Fig. 4.3.5: Extent of aggregation of citrate synthase upon removal of bile salt

12 µM citrate synthase was incubated with 14 mM Na-Cho or 5 mM Na-DOC at either 30°C or 37°C. Aggregation was determined spectroscopically after 1:32 dilution into a buffer containing no subsequent bile salts (final concentration 375 nM).
Insert: Aggregation of citrate synthase during the exposure to Na-Cho or Na-DOC at 37°C

12 µM citrate synthase was incubated with 14 mM Na-Cho or 5 mM Na-DOC at 37°C and protein aggregation was measured spectroscopically over the time course of an hour. At 30°C no aggregation was observed (data not shown).

4.3.1.3 Na-Cho and Na-DOC leads to the unfolding of luciferase at 30°C

Luciferase is the most thermally unstable chaperone client protein tested here, as it starts to unfold at temperatures as low as 39°C. Incubation of luciferase with either 14 mM Na-Cho or 5 mM Na-DOC caused dramatic changes in the secondary structure of the protein already at 30°C. We observed a significant loss in α-helical structure and an increase in random coil formation (minimum at 207 nm) (Fig. 4.3.6). In comparison to the other proteins described in this study, this is the only time that the loss of α-helical structure is indeed accompanied by a visible increase in random coil structure.

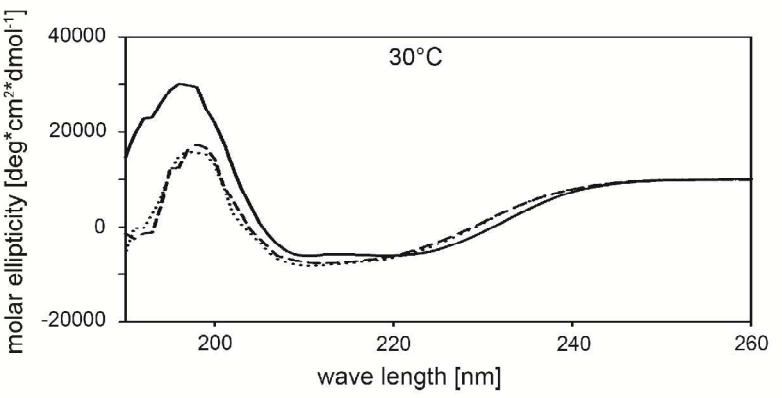

Fig. 4.3.6: Structural changes of luciferase when incubated with Na-Cho or Na-DOC at 30°C

3.3 µM luciferase was incubated in the absence of detergent (solid line), or in the presence of either 14 mM Na-Cho (dashed line), or 5 mM Na-DOC (dotted line) at 30°C. After 1 hour far-UV CD spectra were collected at 30°C to determine the structural changes induced by the bile salts.

The dramatic changes in the structure of luciferase induced by Na-Cho and Na-DOC parallel the rapid loss of its enzymatic activity (Fig. 4.3.7 squares and triangles respectively). Within 20 min of incubation of luciferase with these bile salts, no residual luciferase activity was observed.

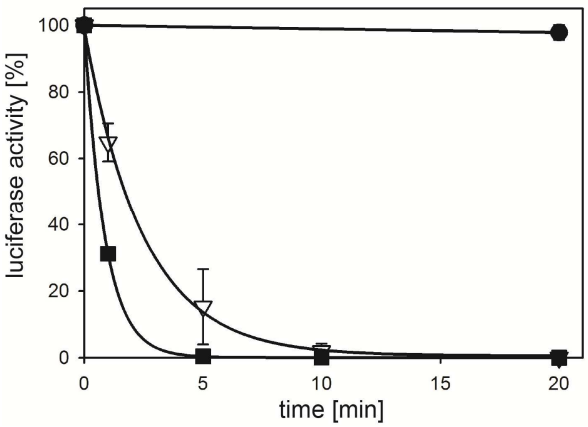

Fig. 4.3.7: Loss of luciferase activity upon incubation with Na-Cho or Na-DOC at 30°C

Luciferase (75 nM) was incubated in the absence of bile salts, or with 14 mM Na-Cho (triangles) or 5 mM Na-DOC (squares) at 30°C. At the indicated time points, aliquots were taken and the luciferase activity was determined.

To determine whether luciferase aggregates in the presence of bile salts or upon its dilution into bile salt free buffer, we monitored light scattering at 30°C. No aggregation of luciferase was detected in the presence of either 14 mM Na-Cho or 5 mM Na-DOC over 60 min of incubation. However, when diluted into buffer containing no bile salts, luciferase rapidly aggregated (Fig. 4.3.8). The aggregation kinetics of Na-Cho-incubated luciferase (dotted line) was faster than the aggregation kinetics following dilution of luciferase from Na-DOC (dashed line).

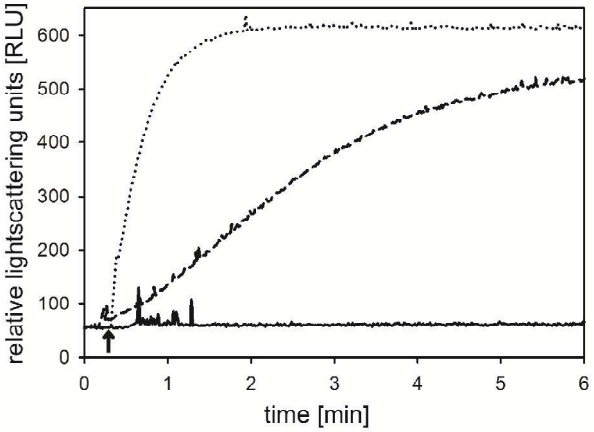

Fig. 4.3.8: Aggregation kinetics of luciferase after incubation in Na-Cho or Na-DOC at 30°C

Luciferase (12 µM) was incubated in the absence of bile salts (solid line) or in the presence of 14 mM Na-Cho (dotted line) or 5 mM Na-DOC (dashed line) for 1 hour at 30°C respectively. Luciferase was then diluted into buffer with a final concentration of 75 nM (as indicated with an arrow) and light scattering was monitored.

Incubation of luciferase and bile salts at 37°C led to even more dramatic structural changes and the aggregation of luciferase even in the presence of Na-Cho or Na-DOC (data not shown). This result confirms our previous conclusions and demonstrates that the effects of bile salts on the structure and function of proteins increase with temperature.

4.3.2 Effects of bile salts on the molecular chaperone Hsp33

Our results showed that bile salts can directly alter the structure of thermolabile proteins and lead to protein aggregation. This raised the question whether molecular chaperones are capable of preventing this bile salt-induced protein aggregation. With this question in mind, we set out to first investigate the effects of bile salts on the activation of the molecular chaperone Hsp33. Reduced, inactive Hsp33 ($Hsp33_{red}$) was incubated with 14 mM Na-Cho or 5 mM Na-DOC at 43°C. After 1 hour of incubation, Hsp33's ability to prevent the aggregation of chemically denatured citrate synthase was tested. Incubation of Hsp33 with H_2O_2 at 43°C served as positive control (Fig. 4.3.9). As shown in Fig. 4.3.9 neither incubation with Na-Cho nor Na-DOC alone caused the activation of $Hsp33_{red}$. In contrast, however, incubation of $Hsp33_{red}$ in the presence of 14 mM Na-Cho or 5 mM Na-DOC and 2 mM peroxide rapidly activated the chaperone at temperatures as low as 30°C (Fig. 4.3.9). These results fully agreed with our previous studies, which showed that activation of Hsp33 requires the presence of both, oxidants and protein unfolding conditions and suggests that both Na-Cho and Na-DOC induce unfolding conditions that shift Hsp33's linker region towards a more unfolded state (Fig. 4.3.9).

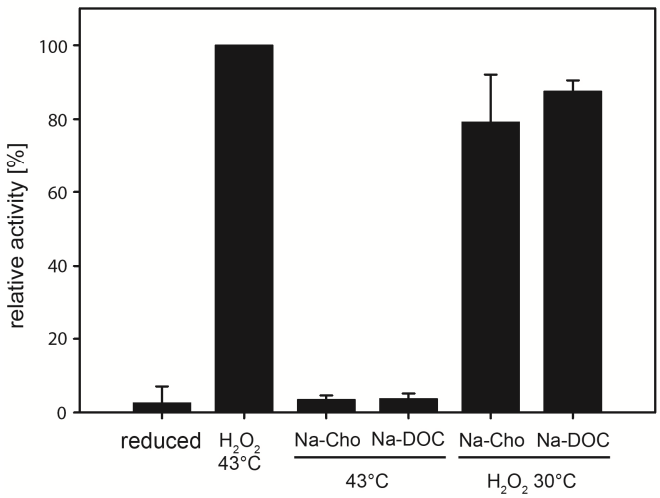

Fig. 4.3.9: Hsp33 activation due to exposure to Na-Cho and Na-DOC
$Hsp33_{red}$ (50 µM) was incubated with 14 mM Na-Cho or 5 mM Na-DOC at either 43°C for 1 hour or 30°C with 2 mM H_2O_2 for 3 hours respectively. After the incubation chaperone activity was measured by the suppression of chemically unfolded citrate synthase aggregation. A positive control for chaperone activity served Hsp33 oxidized at 43°C with 2 mM H_2O_2 (3 h), as a negative control inactive, reduced Hsp33 was used.

Our demonstration that Na-Cho and Na-DOC can mimic the unfolding conditions necessary for Hsp33's activation raised the question whether bile salts unfold Hsp33's linker region. To address this question, we conducted co-incubation studies between Hsp33, the client protein luciferase and bile salts. We reasoned that if bile salts induced unfolding of the linker region, $Hsp33_{red}$ should be active as a chaperone as long as bile salts are present. We thus set up co-incubation reactions of $Hsp33_{red}$ in a four-fold molecular access to luciferase at 30°C. Then, the respective bile salts were added. After 1 hour of co-incubation, we diluted the proteins and determined the aggregation of luciferase by light scattering (fig. 4.3.11, + label). As a control, we used Na-Cho or Na-DOC unfolded luciferase, and diluted it into buffer containing reduced Hsp33 (fig. 4.3.11, - label). Co-incubation of $Hsp33_{red}$ and luciferase with Na-Cho did not lead to inhibition of luciferase aggregation upon dilution, suggesting that Na-Cho was unable to unfold Hsp33's linker region to an extent that would cause activation of Hsp33. In contrast, co-incubation of $Hsp33_{red}$, luciferase and Na-DOC at 30°C led to a partial inhibition of luciferase aggregation upon dilution. If luciferase was incubated with bile salts in the absence Hsp33, and diluted into buffer containing inactive $Hsp33_{red}$, no

inhibition of aggregation was observed. These results suggest that Na-DOC is able to unfold the linker region of Hsp33.

To test whether the Na-DOC mediated unfolding of Hsp33's linker region is reversible, we diluted the Na-DOC treated Hsp33 into bile salt-free buffer and tested its chaperone activity. No inhibition of the aggregation of chemically unfolded citrate synthase was observed, suggesting that the linker unfolding is reversible (figure 4.3.9). It is important to note that HOCl-activated $Hsp33_{ox}$ is able to prevent the aggregation of MDH and CS when co-incubated at 37°C with Na-Cho. This result indicates that the unfolding and subsequent aggregation of Hsp33's client proteins occurs via unfolding intermediates that are recognized by bleach activated $Hsp33_{ox.}$

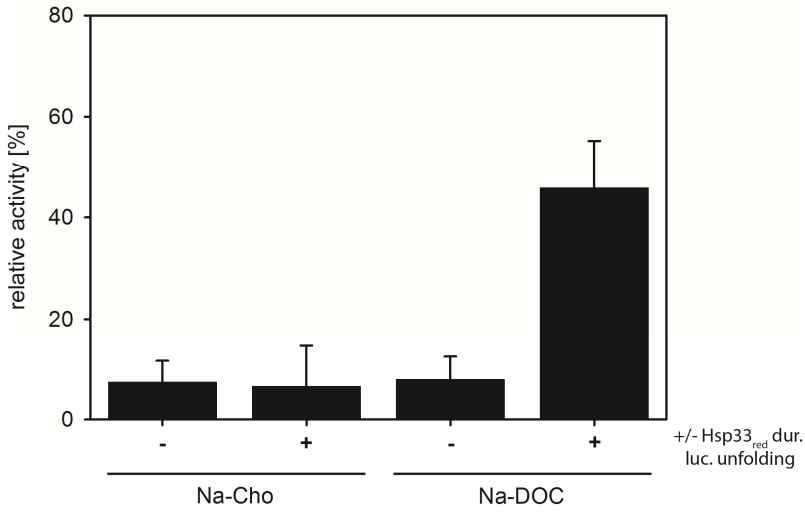

Fig. 4.3.10: Unfolding of Hsp33's linker leads to client binding
$Hsp33_{red}$ (48 µM) was co-incubated with 12 µM luciferase in the presence of either 14 mM Na-Cho or 5 mM Na-DOC at 30°C. After one hour of incubation, the proteins were diluted and light scattering of luciferase was monitored. 100 % activity corresponds to Na-Cho or Na-DOC unfolded luciferase diluted into buffer containing $Hsp33_{ox}$, which inhibited Luciferase aggregation, 0 % activity correspond to the signal obtained, if Na-Cho or Na-DOC unfolded luciferase aggregated in buffer not containing any chaperones.

To directly monitor the unfolding of Hsp33's linker region in response to Na-DOC treatment, we conducted tryptophan measurements. As described in chapter 4.1.4, wild type Hsp33 harbors one tryptophan in its linker region at position 212. Mutation of this residue to phenylalanine and introduction of F187 to tryptophan leads to the Hsp33-F187W W212F mutant variant, whose

linker (un)folding can be directly monitored by tryptophan fluorescence (Ilbert et al., 2007). If Hsp33 is reduced and inactive, the linker is compactly folded on top of Hsp33's N-terminal domain (Graf, 2004; Vijayalakshmi et al., 2001) and the tryptophan is buried within the nonpolar environment of the protein (Fig. 4.3.11, solid line). Activation of Hsp33 leads to unfolding of the linker region, which is reflected by the exposure of W187 to the polar environment of the solvent as indicated by a decrease in tryptophan emission and a dramatic red shift to 346 nm (Fig. 4.3.11, dotted-dashed line). We thus incubated 5 µM Hsp33-F187W W212F$_{red}$ with either 14 mM Na-Cho or 5 mM Na-DOC at 30°C for one hour and monitored the tryptophan fluorescence. In full agreements with our activity studies, we found that incubation of reduced Hsp33-F187W W212F with Na-Cho showed no dramatic change on the Trp-fluorescence spectrum while incubation with Na-DOC yielded in a spectrum that was very similar to the spectrum of activated Hsp33-F187W W212F (Fig. 4.3.11). These results strongly suggest that Na-DOC causes the unfolding of Hsp33's linker region.

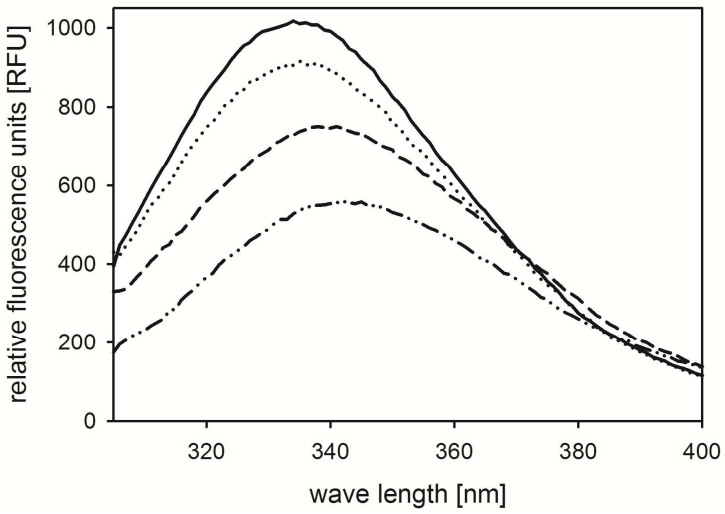

Fig. 4.3.11: Unfolding of Hsp33's linker due to the exposure to Na-DOC
Tryptophan fluorescence of 5 µM Hsp33-F187W W212F in its reduced form (solid line) or upon 3 h oxidation with 2 mM H_2O_2 at 43°C (dotted-dashed line). The spectra were recorded at 30°C. Changes in the linker region upon incubation with 14 mM Na-Cho (dotted line) or 5 mM Na-DOC (dashed line) were determined after one hour of incubation at 30°C.

Taken together, these data suggest that Hsp33 can be directly activated by the presence of Na-DOC, which shifts the folding status of the linker region

towards the unfolded conformation. As shown in chapter 4.1 of this thesis, unfolding of Hsp33's linker region is crucial for its activation as a chaperone. However, to lock Hsp33 in a permanently activated state, simultaneous presence of unfolding conditions (Na-DOC) and oxidants are needed (Ilbert et al., 2007). On the contrary, Na-Cho can only activate Hsp33 in the presence of H_2O_2. When H_2O_2 is present, it seems that Na-Cho is able to shift the equilibrium of Hsp33's linker region to the unfolded form. H_2O_2 is then able to oxidize Hsp33's cysteines and locks the protein in its active conformation.

4.3.3 Hsp33 deletion strains are bile salt sensitive

To investigate whether Hsp33 is able to protect bacteria against bile salt stress, we compared the bile salt sensitivity of *E. coli* MC4100 wild type and MC4100 *hslO*- strains at 37°C. Cells were grown to mid log phase, serially diluted and then spot-titered onto LB-agar plates containing various concentrations of Na-Cho or Na-DOC. After incubation for 18 h hours at 37°C, we found that the wild type strain was able to form viable colonies at 5 mM Na-Cho or 2 mM Na-DOC (Fig. 4.3.12), whereas the Hsp33 deletion strain was no longer capable of forming colonies under these conditions. These results demonstrate that Hsp33 is important for increasing the bile salt resistance of MC4100 cells.

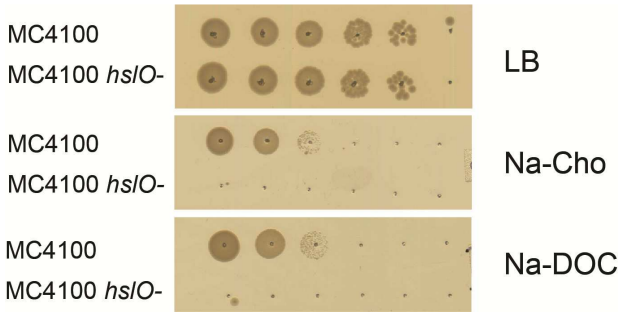

Fig. 4.3.12: Growth of *E. coli* MC4100 strains on plates containing bile salt
MC4100 and the Hsp33 deletion mutant MC4100 *hslO*- were grown at 37°C to an OD_{600} 0.5, serially diluted and spot titered onto LB plates or LB plates containing various concentrations of either Na-Cho or Na-DOC. Plates were incubated at 37°C for 18 h.

Very similar effects were observed with other *E. coli* strains and their corresponding Hsp33 deletion strains, including Bl21 and BB25113. The wild

type strain always grew significantly better in the presence of bile salts than the corresponding Hsp33 deletion strain. No significant difference between Na-DOC and Na-Cho was observed. It should be noted though that MC4100 was the most sensitive strain, and consistently showed the biggest difference in growth on bile salts between wild type and *hslO*- deletion mutant.

Experiments in liquid culture were performed to verify Hsp33's importance in bacterial survival following bile salt treatment. For these experiments, MC4100 or MC4100 *hslO*- cells were grown in LB medium to mid-log phase (OD_{600} ~0.5) at 37°C and then challenged with various concentrations of Na-Cho or Na-DOC (the CMC concentration for bile salts in LB medium has not been determined). Following the treatment, we found a clear lag phase in cell growth, which was significantly longer in the Hsp33 deletion strain (Fig.4.3.13). The most consistent results were obtained upon treatment with 14 mM Na-Cho or 5 mM Na-DOC. Hence, these bile salt concentrations were used for subsequent experiments, if not otherwise stated. These are also the same concentrations that we used in our *in vitro* experiments.

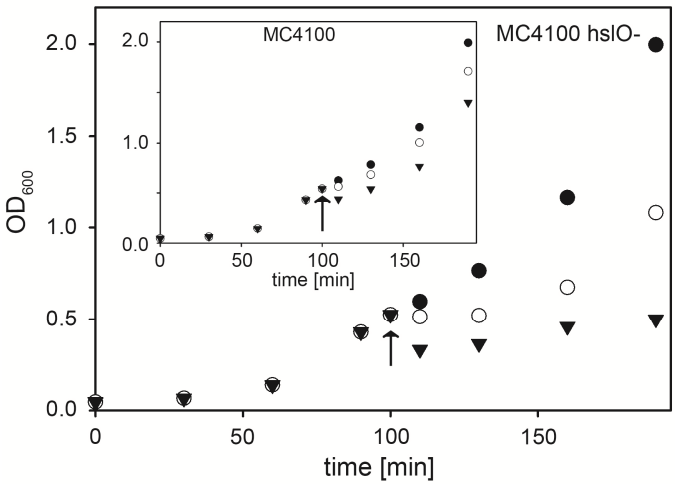

Fig. 4.3.13: Effect of Na-Cho or Na-DOC treatment on the growth of MC4100 and MC4100 *hslO*-

MC4100 (insert) or MC4100 *hslO*- were grown in LB at 37°C to an OD_{600} ~0.5. The arrows in the figures indicate the start of treatment with 14 mM Na-Cho (open circle) or 5 mM Na-DOC (triangle). The closed circles reflect growth in the absence of treatment.

As mentioned before, both MC4100 and the Hsp33 deletion strain showed a lag phase upon treatment with Na-Cho or Na-DOC (Fig. 4.3.13, arrow

indicates start of treatment). In wild type MC4100 (Fig. 4.3.13, insert), this lag phase was less pronounced upon Na-Cho treatment (open circle) and lasted about 30 min in response to Na-DOC treatment (triangle). In contrast, deletion of Hsp33 led to a 60 min growth arrest upon Na-Cho treatment (open circle) and a more than 2 hour growth arrest upon Na-DOC treatment (triangle) (Fig. 4.3.13). The initial 'dip' in OD upon treatment with Na-DOC needs to be further investigated. It may likely be due to the lysis of part of the cell population or to morphological changes in cell shape that effect optical density measurements. The severity of the dip is very similar between wild type and mutant cells, suggesting that it is not affected by the absence of Hsp33.

4.3.4 Hsp33 and DnaK are overexpressed under bile salt stress

The transcriptional up-regulation of several bacterial chaperones, including DnaK, GroEL, and ClpB has been previously described in response to bile salt treatment (Bernstein et al., 1999; Flahaut et al., 1996; Leverrier et al., 2003). As the heat shock response is generally triggered by protein unfolding conditions (Chapter 2.3), these results suggest that proteins might unfold upon exposure of cells to bile salts. We thus tested the expression level of the molecular chaperones Hsp33 and DnaK upon exposure of wild type MC4100 to 14 mM Na-Cho or 5 mM Na-DOC in LB medium, and we found massive up-regulation of both chaperones. The amount of expressed DnaK approximately doubled in response to treatment with either 14 mM Na-Cho or 5 mM Na-DOC (Fig. 4.3.14). This effect was very similar to the degree of DnaK up-regulation observed upon heat shock treatment. In the presence of Na-Cho, increased DnaK-levels were observed within the first 30 minutes of exposure. Presence of Na-DOC treatment caused an increase in DnaK within the first 10 min and a substantial further increased over the next 50 min. Very similar results were obtained for Hsp33, which was significantly up-regulated by both Na-Cho and Na-DOC treatment (Fig. 4.3.14).

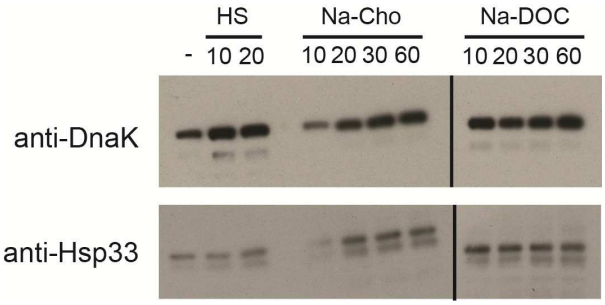

Fig. 4.3.14: DnaK and Hsp33 are up-regulated during Na-Cho and Na-DOC treatment

E. coli MC4100 were grown in LB until mid-log phase and subsequently treated with 14 mM Na-Cho or 5 mM Na-DOC for the indicated times. Aliquots were taken and western blot analysis was conducted to visualize DnaK and Hsp33. As a control for basal expression level, untreated cell lysates were used. As a positive control, cells were shifted from 30°C to 43°C (*i.e.*, heat shock response) for the indicated time. The vertical bar in the blot indicates that the results were combined from two different blots, using cells that were treated at the same time.

4.3.5 Aggregation of bile salt-sensitive proteins *in vivo*

We decided to further investigate to what extent proteins aggregate upon bile salt treatment *in vivo*. MC4100 wild type and *hslO* deletion strains were grown to mid-log phase and then split into pre-warmed flasks containing 14 mM Na-Cho or 5 mM Na-DOC. Samples were taken at defined time points. Potentially aggregated and soluble proteins were separated using an established protocol (Cremers et al., 2010). Protein aggregates were then solubilized and analyzed on SDS-PAGE. We found substantial protein aggregation in the Hsp33 deletion strain upon treatment with either Na-Cho or Na-DOC treatment (Fig. 4.3.15). In contrast, only small amounts of aggregated protein were found in the wild type strain. These results demonstrate two things. First of all, bile salts induce widespread protein unfolding and aggregation in bacteria, and second, Hsp33 protects bacteria against the bile salt toxicity presumably by binding to these proteins and keeping them soluble.

The molecular size of aggregated proteins in the Hsp33 deletion strain reflects the whole physiological range; we found very small proteins (< 15 kDa) in the aggregated fraction as well as very large ones (~150 kDa) (Fig. 4.3.15). Aggregation was detectable within 10 min after bile salt addition and reached a maximum approximately 30 minutes after treatment with Na-Cho,

at which time point cells started to resume growth. Treatment with Na-DOC had more severe effects than Na-Cho. Large amounts of aggregated proteins were detectable in the MC4100 *hslO*- strain (Fig. 4.3.15). 60 min after the treatment started, cells had still not resumed growth although no cell killing was observed (data not shown) (Fig. 4.3.13).

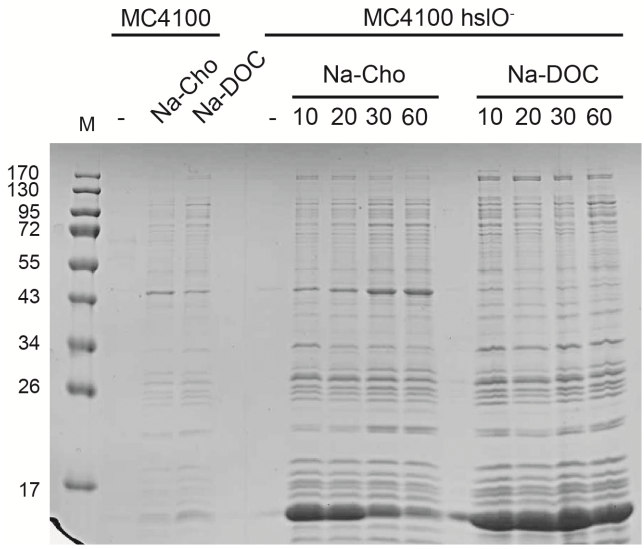

Fig. 4.3.15: Na-Cho and Na-DOC leads to widespread protein aggregation in MC4100 *hslO*- strains

E. coli MC4100 and the deletion mutant MC4100 *hslO*- were grown in LB to an OD600 ~0.5 and then treated with 14 mM Na-Cho or 5 mM Na-DOC. At the indicated time points, samples were taken and aggregated proteins were purified for analysis on SDS PAGE. Samples for the wild type strain were taken 30 min after the treatment.

As shown in Fig. 4.3.15, the pattern of aggregated proteins differed significantly between treatments; while Na-Cho and Na-DOC seemed to affect many proteins to a similar extent, some proteins were affected by one bile salt but not the other. Hsp33 was able to protect most proteins from bile salt-induced aggregation. This became obvious in the wild-type strain, where only very few proteins aggregated (Fig. 4.3.15). It is of note that the severity of the growth phenotype correlated well with the extent of aggregated proteins. As soon as cells exerted a growth defect, aggregates were detected. These results suggest that the growth inhibiting effect of bile salts on *E. coli* is caused by protein aggregation. Hsp33 maintains bacterial proteins in a

soluble state during bile salt treatment, and hence keeping the amount of toxic aggregates low.

To investigate the specific effects of distinct bile salts on the *E. coli* proteome, we decided to visualize the aggregated proteins on 2-dimensional (2D) PAGE, which separate proteins in two dimensions. First, the proteins are separated according to their isoelectric point, which is defined by the number of positively and negatively charged amino acids in the proteins. In the second dimension, the proteins are separated by their size in a SDS-PAGE. 2D gels are very valuable in visualizing complex protein samples. They help to determine the relative amount of proteins present in these samples and aid in the identification of certain proteins.

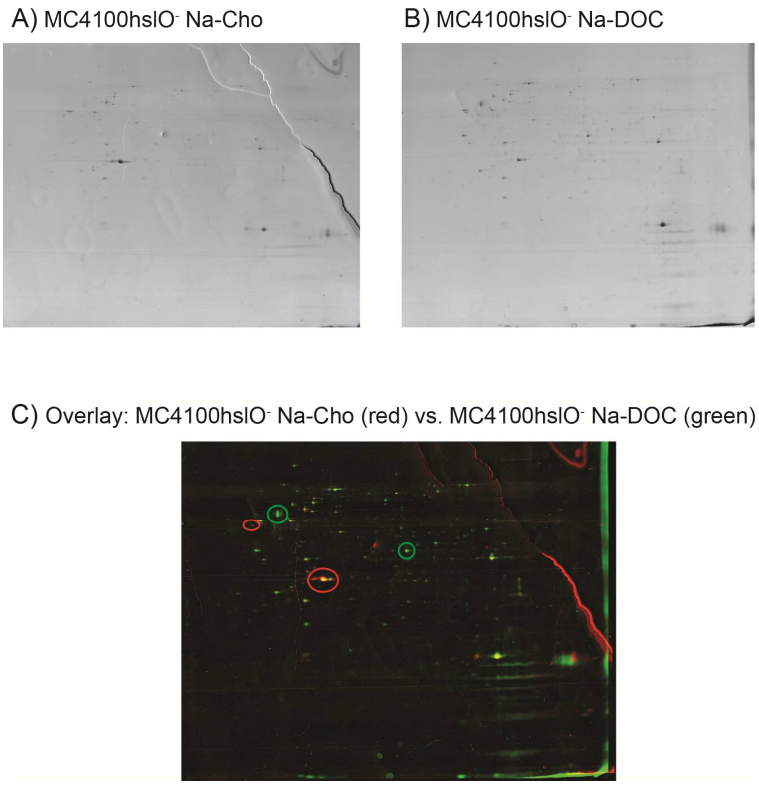

Fig. 4.3.16: 2D gel analysis of aggregated proteins after bile salt treatment
Protein aggregates after Na-Cho and Na-DOC treatment were prepared as described earlier. Protein pellets were then solubilized in 2D gel buffer and proteins were first separated according to their isoelectric point and then according to their size. A) proteins that aggregate during 14 mM Na-Cho treatment in MC4100 *hslO-*; B) proteins that aggregate during 5 mM Na-DOC treatment in MC4100 *hslO-*; C) false colored image of the overlay of proteins aggregating upon Na-Cho treatment (red) or Na-DOC treatment (green).

As seen in Fig. 4.3.16, numerous proteins aggregated to the same extent upon both Na-Cho and Na-DOC treatment (indicated by the yellow spots in figure 4.3.16, C). In contrast, some proteins preferentially aggregated upon Na-Cho treatment (Fig.4.3.16, A, C; green spots) while others aggregated only upon Na-DOC treatment (Fig. 4.3.16, B, C; red spots).

4.3.6 Using SILAC analysis to identify aggregated proteins

We decided to further investigate, which proteins aggregate in Hsp33 deletion strains and what the difference is between the two bile salt treatments. We thus performed SILAC (stable isotope *l*abeling by amino acids in cell culture) experiments. In SILAC experiments, two cell cultures are either cultivated in the presence of either “normal” ($^{12}C_6$-L-Arg) or “heavy” arginine ($^{13}C_6$-L-Arg). Aliquots of the cells are taken and lysed, and equal volumes of the protein samples are mixed. The relative ratio of individual proteins in the two cell cultures is then determined by mass spectrometry and the proteins are identified by tandem MS/MS.

To determine the proteins that aggregate in MC4100 *hslO*- strains upon treatment with Na-DOC or Na-Cho, we prepared two cell cultures. Cells were grown in MOPS minimal media supplemented with all amino acids and either heavy or light arginine. In mid-log phase (OD_{600} ~ 0.5), cells were then challenged with either 42 mM Na-Cho or 7.5 mM DOC (Fig. 4.3.17). It is of note that Na-Cho is significantly less effective in inducing growth defects when administered in MOPS medium as compared to LB medium (Fig. 4.3.13). Na-DOC, by contrast, leads to a severe growth defect in MC4100 *hslO*- in both MOPS minimal media (Fig. 4.3.17) and LB medium (Fig. 4.3.13). One possible explanation for the less severe growth defect observed in MOPS minimal medium is that the growth rate of cells might determine the severity of the growth defect. It is known that cells in stationary phase are much less sensitive towards bile salt-induced toxicity (King et al., 2003). If cells grow faster, they might be more strongly affected by the introduced stress, in this case by Na-Cho or Na-DOC.

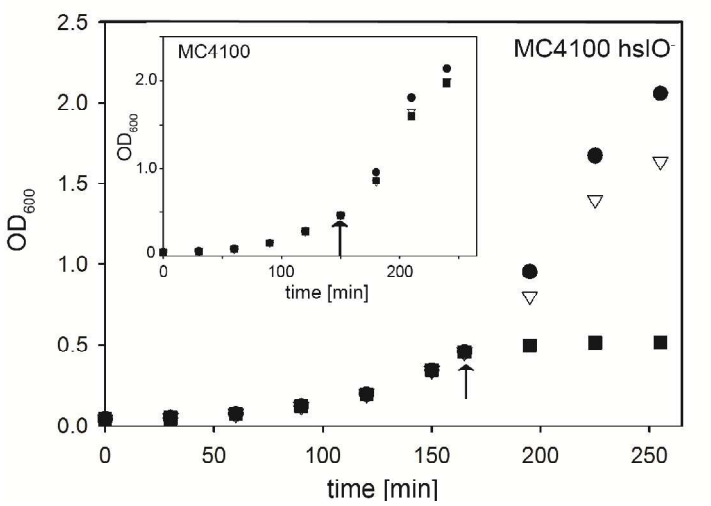

Fig. 4.3.17: Growth curves following the responds upon treatment with Na-Cho or Na-DOC

MC4100 (insert) or MC4100 *hslO*- were grown in MOPS minimal media supplemented with amino acids at 37°C to an OD_{600} ~0.5. The arrows in the figures indicate the start of treatment with 42 mM Na-Cho (triangles) and 7.5 mM Na-DOC (squares). The closed circle reflects untreated growth. Growth was followed 1.5 h after treatment was started.

30 min after the respective bile salt treatment was started, samples were taken and aggregated proteins were prepared. To initially assess the level of protein aggregation in the individual samples, the protein pellets were dissolved in DAB buffer corresponding to the cell OD_{600} and the purified aggregates were analyzed on SDS-PAGE (Fig. 4.3.18). The SDS-PAGE revealed again that significant protein aggregation was detected in MC4100 *hslO*- cells treated with Na-DOC or Na-Cho. Wild type cells that were used as negative control showed very little protein aggregation. The amount of aggregates in cells treated with Na-Cho was much lower than the amount of aggregates detectable upon Na-DOC, confirming our previous observation that higher levels of protein aggregates correlate with stronger growth defects.

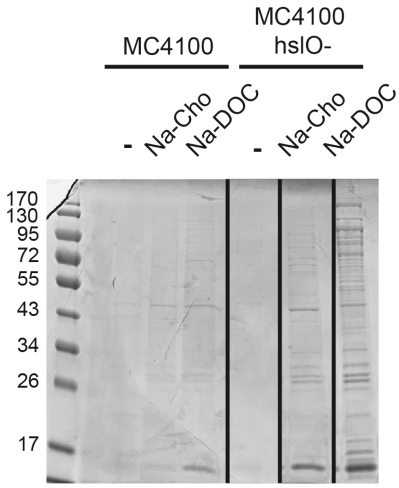

Fig. 4.3.18: Na-Cho and Na-DOC lead to widespread protein aggregation in cells not expressing Hsp33 when grown in MOPS minimal media

E. coli MC4100 and the deletion mutant MC4100 *hslO*- were grown in MOPS minimal media to an OD600 ~0.5 and then treated with 42 mM Na-Cho or 7.5 mM Na-DOC, 60 min after treatment was started samples were taken and aggregated proteins were purified for analysis on SDS-Page, amounts of proteins loaded is normalized to OD_{600}. Bars in the gel indicate that samples not important for this image were cut out.

Equal volumes of the aggregated proteins prepared from Na-DOC and Na-Cho treated MC4100 *hslO*- strains were mixed and separated on SDS-PAGE. The bands were excised, trypsin digested, and the peptides were subsequently purified and analyzed by LC-MS/MS. We identified a total of 83 aggregated proteins in the samples treated with either Na-Cho or Na-DOC for 30 minutes. Six additional proteins were only identified in lysates of cells treated with Na-DOC (Table 2).

The affected proteins fell into several different functional classes. Ribosomal proteins as well as proteins important for cellular metabolism contributed about 50 % of all identified proteins. In addition, we found chaperones, as well as transcriptional and translational regulators to be affected by the individual bile salt treatments. Furthermore some membrane proteins were also identified. Whether these aggregated in response to the bile salt treatment or were simply precipitated during the preparation needs to be further investigated (Fig. 4.3.19).

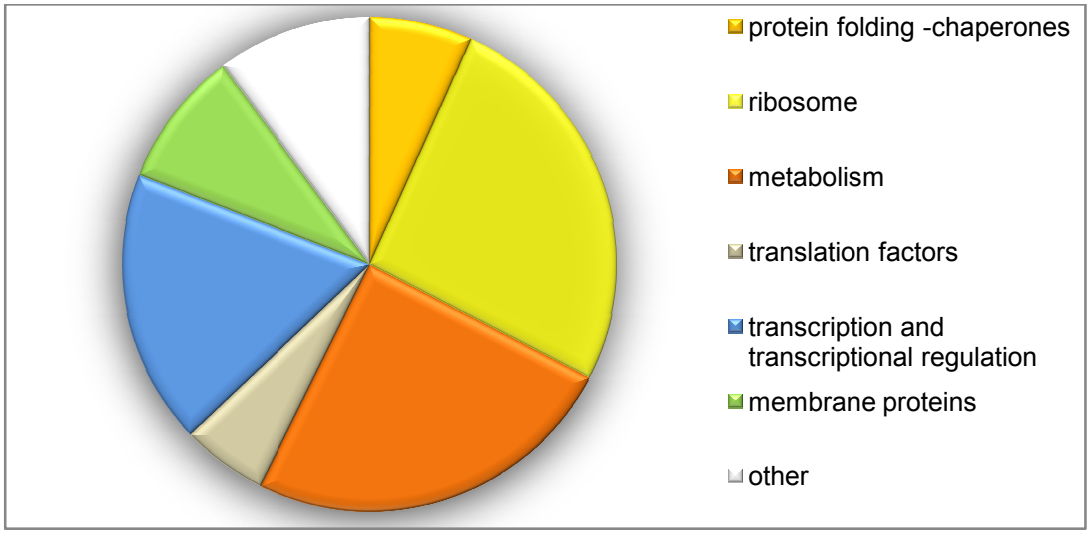

Fig. 4.3.19: Protein classes identified by SILAC
Pie-chart of protein classes identified by SILAC and subsequent LC-MS/MS studies. Proteins belonged to several classes important for cellular survival.

Our analysis revealed 24 ribosomal proteins that are prone to aggregate upon bile salt treatment in the absence of Hsp33 (Table 2). Other aggregation studies conducted to identify Hsp33 client proteins (Winter et al., 2008; Winter et al., 2005) revealed only one ribosomal protein, the 30S ribosomal protein S1. This protein was also identified in this study. Our discovery that 24 ribosomal proteins aggregate upon bile salt treatment would already explain why the growth defect was significantly more pronounced in Hsp33 deletion strains. Protein synthesis is essential for growth and survival of prokaryotic and eukaryotic cells, and reduction in translation is known to lead to slower growth.

We additionally identified 23 proteins important for metabolic functions, including enzymes involved in glycolysis, TCA-cycle, and energy production, as well as amino acid synthesis (Table 2). Some of these proteins have been identified as Hsp33 client proteins in previous studies (Winter et al., 2008; Winter et al., 2005) while others have not been identified before. Furthermore, we identified 15 proteins involved in transcription and transcriptional regulation, as well as in DNA repair.

Table 2: Aggregated proteins identified with LC-MS/MS upon Na-Cho and Na-DOC treatment

category	gene	protein	Intensity light Na-DOC	Intensity heavy Na-Cho	ratio Cho/DOC	Essential gene
ribosome	rpsJ	30S ribosomal protein S10	65224	97485	1.495	*
	rplF	50S ribosomal protein L6	329633	460479	1.397	*
	rplP	50S ribosomal protein L16	215973	284017	1.315	
	rplE	50S ribosomal protein L5	164771	195009	1.184	
	rplC	50S ribosomal protein L3	613456	596034	0.972	*
	rplN	50S ribosomal protein L14	357564	277915	0.777	*
	rplM	50S ribosomal protein L13	20697	16040	0.775	*
	rplK	50S ribosomal protein L11	1108155	812718	0.733	
	rplB	50S ribosomal protein L2	318787	221658	0.695	
	rplI	50S ribosomal protein L9	55501	32465	0.585	
	rplO	50S ribosomal protein L15	885821	420154	0.474	*
	rpsF	30S ribosomal protein S6	154852	72952	0.471	*
	rplD	50S ribosomal protein L4	232895	101699	0.437	*
	rpsD	30S ribosomal protein S4	3558104	1523538	0.428	
	rpsC	30S ribosomal protein S3	2042813	814786	0.399	
	rpsG	30S ribosomal protein S7	1101631	425915	0.387	
	rpsD	30S ribosomal protein S2	1920082	673658	0.351	
	rpsR	30S ribosomal protein S18	245790	73506	0.299	
	rpsE	30S ribosomal protein S5	2462181	698615	0.284	
	rpsI	30S ribosomal protein S9	150744	26306	0.175	*
	rpsA	30S ribosomal protein S1	224659	37309	0.166	
	rpsM	30S ribosomal protein S13	94955	13859	0.146	*
	rpsK	30S ribosomal protein S11	3140775	350205	0.112	

Table 2 continued: Aggregated proteins identified with LC-MS/MS upon Na-Cho and Na-DOC treatment

category	gene	protein	Intensity light Na-DOC	Intensity heavy Na-Cho	ratio Cho/DOC	Essential gene
metabolism	pykF	Pyruvate kinase	18212	246598	13.540	
	thrA	Aspartokinase I	113293	196838	1.737	
	prsA	Ribose-phosphate pyrophosphokinase	21554	15412	0.715	
	speA	Biosynthetic arginine decarboxylase	47411	21685	0.457	
	proS	Prolyl-tRNA synthetase	413761	174376	0.421	*
	pflB	Formate acetyltransferase 1	102467	38243	0.373	
	metH	Methionine synthase	62551	20444	0.327	
	asnA	Aspartate--ammonia ligase	24277	7174	0.296	
	accC	Acetyl CoA carboxylase, biotin carboxylase subunit	33135	9738	0.294	*
	atpD	ATP synthase subunit beta	211315	59704	0.283	
	ndh	NADH dehydrogenase	331896	88185	0.266	
	serA	D-3-phosphoglycerate dehydrogenase	44234	11526	0.261	
	sucA	2-oxoglutarate dehydrogenase E1 component	210357	39839	0.189	
	pta	Phosphate acetyltransferase	1142915	200496	0.175	
	plsB	Glycerol-3-phosphate acyltransferase	65617	8668	0.132	
	suhB	Inositol-1-monophosphatase	33668	4251	0.126	
	adhE	Aldehyde-alcohol dehydrogenase	1086035	101207	0.093	
	accD	Acetyl-coenzyme A carboxylase carboxyl transferase subunit beta	80580	6448	0.080	*
	aceE	Pyruvate dehydrogenase E1 component	1686239	143508	0.085	
	pheT	Phenylalanyl-tRNA synthetase beta chain	212936	14283	0.067	
	guaA	GMP synthase [glutamine-hydrolyzing]	63379	3644	0.057	
	ptsG	Glucose phophotransferase	335494	10124	0.030	
	argS	Arginyl-tRNA synthetase	17412			*

Table 2 continued: Aggregated proteins identified with LC-MS/MS upon Na-Cho and Na-DOC treatment

category	gene	protein	Intensity light Na-DOC	Intensity heavy Na-Cho	ratio Cho/DOC	Essential gene
transcription and transcriptional regulation	recA	Protein recA	58337	115836	1.986	
	nrdA	Ribonucleoside-diphosphate reductase 1 subunit alpha	217054	227248	1.047	*
	deaD	ATP-dependent RNA helicase	1581244	1434051	0.907	
	rho	Transcription termination factor Rho	461713	189350	0.410	
	rapA	RNA polymerase-associated protein rapA	147808	56885	0.385	
	topA	DNA topoisomerase	150836	53027	0.352	*
	crp	Catabolite gene activator	132008	42708	0.324	
	ybeZ	Putative ATP-binding protein in pho regulon	22661	6766	0.299	
	pcnB	Poly(A) polymerase	126544	35874	0.283	
	nemR	HTH-type transcriptional repressor nemR	435831	106410	0.244	
	nusG	Transcription antitermination protein nusG	48857	10824	0.222	*
	rne	Ribonuclease	1568909	195829	0.125	
	rpoB	DNA-directed RNA polymerase subunit beta	3537003	404821	0.114	
	rpoC	DNA-directed RNA polymerase subunit beta	1538634	130297	0.085	*
	gyrA	DNA gyrase subunit A	87080			*
protein folding – chaperones	hslU	ATP-dependent protease ATPase subunit HslU	156351	936171	5.988	
	lon	ATP-dependent protease La	204873	89926	0.439	
	clpB	Heat shock protein clpB	189439	66255	0.350	
	hslK/A	Modulator of FtsH protease HflK	185576	56891	0.307	
	dnaJ	Chaperone protein dnaJ	122100	30451	0.249	
	tig	Trigger factor	179704	19995	0.111	

Table 2 continued: Aggregated proteins identified with LC-MS/MS upon Na-Cho and Na-DOC treatment

category	gene	protein	Intensity light Na-DOC	Intensity heavy Na-Cho	ratio Cho/DOC	
translation factors	tuf2	Elongation factor Tu-2	1432620	1761368	1.229	*
	fusA	Elongation factor G	215413	191402	0.889	*
	infB	Translation initiation factor IF-2	1969419	765692	0.389	*
	srmB	ATP-dependent RNA helicase srmB	307931	118333	0.384	
	infC	Translation initiation factor IF-3	503629	73292	0.146	
membrane proteins	mrcB	Penicillin-binding protein 1B	36873	84130	2.282	
	ffh	Signal recognition particle protein	198440	50708	0.256	
	secF	Export membrane protein SecF	44380	7662	0.173	
	secY	Preprotein translocase subunit SecY	99258	4047	0.041	*
	secB	Protein-export membrane protein secD	412181	15543	0.038	
	oxaA	Inner membrane protein oxaA	234434			
	kefA	Potassium efflux system KefA	13549			
other	yeeF	Predicted amino acid transporter	11786	12794	1.086	
	typA	GTP-binding protein TypA/BipA	312243	165173	0.529	
	mukB	Chromosome partition protein mukB	723629	242427	0.335	
	mreB	Regulator of FtsI	155494	50062	0.322	
	glyS	Glycyl-tRNA synthetase beta subunit	179154	32868	0.183	
	yfiF	Hypothetical tRNA/rRNA methyltransferase YfiF	142192	17217	0.121	
	yicC	protein yicC	16232			
	wbbJ	Putative lipopolysaccharide biosynthesis O-acetyl transferase wbbJ	25439			

4.3.7 Bile salt treatment leads to oxidative stress *in vivo*

Realizing that bile salts lead to widespread protein unfolding *in vivo* and that Hsp33 has a highly protective function, we wondered about the activation mechanism of Hsp33 *in vivo*, given that Hsp33 activation requires both unfolding and oxidizing conditions (Ilbert et al., 2007; Winter et al., 2008; Winter and Jakob, 2004). Several papers have previously described induction of oxidative stress in hepatocytes upon exposure to hydrophobic bile salts yet little has been done in regards to bacteria (Fang et al., 2004; Sokol et al., 2005; Sokol et al., 1993).

To first examine whether bile salt treatment leads to Hsp33 oxidation *in vivo*, we performed thiol trapping assays. In this assay, we covalently label all *in vivo* reduced cysteines with iodoacetamide (IAA), reduce all *in vivo* oxidized protein thiols with DTT, and label all newly accessible, reduced cysteines with 4-acetamido-4"-maleimidylstilbene-2'-disulfonate (AMS), an alkylating reagent that introduces 500 Da mass per labeled cysteine. This increase in mass can be detected in SDS-PAGE. The results in Fig. 4.3.20 show that treatment of *E. coli* with either 14 mM Na-Cho or 5 mM Na-DOC in LB medium leads to the oxidation of Hsp33. These results provide a clear indication that bile salts induce oxidative stress in *E. coli*.

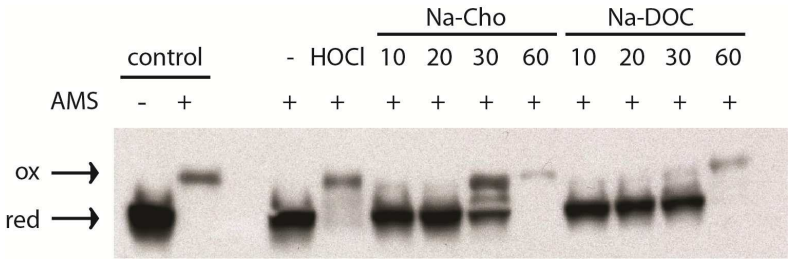

Fig. 4.3.20: Thiol-trapping of Hsp33 to determine its oxidation status
Wild type E. coli was treated with 4 mM HOCl, 14 mM Na-Cho or 5 mM Na-DOC for the indicated time points in LB medium. To quantify Hsp33's *in vivo* oxidation status, samples were taken a differentially thiol-trapped. First, all *in vivo* reduced cysteines were labeled with IAA. Second, *in vivo* oxidized cysteines were reduced and labeled with AMS. Proteins with AMS-labeled cysteines are migrating higher in the SDS PAGE. Hsp33 was identified after western blot using specific anti-Hsp33 antibodies.

As shown in Fig. 4.3.20, bleach shifts most of Hsp33 into the oxidized state within 20 min of treatment. In contrast, oxidation of Hsp33 upon exposure to bile salts appears to be slower. Upon Na-Cho treatment, Hsp33 starts to get significantly oxidized approximately 30 min after start of the treatment and the protein seems to be fully oxidized within 60 min. Na-DOC-mediated oxidation appears to start after 30 min (Fig. 4.3.20, very faint oxidized band) and the protein is again fully oxidized within 60 min of treatment.

4.3.8 *E. coli* strains defective in antioxidant defense are bile salt sensitive

To test whether strains defective in the cellular antioxidant response are more sensitive to bile salt treatment, we investigated the bile salt sensitivity of DHB4 strains with deletions in either the glutaredoxin system or the thioredoxin system under aerobic conditions on plates. It was striking that nearly all mutant strains were more sensitive towards bile salt stress under aerobic conditions (Fig. 4.3.21, 4.3.22, 4.3.23). It was also interesting that Na-DOC and Na-Cho treatment exerted different effects on the mutant strains, suggesting that they trigger slightly different responses in bacteria.

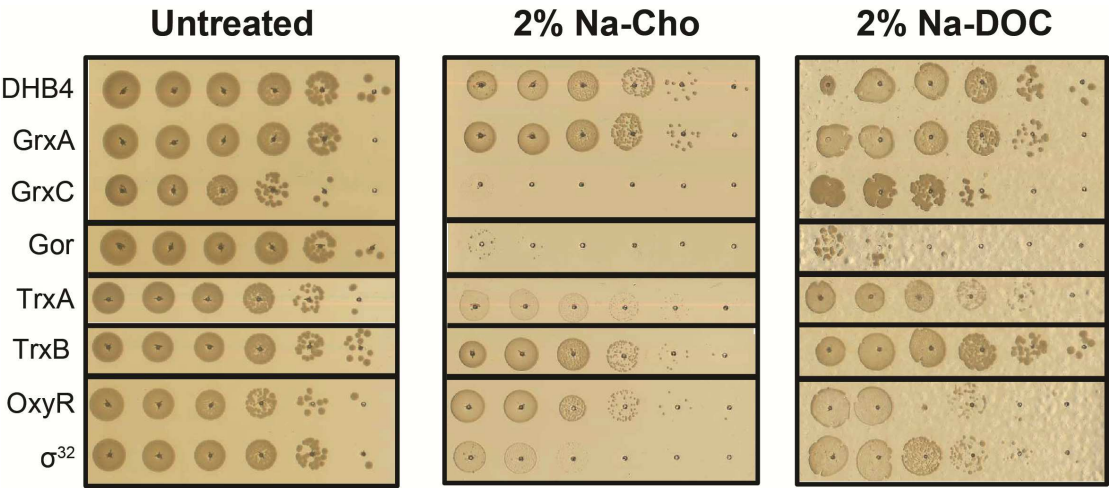

Fig. 4.3.21: Phenotyping of DHB4 strains with deletions in redox regulating genes on plates containing various concentrations of Na-Cho and Na-DOC

DHB4 strains were grown in LB medium at 30°C until mid-log phase, serial diluted in LB medium and spot titered on LB plates containing various concentrations of Na-Cho and Na-DOC (0-2.5%). After incubation overnight at 37°C log differences in growth were analyzed and compared. Strains: DHB4= wild type, deletion of the genes *grxA*= glutaredoxin A, *grxC*= glutaredoxin C, *gorA*= glutaredoxin

oxidoreductase, *trxA*= thioredoxin A, *trxB*= thioredoxin reductase, *oxyR*= transcriptional regulator, H_2O_2 response, *rpoH*= σ^{32}, transcriptional regulator, heat shock response.

To more precisely assess the growth defects of the individual mutants, we spot titered the individual mutant strains on plates containing increasing amounts of either Na-DOC or Na-Cho and plotted the surviving colonies against the bile salt concentrations. A representative result of the experiments (3 repeats) is shown in Fig. 22 and 23. The wild type strain grew well until 2 % Na-Cho and 2.5 % Na-DOC, respectively (Fig. 4.3.22, black and green line). At the higher bile salt concentrations, the colony size decreased, indicating slower growth due to bile salt stress. Deletion of the heat shock factor σ^{32} caused a significant increase in bile salt sensitivity, confirming that increased expression of chaperones is necessary to survive bile salt stress (Fig. 4.3.22, blue and red line).

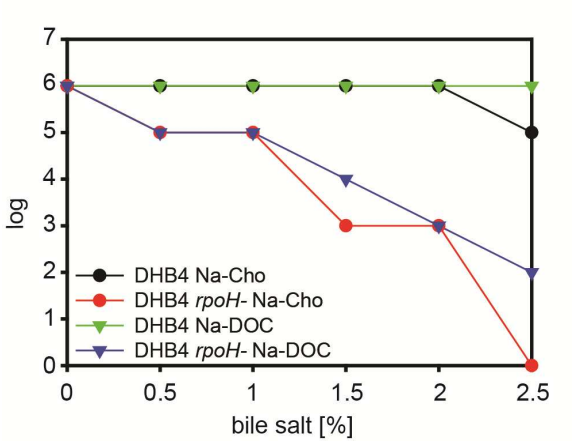

Fig. 4.3.22: *RpoH* deletion strains are highly bile salt sensitive
DHB4 wild type and *rpoH* deletion strain were grown in LB medium at 30°C until mid-log phase, serially diluted in LB medium and spot-titered onto LB plates containing various concentrations of Na-Cho and Na-DOC (0-2.5 %). After incubation overnight at 30°C, colonies were counted. Traces reflect the average of 3 independent proteins.

Other mutant strains of DHB4 that were sensitive towards bile salt treatment were those that harbored deletion in *oxyR, gorA, grxC*, and *trxA* (Fig. 4.3.23).

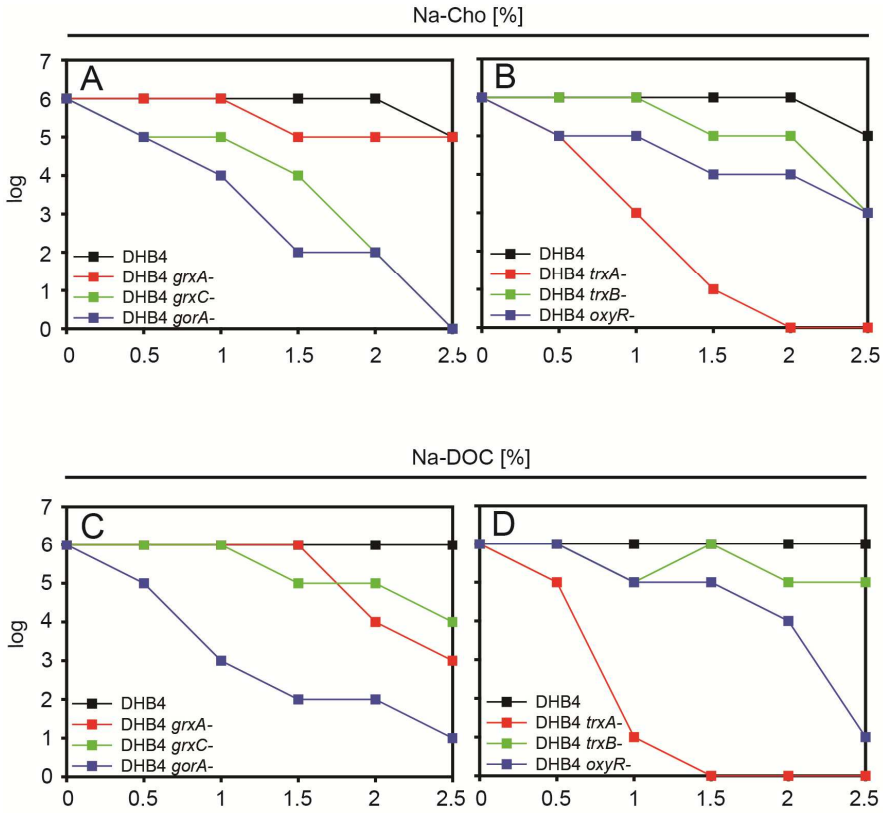

Fig. 4.3.23: Phenotyping of DHB4 strains with deletions in redox regulating genes on plates containing various concentrations of bile salts

DHB4 strains were grown in LB medium at 30°C until mid-log phase, serially diluted in LB medium and spot-titered on LB plates containing various concentrations of Na-Cho and Na-DOC (0-2.5 %). After incubation overnight at 30°C log of growth differences were analyzed and compared. Strains: DHB4= wild type, deletion of the genes *grxA*= glutaredoxin A, *grxC*= glutaredoxin C, *gorA*= glutaredoxin oxidoreductase, *trxA*= thioredoxin A, *trxB*= thioredoxin reductase, *oxyR*= transcriptional regulator, H_2O_2 response.

OxyR is a transcriptional regulator, which is activated under H_2O_2 stress and responsible for the induction of numerous antioxidant genes, including some that have been tested here: *gorA, trxA, trxB,* and *grxA (Zheng et al., 1998)*. The fact that this strain is significantly more sensitive to bile salt treatment than the wild type strain strongly suggests that bile salts generate peroxide stress in bacteria (Fig. 4.3.23, B, D; blue line). Another gene, whose deletion made *E. coli* highly sensitive to bile salts is thioredoxin A (TrxA), which has two distinct functions in *E. coli*. First, it is important for the reduction of oxidized proteins during oxidative stress; second, it transfers electrons to the periplasm via interaction with DsbD in the cytoplasmic membrane. DsbD keeps the disulfide isomerase DsbC reduced (Missiakas et al., 1995; Rietsch

and Beckwith, 1998). Surprisingly, deletion of thioredoxin reductase (TrxB), the enzyme responsible for re-reducing TrxA, does only causes a mild growth defect on Na-Cho or Na-DOC plates in comparison to the wild type strain (Fig. 4.3.23, B, D; green line). It is conceivable that other proteins are able to reduce oxidized TrxA.

Deletion of either glutathione reductase (GorA) or glutaredoxin C (GrxC) in DHB4 strains had a very negative effect on bacterial bile salt survival (Fig. 4.3.23, A, C; blue and green line respectively). While the glutathione oxidoreductase is important for keeping glutathione in its reduced form, is GrxC important in keeping cytosolic proteins reduced and de-glutathiolylated (Aslund et al., 1994; Aslund et al., 1996). In contrast, deletion of *grxA* does not cause a severe bile salt stress phenotype, which could be due to the fact that the Trx-system is still functional and reduces oxidized proteins.

4.3.9 Glutathione redox potential is more oxidized during the first 30 min of exposure to bile salts

The GSH/GSSG standard redox potential in *E. coli* is about -240 mV (Aslund et al., 1997), which becomes more positive during oxidative stress. Our finding that the *grxC* deletion strain is more sensitive towards Na-Cho and Na-DOC treatment suggested that the GSH/GSSG levels might be affected by bile salt treatment.

E. coli was grown in LB until mid-log phase and subsequently treated with 21 mM Na-Cho or 7.5 mM Na-DOC for 30 or 60 minutes. The increase in bile salt concentration was necessary to increase the lag phase. Cells were then harvested and prepared with slight modifications according to (Reed et al., 1980) to determine the cellular GSH and GSSH concentrations. The redox potential was then calculated using the Nernst equation:

$$E = E^0 - \frac{RT}{nF} * \log \frac{[red]^2}{[ox]}$$

With E^0 for reduced GSH of -240mV at 25°C (*T* absolute temperature, *n* number of electrons transferred, *F* Faraday constant (96 406 J V^{-1})) we get the following equation to calculate the GSH/GSSG redox potential:

$$E = -240 - \frac{59.1}{2} * \log\frac{[GSH]^2}{[GSSG]}$$

We found that treatment of *E. coli* leads to an increase in redox potential from ~ -240 mV to ~ -230 mV upon Na-Cho and to ~ -215 mV upon treatment with Na-DOC (Fig. 4.3.24). After 60 min, the redox potential seems to recover and decreases again to ~ -235 mV (Fig. 4.3.24). This corresponds to the onset of growth after the lag phase again (Fig. 4.3.16), indicating that *E. coli* recovers from the stress.

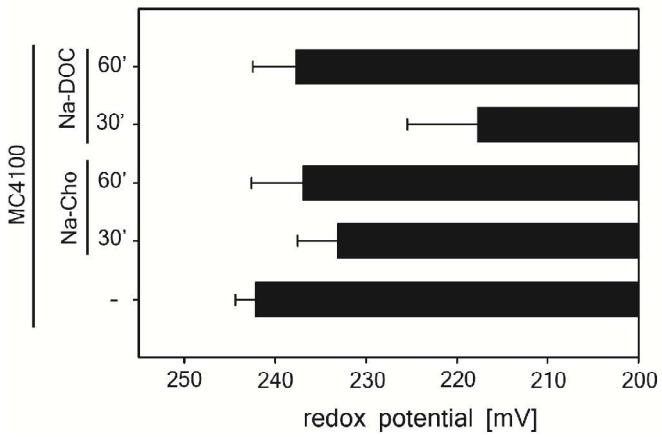

Fig. 4.3.24: GSH/GSSG redox potential in *E. coli* during bile salt stress
The redox potential of *E. coli* was determined using the molar ratios of GSH/GSSG during bile salt treatment.

4.3.10 Protein carbonylation – An alternative read-out for oxidative stress *in vivo*

Protein carbonylation is an irreversible oxidative protein modification, which affects the side chains of several amino acid residues, including arginine, histidine, lysine, and proline (Dalle-Donne et al., 2003). It is commonly used to monitor oxidative stress *in vivo*. To determine whether bile salt treatment causes oxidative protein carbonylation, we cultivated cells until mid-log phase and then treated them with 14 mM Na-Cho or 5 mM Na-DOC as before. As positive control for protein carbonylation, we treated cells with HOCl for 20 min. As negative control, we exposed cells to heat shock. Samples were taken at the indicated time points and the carbonyl groups in proteins were derivatized with 2,4-dinitrophenylhydrazine (DNPH). This leads to the formation of a stable dinitrophenyl hydrazine product, which is

detectable with specific antibodies after separation of the proteins on SDS PAGE and subsequent transfer onto a nitrocellulose membrane.

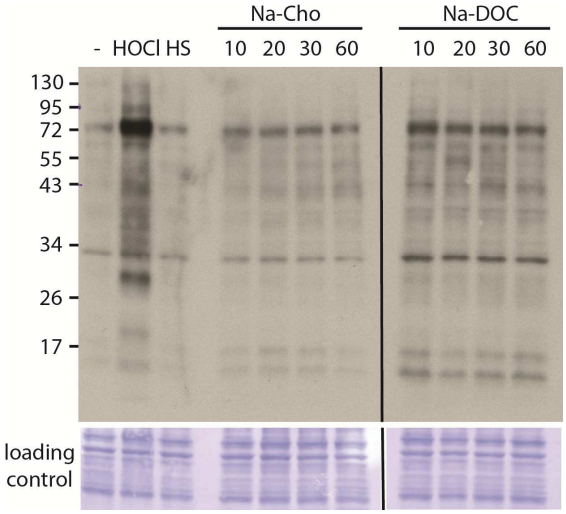

Fig. 4.3.25: Detection of carbonylated proteins during bile salt stress
Protein carbonylation was detected with specific antibodies against the derivatization product of the carbonyl group and DNPH. Bacteria were harvested and derivatized, separated on an SDS page and transferred onto a nitrocellulose membrane, followed by western blot detection. The bar in the figures indicates the combination of two membranes processed in parallel. As loading control served the blue stained PVDF membrane after detection of the carbonylation was detected.

The amount of proteins that were carbonylated upon bile salt treatment was not as high as the amount of carbonylation induced by HOCl treatment (Fig. 4.3.25). Nevertheless, the intensity of some of the bands increased with increasing exposure time to bile salts, indicative of oxidative damage. Although we were unable to identify which proteins are affected by bile salt or HOCl-induced oxidative stress, these results clearly show that bacteria encounter oxidative stress during bile salt treatment. In contrast, heat shock (HS) treatment does not seem to induce significant oxidative stress.

4.3.11 Conclusion

Bile salts are amphipathic molecules in our intestine, which are known as soft detergents. They have numerous important physiological functions in food digestion, and play an important role in keeping the microbial flora in equilibrium due to their antimicrobial function. It is interesting that the mechanism by which bile salts kill bacteria has not been very well

characterized. Here we demonstrate that bile salts (1) cause protein unfolding and aggregation *in vitro*, and (2) lead to both oxidative stress and protein unfolding *in vivo*. These are the precise stress conditions that have been previously shown to activate Hsp33 (Ilbert et al., 2007; Winter et al., 2008). Resistance of *E. coli* toward bile salt stress is hence significantly increased when Hsp33 is expressed. These results provide evidence that bile salt-mediated toxicity is not only due to membrane permeabilization but also due to oxidative protein unfolding and aggregation.

Our *in vitro* results indicate that Na-Cho and Na-DOC have different effects on different proteins and appear to correlate with the thermodynamic stability of the test proteins. The more thermolabile, the larger the effect of Na-Cho and Na-DOC on protein structure and function. Hence, it is conceivable that hydrophobic interactions between bile salts and the protein shift the equilibrium of proteins toward the more unfolded stage. These results fit well with results obtained by Gass et al., who showed that some proteins are more sensitive to structural loss than others when exposed to conjugated bile salts (Gass et al., 2007). Our studies showed that under the appropriate temperature conditions, some of our test proteins even aggregate while incubating with bile salts, such as Na-Cho. Most of the proteins, however, aggregate upon dilution from bile salts, which speaks for the non-covalent character of the bile salt-protein interaction. Upon dilution, proteins seem to be unable to refold and are segregated into aggregates. Taking our *in vitro* results and the outcome of previous studies together, it appears that more thermolabile proteins are more prone to bile salt-induced unfolding and subsequent aggregation. Yet at this point it is still unclear why some proteins are more sensitive to unfolding by one particular bile salt and resistant to the other. One good example is Hsp33, which seems to be significantly more affected by Na-DOC than by Na-Cho. Incubation with Na-DOC causes the unfolding of Hsp33's linker region and hence the activation of the chaperone. Na-Cho, however, is unable to affect the stability of Hsp33's linker region to a degree that would activate the chaperone. More studies need to be conducted to obtain a precise understanding as to the types of interactions that individual bile salts can participate in.

Our *in vivo* results obtained with the SILAC/LC-MS/MS experiments revealed 83 proteins, which are vulnerable to bile salt-mediated protein aggregation *in vivo* and are protected against aggregation by functional Hsp33. Some of these proteins have been identified as Hsp33 client-proteins in thermal aggregation studies or HOCl-aggregation experiments (Winter et al., 2008; Winter et al., 2005). Most of the proteins that we identified in this study, however, have neither been identified as particularly thermally unstable nor as sensitive to oxidative unfolding. We found 24 different ribosomal proteins to be sensitive to bile salt mediated aggregation in the absence of Hsp33. This was surprising as ribosomal proteins are classified as stable and usually not aggregation-prone. It has been suggested that proteins are most sensitive towards oxidation during their synthesis, and that the final structure protects them against oxidative and other damage (Holland et al., 2007; Medicherla and Goldberg, 2008; Winter et al., 2008; Winter et al., 2005). This could be true for bile salt-induced protein unfolding and aggregation as well. If bile salts bind indeed preferentially to hydrophobic patches in nascent polypeptide chains, they might interact with proteins during the translation process, and hence trigger protein aggregation. Ribosomal proteins might then simply co-aggregate with the nascent polypeptide chains. It is of note that we also identified the chaperone trigger factor to aggregate upon bile salt treatment. This chaperone is associated with the ribosome and is important for the initial protein folding on the ribosome exit tunnel (Merz et al., 2008). Given its tight association with the ribosome, it is likely that trigger factor co-aggregates with one or several of the newly synthesized proteins.

Three of the aggregated proteins that we identified are transcriptional regulators, including the transcriptional repressor NemR, the catabolite gene activator CRP, and RNA polymerase-associated protein RapA. While NemR has been recently identified as a HOCl-specific transcriptional regulator in *E. coli* (M. Gray, personal communication), CRP is a transcriptional regulator involved in the regulation of more than 100 genes, most of which involved in energy metabolism (Semsey et al., 2007; Zheng et al., 2004). The last regulator that we identified is RapA, which belongs to the RNA polymerase

complex and is relative abundant in *E. coli* (Sukhodolets et al., 2001; Sukhodolets and Jin, 1998, 2000).

We also found six chaperones within the aggregated samples (including trigger factor), most of which are known to be important for protein disaggregation or the degradation of otherwise toxic protein aggregates. The proteases Lon, HslU, and the modulator of HflK- a membrane-bound protease complex, were found to associate with aggregates. One chaperone that we identified was DnaJ, a co-chaperone of DnaK, which is important for binding client proteins and transferring them to DnaK (Greene et al., 1998) (Chapter 2.4.2). A complex of DnaK, DnaJ, and the nucleotide exchange factor GrpE supports *de novo* protein folding and plays an important role in disaggregating aggregates in concert with ClpB. It is of note that we also identified ClpB in our bile salt-induced protein aggregates. These results confirm previous studies, which reported that protein aggregates often contain chaperones and proteases (Winkler et al., 2010).

While the amount of many of the identified proteins is significantly lower in protein aggregates isolated from Na-Cho treated cells than from Na-DOC treated *E. coli*, several proteins are massively over-represented in the Na-Cho sample. These proteins include pyruvate kinase, which aggregates 13.5-fold more upon Na-Cho treatment than upon Na-DOC treatment as well as aspartokinase, RecA, HslU, and elongation factor TU (EF-Tu). Other proteins are completely absent from Na-Cho aggregates, suggesting that their aggregation is Na-DOC specific. These proteins include arginyl-tRNA synthetase, DNA gyrase subunit A, potassium efflux system KefA, inner membrane protein OxaA, protein YicC, and a putative O-acetyl transferase (Table 2). Given the difference in the efficacy of the individual bile salt treatments, targeting any one these proteins for irreversible aggregation might explain the more severe growth inhibitory effect observed upon Na-DOC treatment.

It is of note that 23 of our identified 89 gene products (25%) were previously identified to be essential gene products in *E. coli* (marked * in Table 2). This is a surprisingly high proportion, given that only 171 *E. coli* genes

(less than 4%) fall into this category (Gerdes et al., 2003). One of these essential proteins is EF-Tu, which has been recently identified to be a central Hsp33 target protein under HOCl stress in *Vibrio cholera* (Wholey and Jakob, 2012). We identified EF-Tu now also as a target protein of Hsp33 under bile salt stress. Aggregation of EF-Tu or any other essential protein likely contributes to the observed growth defect in bile salt treated *E. coli* cells lacking Hsp33.

Bile salts induce oxidative stress in *E. coli.* Winter et al. showed that slow reacting oxidants like H_2O_2 together with unfolding conditions, or fast acting oxidants like HOCl, lead to widespread protein-unfolding and aggregation *in vivo* (Winter 2005 2008). Under both conditions the molecular chaperone Hsp33 is activated and subsequently prevents the aggregation of these proteins (Graumann et al., 2001; Ilbert et al., 2007; Winter et al., 2008; Winter et al., 2005). We show here that Hsp33 is crucial for bacterial survival during bile salt treatment, indicating that oxidative unfolding conditions exist. The DnaK/J/E system, as well GroEL/ES are central chaperone machineries, protecting proteins against stress-induced protein aggregation (Georgopoulos, 2006; Houry, 2001). Whether they can function under bile salt-induced stress conditions, remains to be further investigated. Nevertheless, Hsp33 seems to work in the first line of defense against bile salt-induced protein unfolding and aggregation.

At this point the source of bile salt-induced oxidative stress is still unclear. Our results agree, however, with the literature that states that numerous genes important for oxidative defense are up-regulated during bile salt stress (Begley et al., 2005b; Kristoffersen et al., 2007). Analysis of *E. coli* mutant strains defective in antioxidant response furthermore revealed several genes that appear to be essential for cellular survival under bile salt stress. One of the most sensitive DHB4 mutant strains contained a deletion in the *grxC* gene. This was interesting as deletion of the closely related glutaredoxin A (*grxA*) showed little effect on the sensitivity of DHB4 to bile salt stress. While both GrxA and thioredoxin A (TrxA) are responsible for the reduction of oxidized proteins in the *E. coli* cytosol, GrxC is specifically responsible for

removing glutathione from S-glutathionylated proteins (Aslund et al., 1994; Aslund et al., 1996). These results provide a first indication that bile salts, or at least Na-Cho, might induce widespread S-glutathionylation in proteins, which requires GrxC's enzymatic activity for reduction. In agreement with these conclusions, we found that strains defective for glutathione reductase (*gorA*$^{-}$) are also highly sensitive to bile salts. Reduction of oxidized Grx is initiated by glutathione, which, in turn, is reduced by glutathione reductase GorA (Holmgren, 1989a; Holmgren and Aslund, 1995). GorA is hence essential for maintaining the GSH:GSSG ratio and thus the redox potential of the cytosol. Interestingly, we found a significant increase in the cell's redox potential, which was largely due to a decrease in cellular GSH levels. These results suggest that the reduction of GSH might be due to S-glutathionylation of proteins. This would explain why absence of either *grxC* or *gorA* is so disadvantageous for bacteria during bile salt stress.

Reactive oxygen species are typically produced in the electron transport chain due to the incomplete reduction of oxygen. Our findings that bile salts are more toxic when cells grow faster (*i.e.,* LB versus MOPS) strongly suggests the involvement of the electron transport chain in bile salt-mediated ROS production. To directly test this hypothesis, bile salt sensitivity assays should be performed under anaerobic growth conditions. This would eliminate the oxygen and should therefore eliminate the production of ROS. Hence, *E. coli* mutants lacking antioxidant genes should grow better. To identify where in the electron transport chain the back flow of electrons to oxygen occurs, members of the electron transport chain could be deleted and tested for their sensitivity toward bile salts.

Taken together our results demonstrate that bile salts cause oxidative protein unfolding and aggregation in *E. coli,* the precise stress conditions that lead to the activation of Hsp33. These studies provide insights into the mechanism of physiological antimicrobials and the strategies that bacteria developed to defend themselves against the insult. This information is crucial for the development of alternative antimicrobial therapies.

5 Supplementary Section

5.1 Publications

Unfolding of metastable linker region is at the core of Hsp33 activation as a redox-regulated chaperone.
Claudia M. Cremers, Dana Reichmann, Jens Hausmann, Marianne Ilbert, and Ursula Jakob
J Biol Chem. 2010 Apr 9; 285(15):11243-51

Are zinc-finger domains of protein kinase C dynamic structures that unfold by lipid or redox activation?
Feng Zhao, Marianne Ilbert, Ranjani Varadan, Claudia M. Cremers, Beatrice Hoyos, Rebeca Acin-Perez, Valerie Vinogradov, David Cowburn, Ursula Jakob, and Ulrich Hammerling
Antioxid Redox Signal. 2011 Mar 1; 14(5):757-66

Chlorinated phenols control the expression of the multi-drug resistance efflux pump MexAB-OprM in Pseudomonas aeruginosa by activating NalC.
Sudeshna Ghosh, Claudia M. Cremers, Ursula Jakob, and Nancy G. Love
Mol Microbiol. 2011 Jan 14; 79(6):1547-1556

Order out of Disorder – Working Cycle of an Intrinsically Unfolded Chaperone
Dana Reichmann, Ying Xu, Claudia M. Cremers, Marianne Ilbert, Roni Mittelman, Michael C. Fitzgerald, and Ursula Jakob
Cell. 2012 Mar 2; 148(5):947-57

How cells defend against bleach
Michael J. Gray, Wei-Yun Wholey, Minwook Kim, Erica M. Smith, Claudia M. Cremers, Robert A. Bender, Ursula Jakob
Science. In review

The antimicrobial effects of bile salt
Claudia M. Cremers, Victor Vitvitsky, Ruma Banerjee, Ursula Jakob
In preparation

5.2 Oral Presentations

Midwest Stress Response and Molecular Chaperone Meeting (January 2009)
Northwestern University, Evanston, Illinois
Turning Hsp33 loose by loss of redox regulation
Claudia M. Cremers and Ursula Jakob

Symposium on Molecular Chaperones and Protein Quality Control (May 2012)
University of Michigan, Ann Arbor, Michigan
Hsp33 Protects Cells Against Bile Salt Induced Protein Aggregation
Claudia M. Cremers and Ursula Jakob

5.3 Poster presentations

Annual Midwest Conference on Protein Folding, Assembly and Molecular Motions (May 2008)
University of Notre Dame, Notre Dame, Indiana
Redox-Modulated Changes in the Stability of Linker Region Control the Chaperone Activity of Hsp33
Claudia M. Cremers, Marianne Ilbert, and Ursula Jakob

Redox Signaling and Disease - Symposium (September 2009)
University of Michigan, Ann Arbor, Michigan
Redox-Modulated Changes in the Stability of Linker Region Control the Chaperone Activity of Hsp33
Claudia M. Cremers, Marianne Ilbert, and Ursula Jakob

Molecular Chaperones & Stress Responses (May 2010)
Cold Spring Harbor Laboratory, Cold Spring Harbor, New York
The core of Hsp33's activation is the unfolding of the metastable linker region
Claudia M. Cremers, Dana Reichmann, and Ursula Jakob

The Biology of Molecular Chaperones (May 2011)
Grundelsee, Austria
Hsp33 Prevents *E. coli* from Bile Salt Induced Cell death by Preventing Protein Aggregation
Claudia M. Cremers and Ursula Jakob

6 Acknowledgements

First and foremost, I would like to thank my ‘Dr. Mutter’, Dr. Ursula Jakob who brought me to Michigan and inspired me from the beginning on. Her unwavering support, encouragement, and guidance have gotten me this far. She gave me the support to finally grow up. To have a mentor who is both academically, professionally, and personally invested in you is more than any graduate student could hope for. I would also like to thank my ‘Dr. Vater’, Dr. Johannes Buchner for being my advisor in München, without him, this dissertation would never have been possible.

I would like to express my gratitude to the entire Jakob lab. Their collegiality and teamwork inspired me. My special thanks go to Dana Reichmann and Marianne Ilbert, they shared their knowledge in the protein field, and especially about Hsp33, with me. Working on the same project, we had many fruitful discussions. Further I want to thank Winnie Chen – now Wholey, Daniela Knöfler, Antje Müller, and Heather Tienson for their scientific input, but more importantly, their friendship and support throughout the time this voyage - called PhD - took. I am glad I met them all and that we are more than ‘just colleagues’. Far away from home, these people became part of my family. I also want to thank Mike Gray for many scientific discussions. Further I would like to thank the students I had the pleasure to supervise during my time in Ann Arbor, you taught me how to teach, and particularly taught me patience. I also would also like to thank the Bardwell lab, especially Dr. James Bardwell, for scientific discussions and support.

I would never have gotten to this point without my wonderful support network. Thanks to my friends in Germany, Diane and Marc Venmanns, and Silke and Heinz-Gert Feyen, who supported me through the years before graduate school and continued to be there for me no matter where my degree took me. The friends I made in Ann Arbor have made this journey so much more fun than I expected. There are too many to mention them all, but special thanks to Roisin O’Mara, Ferdinand Kappes, Christopher Champion, and Fabio Albano for being my comrades on this whirlwind ride! They were always there for me, no matter what happened. THANK YOU! I would also like to

thank a new member in this club, Serge Farinas, thank you for the support, patience, and friendship you showed me in the last month.

Last but not least: möchte ich meiner Familie danken, meinen Eltern, Maria und Dieter und meinen Geschwister, Andrea und Lukas, sowie meinen Grosseltern, die diesen Moment leider nicht mehr mit mir teilen können. Sie sind mein Fels in der Brandung. Ohne ihre Hilfe und kontinuierliche Unterstützung wäre ich nie soweit gekommen. Meine Familie hat meine Kuriosität und Wissbegierde immer gefördert und mir das Gefühl gegeben, dass ich schaffen kann, was ich erreichen will. DANKE EUCH ALLEN!

7 References

Ago, T., Nunoi, H., Ito, T., and Sumimoto, H. (1999). Mechanism for phosphorylation-induced activation of the phagocyte NADPH oxidase protein p47(phox). Triple replacement of serines 303, 304, and 328 with aspartates disrupts the SH3 domain-mediated intramolecular interaction in p47(phox), thereby activating the oxidase. J Biol Chem *274*, 33644-33653.

Akhtar, M.W., Srinivas, V., Raman, B., Ramakrishna, T., Inobe, T., Maki, K., Arai, M., Kuwajima, K., and Rao Ch, M. (2004). Oligomeric Hsp33 with enhanced chaperone activity: gel filtration, cross-linking, and small angle x-ray scattering (SAXS) analysis. J Biol Chem *279*, 55760-55769.

Albalak, A., Zeidel, M.L., Zucker, S.D., Jackson, A.A., and Donovan, J.M. (1996). Effects of submicellar bile salt concentrations on biological membrane permeability to low molecular weight non-ionic solutes. Biochemistry *35*, 7936-7945.

Allen, R.C., Yevich, S.J., Orth, R.W., and Steele, R.H. (1974). The superoxide anion and singlet molecular oxygen: their role in the microbicidal activity of the polymorphonuclear leukocyte. Biochem Biophys Res Commun *60*, 909-917.

Allen, S.P., Polazzi, J.O., Gierse, J.K., and Easton, A.M. (1992). Two novel heat shock genes encoding proteins produced in response to heterologous protein expression in Escherichia coli. J Bacteriol *174*, 6938-6947.

Altuvia, S., WeinsteinFischer, D., Zhang, A.X., Postow, L., and Storz, G. (1997). A small, stable RNA induced by oxidative stress: Role as a pleiotropic regulator and antimutator. Cell *90*, 43-53.

Aslund, F., Berndt, K.D., and Holmgren, A. (1997). Redox potentials of glutaredoxins and other thiol-disulfide oxidoreductases of the thioredoxin superfamily determined by direct protein-protein redox equilibria. J Biol Chem *272*, 30780-30786.

Aslund, F., Ehn, B., Miranda-Vizuete, A., Pueyo, C., and Holmgren, A. (1994). Two additional glutaredoxins exist in Escherichia coli: glutaredoxin 3 is a hydrogen donor for ribonucleotide reductase in a thioredoxin/glutaredoxin 1 double mutant. Proc Natl Acad Sci U S A *91*, 9813-9817.

Aslund, F., Nordstrand, K., Berndt, K.D., Nikkola, M., Bergman, T., Ponstingl, H., Jornvall, H., Otting, G., and Holmgren, A. (1996). Glutaredoxin-3 from Escherichia coli. Amino acid sequence, 1H AND 15N NMR assignments, and structural analysis. J Biol Chem *271*, 6736-6745.

Aslund, F., Zheng, M., Beckwith, J., and Storz, G. (1999). Regulation of the OxyR transcription factor by hydrogen peroxide and the cellular thiol - disulfide status. P Natl Acad Sci USA *96*, 6161-6165.

Baneyx, F., and Mujacic, M. (2004). Recombinant protein folding and misfolding in Escherichia coli. Nat Biotechnol *22*, 1399-1408.

Bardwell, J.C., and Craig, E.A. (1984). Major heat shock gene of Drosophila and the Escherichia coli heat-inducible dnaK gene are homologous. Proc Natl Acad Sci U S A *81*, 848-852.

Barrette, W.C., Hannum, D.M., Wheeler, W.D., and Hurst, J.K. (1989). General Mechanism for the Bacterial Toxicity of Hypochlorous Acid - Abolition of Atp Production. Biochemistry *28*, 9172-9178.

Begley, M., Gahan, C.G.M., and Hill, C. (2005a). The interaction between bacteria and bile. FEMS Microbiology Reviews *29*, 625-651.

Begley, M.i., Gahan, C.G.M., and Hill, C. (2005b). The interaction between bacteria and bile. FEMS Microbiology Reviews *29*, 625-651.

Beissinger, M., and Buchner, J. (1998). How chaperones fold proteins. Biol Chem *379*, 245-259.

Bernstein, C., Bernstein, H., Payne, C.M., Beard, S.E., and Schneider, J. (1999). Bile salt activation of stress response promoters in Escherichia coli. Curr Microbiol *39*, 68-72.

Bertelsen, E.B., Chang, L., Gestwicki, J.E., and Zuiderweg, E.R.P. (2009). Solution conformation of wild-type E. coli Hsp70 (DnaK) chaperone complexed with ADP and substrate. Proceedings of the National Academy of Sciences *106*, 8471-8476.

Blanchard, J.L., Wholey, W.Y., Conlon, E.M., and Pomposiello, P.J. (2007). Rapid changes in gene expression dynamics in response to superoxide reveal SoxRS-dependent and independent transcriptional networks. PLoS ONE *2*, e1186.

Bowie, J.U., and Sauer, R.T. (1989). Equilibrium dissociation and unfolding of the Arc repressor dimer. Biochemistry *28*, 7139-7143.

Braig, K., Otwinowski, Z., Hegde, R., Boisvert, D.C., Joachimiak, A., Horwich, A.L., and Sigler, P.B. (1994). The crystal structure of the bacterial chaperonin GroEL at 2.8 A. Nature *371*, 578-586.

Brandes, H.K., Larimer, F.W., Geck, M.K., Stringer, C.D., Schurmann, P., and Hartman, F.C. (1993). Direct Identification of the Primary Nucleophile of Thioredoxin-F. Journal of Biological Chemistry *268*, 18411-18414.

Brehmer, D., Gassler, C., Rist, W., Mayer, M.P., and Bukau, B. (2004). Influence of GrpE on DnaK-substrate interactions. J Biol Chem *279*, 27957-27964.

Brockwell, D.J., and Radford, S.E. (2007). Intermediates: ubiquitous species on folding energy landscapes? Curr Opin Struct Biol *17*, 30-37.

Brynildsen, M.P., and Liao, J.C. (2009). An integrated network approach identifies the isobutanol response network of Escherichia coli. Mol Syst Biol *5*, 277.

Buchberger, A., Schroder, H., Buttner, M., Valencia, A., and Bukau, B. (1994). A conserved loop in the ATPase domain of the DnaK chaperone is essential for stable binding of GrpE. Nat Struct Biol *1*, 95-101.

Buchner, J., Ehrnsperger, M., Gaestel, M., and Walke, S. (1998). Purification and characterization of small heat shock proteins. Methods Enzymol *290*, 339-349.

Bukau, B. (1993). Regulation of the Escherichia coli heat-shock response. Mol Microbiol *9*, 671-680.

Bukau, B., and Horwich, A.L. (1998). The Hsp70 and Hsp60 chaperone machines. Cell *92*, 351-366.

Bukau, B., Weissman, J., and Horwich, A. (2006). Molecular chaperones and protein quality control. Cell *125*, 443-451.

Bury-Mone, S., Nomane, Y., Reymond, N., Barbet, R., Jacquet, E., Imbeaud, S., Jacq, A., and Bouloc, P. (2009). Global analysis of extracytoplasmic stress signaling in Escherichia coli. PLoS Genet *5*, e1000651.

Bushweller, J.H., Aslund, F., Wuthrich, K., and Holmgren, A. (1992). Structural and functional characterization of the mutant Escherichia coli glutaredoxin (C14----S) and its mixed disulfide with glutathione. Biochemistry *31*, 9288-9293.

Cabral, D.J., Small, D.M., Lilly, H.S., and Hamilton, J.A. (1987). Transbilayer movement of bile acids in model membranes. Biochemistry *26*, 1801-1804.

Campioni, S., Mannini, B., Zampagni, M., Pensalfini, A., Parrini, C., Evangelisti, E., Relini, A., Stefani, M., Dobson, C.M., Cecchi, C.*, et al.* (2010). A causative link between the structure of aberrant protein oligomers and their toxicity. Nat Chem Biol *6*, 140-147.

Carey, M.C., and Small, D.M. (1972). Micelle formation by bile salts. Physical-chemical and thermodynamic considerations. Arch Intern Med *130*, 506-527.

Caspers, G.J., Leunissen, J.A., and de Jong, W.W. (1995). The expanding small heat-shock protein family, and structure predictions of the conserved "alpha-crystallin domain". J Mol Evol *40*, 238-248.

Chen, X., Lee, K.A., Ha, E.M., Lee, K.M., Seo, Y.Y., Choi, H.K., Kim, H.N., Kim, M.J., Cho, C.S., Lee, S.Y.*, et al.* (2011). A specific and sensitive method for detection of hypochlorous acid for the imaging of microbe-induced HOCl production. Chem Commun (Camb) *47*, 4373-4375.

Chen, Y., and Barkley, M.D. (1998). Toward understanding tryptophan fluorescence in proteins. Biochemistry *37*, 9976-9982.

Chen, Z., Kurt, N., Rajagopalan, S., and Cavagnero, S. (2006). Secondary structure mapping of DnaK-bound protein fragments: chain helicity and local helix unwinding at the binding site. Biochemistry *45*, 12325-12333.

Chiang, S.M., and Schellhorn, H.E. (2012). Regulators of oxidative stress response genes in Escherichia coli and their functional conservation in bacteria. Archives of Biochemistry and Biophysics.

Choi, H.-I., Lee, S.P., Kim, K.S., Hwang, C.Y., Lee, Y.-R., Chae, S.-K., Kim, Y.-S., Chae, H.Z., and Kwon, K.-S. (2006). Redox-regulated cochaperone activity of the human DnaJ homolog Hdj2. Free Radical Biology and Medicine *40*, 651-659.

Choi, H., Kim, S., Mukhopadhyay, P., Cho, S., Woo, J., Storz, G., and Ryu, S.E. (2001). Structural basis of the redox switch in the OxyR transcription factor. Cell *105*, 103-113.

Chowdhury, R., Sahu, G.K., and Das, J. (1996). Stress response in pathogenic bacteria. J Bioscience *21*, 149-160.

Christiaens, H., Leer, R.J., Pouwels, P.H., and Verstraete, W. (1992). Cloning and expression of a conjugated bile acid hydrolase gene from Lactobacillus plantarum by using a direct plate assay. Appl Environ Microbiol *58*, 3792-3798.

Christman, M.F., Morgan, R.W., Jacobson, F.S., and Ames, B.N. (1985). Positive control of a regulon for defenses against oxidative stress and some heat-shock proteins in Salmonella typhimurium. Cell *41*, 753-762.

Christman, M.F., Storz, G., and Ames, B.N. (1989). OxyR, a positive regulator of hydrogen peroxide-inducible genes in Escherichia coli and Salmonella typhimurium, is homologous to a family of bacterial regulatory proteins. Proc Natl Acad Sci U S A *86*, 3484-3488.

Coleman, R. (1987). Biochemistry of bile secretion. Biochem J *244*, 249-261.

Craven, P.A., Pfanstiel, J., and DeRubertis, F.R. (1987). Role of activation of protein kinase C in the stimulation of colonic epithelial proliferation and reactive oxygen formation by bile acids. J Clin Invest *79*, 532-541.

Cremers, C.M., Reichmann, D., Hausmann, J., Ilbert, M., and Jakob, U. (2010). Unfolding of metastable linker region is at the core of Hsp33 activation as a redox-regulated chaperone. J Biol Chem *285*, 11243-11251.

Dalle-Donne, I., Rossi, R., Giustarini, D., Milzani, A., and Colombo, R. (2003). Protein carbonyl groups as biomarkers of oxidative stress. Clin Chim Acta *329*, 23-38.

De Biase, D., Tramonti, A., Bossa, F., and Visca, P. (1999). The response to stationary-phase stress conditions in Escherichia coli: role and regulation of the glutamic acid decarboxylase system. Mol Microbiol *32*, 1198-1211.

De, S., Das, S., and Girigoswami, A. (2007). Spectroscopic probing of bile salt-albumin interaction. Colloids Surf B Biointerfaces *54*, 74-81.

Desmet, I., Vanhoorde, L., Woestyne, M.V., Christiaens, H., and Verstraete, W. (1995). Significance of Bile-Salt Hydrolytic Activities of Lactobacilli. J Appl Bacteriol *79*, 292-301.

Deuerling, E., Schulze-Specking, A., Tomoyasu, T., Mogk, A., and Bukau, B. (1999). Trigger factor and DnaK cooperate in folding of newly synthesized proteins. Nature *400*, 693-696.

Ding, J.W., Andersson, R., Soltesz, V., Willen, R., and Bengmark, S. (1993). The role of bile and bile acids in bacterial translocation in obstructive jaundice in rats. Eur Surg Res *25*, 11-19.

Dinner, A.R., Sali, A., Smith, L.J., Dobson, C.M., and Karplus, M. (2000). Understanding protein folding via free-energy surfaces from theory and experiment. Trends Biochem Sci *25*, 331-339.

Dubuisson, J.F., Vianney, A., Hugouvieux-Cotte-Pattat, N., and Lazzaroni, J.C. (2005). Tol-Pal proteins are critical cell envelope components of Erwinia chrysanthemi affecting cell morphology and virulence. Microbiol-Sgm *151*, 3337-3347.

Dukan, S., and Nystrom, T. (1999). Oxidative stress defense and deterioration of growth-arrested Escherichia coli cells. J Biol Chem *274*, 26027-26032.

Dunker, A.K., Lawson, J.D., Brown, C.J., Williams, R.M., Romero, P., Oh, J.S., Oldfield, C.J., Campen, A.M., Ratliff, C.M., Hipps, K.W*., et al.* (2001). Intrinsically disordered protein. J Mol Graph Model *19*, 26-59.

Dyson, H.J., Holmgren, A., and Wright, P.E. (1989). Assignment of the proton NMR spectrum of reduced and oxidized thioredoxin: sequence-specific assignments, secondary structure, and global fold. Biochemistry *28*, 7074-7087.

Ehrnsperger, M., Graber, S., Gaestel, M., and Buchner, J. (1997). Binding of non-native protein to Hsp25 during heat shock creates a reservoir of folding intermediates for reactivation. EMBO J *16*, 221-229.

Ehrnsperger, M., Lilie, H., Gaestel, M., and Buchner, J. (1999). The dynamics of Hsp25 quaternary structure. Structure and function of different oligomeric species. J Biol Chem *274*, 14867-14874.

Ellis, J. (1987). Proteins as molecular chaperones. Nature *328*, 378-379.

Ellis, R.J., and Minton, A.P. (2006). Protein aggregation in crowded environments. Biol Chem *387*, 485-497.

Evans, M.S., Sander, I.M., and Clark, P.L. (2008). Cotranslational folding promotes beta-helix formation and avoids aggregation in vivo. J Mol Biol *383*, 683-692.

Ewalt, K.L., Hendrick, J.P., Houry, W.A., and Hartl, F.U. (1997). In vivo observation of polypeptide flux through the bacterial chaperonin system. Cell *90*, 491-500.

Fang, Y., Han, S.I., Mitchell, C., Gupta, S., Studer, E., Grant, S., Hylemon, P.B., and Dent, P. (2004). Bile acids induce mitochondrial ROS, which promote activation of receptor tyrosine kinases and signaling pathways in rat hepatocytes. Hepatology *40*, 961-971.

Fenton, W.A., and Horwich, A.L. (1997). GroEL-mediated protein folding. Protein Sci *6*, 743-760.

Fenton, W.A., and Horwich, A.L. (2003). Chaperonin-mediated protein folding: fate of substrate polypeptide. Q Rev Biophys *36*, 229-256.

Ferbitz, L., Maier, T., Patzelt, H., Bukau, B., Deuerling, E., and Ban, N. (2004). Trigger factor in complex with the ribosome forms a molecular cradle for nascent proteins. Nature *431*, 590-596.

Fink, A.L., Calciano, L.J., Goto, Y., Kurotsu, T., and Palleros, D.R. (1994). Classification of acid denaturation of proteins: intermediates and unfolded states. Biochemistry *33*, 12504-12511.

Flahaut, S., Hartke, A., Giard, J.C., Benachour, A., Boutibonnes, P., and Auffray, Y. (1996). Relationship between stress response toward bile salts, acid and heat treatment in Enterococcus faecalis. FEMS Microbiol Lett *138*, 49-54.

Frydman, J., Erdjument-Bromage, H., Tempst, P., and Hartl, F.U. (1999). Co-translational domain folding as the structural basis for the rapid de novo folding of firefly luciferase. Nat Struct Biol *6*, 697-705.

Frydman, J., Nimmesgern, E., Ohtsuka, K., and Hartl, F.U. (1994). Folding of nascent polypeptide chains in a high molecular mass assembly with molecular chaperones. Nature *370*, 111-117.

Gajiwala, K.S., and Burley, S.K. (2000). HDEA, a periplasmic protein that supports acid resistance in pathogenic enteric bacteria. J Mol Biol *295*, 605-612.

Garbe, T.R., Kobayashi, M., and Yukawa, H. (2000). Indole-inducible proteins in bacteria suggest membrane and oxidant toxicity. Arch Microbiol *173*, 78-82.

Gass, J., Vora, H., Hofmann, A.F., Gray, G.M., and Khosla, C. (2007). Enhancement of dietary protein digestion by conjugated bile acids. Gastroenterology *133*, 16-23.

Geiszt, M., Witta, J., Baffi, J., Lekstrom, K., and Leto, T.L. (2003). Dual oxidases represent novel hydrogen peroxide sources supporting mucosal surface host defense. FASEB J *17*, 1502-1504.

Georgopoulos, C. (2006). Toothpicks, serendipity and the emergence of the Escherichia coli DnaK (Hsp70) and GroEL (Hsp60) chaperone machines. Genetics *174*, 1699-1707.

Georgopoulos, C., and Welch, W.J. (1993). Role of the Major Heat-Shock Proteins as Molecular Chaperones. Annu Rev Cell Biol *9*, 601-634.

Georgopoulos, C.P. (1977). A new bacterial gene (groPC) which affects lambda DNA replication. Mol Gen Genet *151*, 35-39.

Gerdes, S.Y., Scholle, M.D., Campbell, J.W., Balazsi, G., Ravasz, E., Daugherty, M.D., Somera, A.L., Kyrpides, N.C., Anderson, I., Gelfand, M.S.*, et al.* (2003). Experimental determination and system level analysis of essential genes in Escherichia coli MG1655. J Bacteriol *185*, 5673-5684.

Giese, K.C., and Vierling, E. (2002). Changes in oligomerization are essential for the chaperone activity of a small heat shock protein in vivo and in vitro. J Biol Chem *277*, 46310-46318.

Goffin, L., and Georgopoulos, C. (1998). Genetic and biochemical characterization of mutations affecting the carboxy-terminal domain of the Escherichia coli molecular chaperone DnaJ. Mol Microbiol *30*, 329-340.

Gonzalez-Flecha, B., and Demple, B. (1997). Homeostatic regulation of intracellular hydrogen peroxide concentration in aerobically growing Escherichia coli. J Bacteriol *179*, 382-388.

Graf, P.C., and Jakob, U. (2002). Redox-regulated molecular chaperones. Cell Mol Life Sci *59*, 1624-1631.

Graf, P.C.F. (2004). Activation of the Redox-regulated Chaperone Hsp33 by Domain Unfolding. Journal of Biological Chemistry *279*, 20529-20538.

Graumann, J., Lilie, H., Tang, X., Tucker, K.A., Hoffmann, J.H., Vijayalakshmi, J., Saper, M., Bardwell, J.C., and Jakob, U. (2001). Activation of the redox-regulated molecular chaperone Hsp33--a two-step mechanism. Structure *9*, 377-387.

Greene, M.K., Maskos, K., and Landry, S.J. (1998). Role of the J-domain in the cooperation of Hsp40 with Hsp70. P Natl Acad Sci USA *95*, 6108-6113.

Griffith, K.L., Shah, I.M., and Wolf, R.E., Jr. (2004). Proteolytic degradation of Escherichia coli transcription activators SoxS and MarA as the mechanism for reversing the induction of the superoxide (SoxRS) and multiple antibiotic resistance (Mar) regulons. Mol Microbiol *51*, 1801-1816.

Grimshaw, J.P., Siegenthaler, R.K., Zuger, S., Schonfeld, H.J., Z'Graggen B, R., and Christen, P. (2005). The heat-sensitive Escherichia coli grpE280 phenotype: impaired interaction of GrpE(G122D) with DnaK. J Mol Biol *353*, 888-896.

Ha, E.M. (2005). A Direct Role for Dual Oxidase in Drosophila Gut Immunity. Science *310*, 847-850.

Ha, E.M., Oh, C.T., Bae, Y.S., and Lee, W.J. (2005). A direct role for dual oxidase in Drosophila gut immunity. Science *310*, 847-850.

Haley, D.A., Bova, M.P., Huang, Q.L., McHaourab, H.S., and Stewart, P.L. (2000). Small heat-shock protein structures reveal a continuum from symmetric to variable assemblies. J Mol Biol *298*, 261-272.

Haley, D.A., Horwitz, J., and Stewart, P.L. (1998). The small heat-shock protein, alphaB-crystallin, has a variable quaternary structure. J Mol Biol *277*, 27-35.

Hamon, E., Horvatovich, P., Bisch, M., Bringel, F., Marchioni, E., Aoudé-Werner, D., and Ennahar, S. (2012). Investigation of Biomarkers of Bile Tolerance inLactobacillus caseiUsing Comparative Proteomics. Journal of Proteome Research *11*, 109-118.

Harrison, C.J., Hayer-Hartl, M., Di Liberto, M., Hartl, F., and Kuriyan, J. (1997). Crystal structure of the nucleotide exchange factor GrpE bound to the ATPase domain of the molecular chaperone DnaK. Science *276*, 431-435.

Harrison, J.E., and Schultz, J. (1976). Studies on the chlorinating activity of myeloperoxidase. J Biol Chem *251*, 1371-1374.

Hartl, F.U. (1996). Molecular chaperones in cellular protein folding. Nature *381*, 571-579.

Hartl, F.U., and Hayer-Hartl, M. (2002). Molecular chaperones in the cytosol: from nascent chain to folded protein. Science *295*, 1852-1858.

Hartl, F.U., and Hayer-Hartl, M. (2009). Converging concepts of protein folding in vitro and in vivo. Nat Struct Mol Biol *16*, 574-581.

Haslbeck, M., Franzmann, T., Weinfurtner, D., and Buchner, J. (2005). Some like it hot: the structure and function of small heat-shock proteins. Nat Struct Mol Biol *12*, 842-846.

Hausladen, A., Privalle, C.T., and Stamler, J.S. (1996). Direct activation of the prokaryotic transcription factor oxyR by S-nitrosylation. Portl Pr P *10*, 28-28.

Healy, E.F. (2012). A model for heterooligomer formation in the heat shock response of Escherichia coli. Biochemical and Biophysical Research Communications *420*, 639-643.

Herman, C., Thevenet, D., D'Ari, R., and Bouloc, P. (1995). Degradation of sigma 32, the heat shock regulator in Escherichia coli, is governed by HflB. Proc Natl Acad Sci U S A *92*, 3516-3520.

Hidalgo, E., Bollinger, J.M., Jr., Bradley, T.M., Walsh, C.T., and Demple, B. (1995). Binuclear [2Fe-2S] clusters in the Escherichia coli SoxR protein and role of the metal centers in transcription. J Biol Chem *270*, 20908-20914.

Hidalgo, E., and Demple, B. (1994). An iron-sulfur center essential for transcriptional activation by the redox-sensing SoxR protein. EMBO J *13*, 138-146.

Hiniker, A., and Bardwell, J.C. (2004). In vivo substrate specificity of periplasmic disulfide oxidoreductases. J Biol Chem *279*, 12967-12973.

Hjelmeland, L.M. (1980). A nondenaturing zwitterionic detergent for membrane biochemistry: design and synthesis. Proc Natl Acad Sci U S A *77*, 6368-6370.

Hoffmann, J.H., Linke, K., Graf, P.C., Lilie, H., and Jakob, U. (2004). Identification of a redox-regulated chaperone network. EMBO J *23*, 160-168.

Hofmann, A.F. (1994). Enterohepatic Circulation of Bile Acids in Mammals. Falk Symp *75*, 23-37.

Hofmann, A.F. (1999). Bile Acids: The Good, the Bad, and the Ugly. News Physiol Sci *14*, 24-29.

Hofmann, A.F., and Mysels, K.J. (1992). Bile-Acid Solubility and Precipitation Invitro and Invivo - the Role of Conjugation, Ph, and Ca2+ Ions. Journal of Lipid Research *33*, 617-626.

Hofmann, A.F., and Roda, A. (1984). Physicochemical properties of bile acids and their relationship to biological properties: an overview of the problem. J Lipid Res *25*, 1477-1489.

Holland, S., Lodwig, E., Sideri, T., Reader, T., Clarke, I., Gkargkas, K., Hoyle, D.C., Delneri, D., Oliver, S.G., and Avery, S.V. (2007). Application of the comprehensive set of heterozygous yeast deletion mutants to elucidate the molecular basis of cellular chromium toxicity. Genome Biol *8*, R268.

Holmgren, A. (1989a). Thioredoxin and glutaredoxin systems. J Biol Chem *264*, 13963-13966.

Holmgren, A. (1989b). Thioredoxin and Glutaredoxin Systems. Journal of Biological Chemistry *264*, 13963-13966.

Holmgren, A., and Aslund, F. (1995). Glutaredoxin. Methods Enzymol *252*, 283-292.

Hong, W., Jiao, W., Hu, J., Zhang, J., Liu, C., Fu, X., Shen, D., Xia, B., and Chang, Z. (2005). Periplasmic protein HdeA exhibits chaperone-like activity exclusively within stomach pH range by transforming into disordered conformation. J Biol Chem *280*, 27029-27034.

Horovitz, A., and Willison, K.R. (2005). Allosteric regulation of chaperonins. Curr Opin Struct Biol *15*, 646-651.

Horwich, A.L., Apetri, A.C., and Fenton, W.A. (2009). The GroEL/GroES cis cavity as a passive anti-aggregation device. FEBS Lett *583*, 2654-2662.

Horwich, A.L., Fenton, W.A., Chapman, E., and Farr, G.W. (2007). Two Families of Chaperonin: Physiology and Mechanism. Annual Review of Cell and Developmental Biology *23*, 115-145.

Houry, W.A. (2001). Chaperone-assisted protein folding in the cell cytoplasm. Curr Protein Pept Sci *2*, 227-244.

Houry, W.A., Frishman, D., Eckerskorn, C., Lottspeich, F., and Hartl, F.U. (1999). Identification of in vivo substrates of the chaperonin GroEL. Nature *402*, 147-154.

Hunt, J.B., Rhee, M.J., and Storm, C.B. (1977). A rapid and convenient preparation of apocarbonic anhydrase. Anal Biochem *79*, 614-617.

Hunt, J.F., Weaver, A.J., Landry, S.J., Gierasch, L., and Deisenhofer, J. (1996). The crystal structure of the GroES co-chaperonin at 2.8 A resolution. Nature *379*, 37-45.

Ilbert, M., Horst, J., Ahrens, S., Winter, J., Graf, P.C., Lilie, H., and Jakob, U. (2007). The redox-switch domain of Hsp33 functions as dual stress sensor. Nat Struct Mol Biol *14*, 556-563.

Imlay, J.A. (2003). Pathways of oxidative damage. Annu Rev Microbiol *57*, 395-418.

Imlay, J.A., Chin, S.M., and Linn, S. (1988). Toxic DNA damage by hydrogen peroxide through the Fenton reaction in vivo and in vitro. Science *240*, 640-642.

Inagaki, T. (2006). Regulation of antibacterial defense in the small intestine by the nuclear bile acid receptor. Proceedings of the National Academy of Sciences *103*, 3920-3925.

Jakob, U. (2000). Redox Switch of Hsp33 Has a Novel Zinc-binding Motif. Journal of Biological Chemistry *275*, 38302-38310.

Jakob, U., Muse, W., Eser, M., and Bardwell, J.C. (1999). Chaperone activity with a redox switch. Cell *96*, 341-352.

Janda, I., Devedjiev, Y., Derewenda, U., Dauter, Z., Bielnicki, J., Cooper, D.R., Graf, P.C., Joachimiak, A., Jakob, U., and Derewenda, Z.S. (2004). The crystal structure of the reduced, Zn2+-bound form of the B. subtilis Hsp33 chaperone and its implications for the activation mechanism. Structure *12*, 1901-1907.

Jaya, N., Garcia, V., and Vierling, E. (2009). Substrate binding site flexibility of the small heat shock protein molecular chaperones. Proceedings of the National Academy of Sciences *106*, 15604-15609.

Kandell, R.L., and Bernstein, C. (1991). Bile salt/acid induction of DNA damage in bacterial and mammalian cells: implications for colon cancer. Nutr Cancer *16*, 227-238.

Kanemori, M., Mori, H., and Yura, T. (1994). Induction of heat shock proteins by abnormal proteins results from stabilization and not increased synthesis of sigma 32 in Escherichia coli. J Bacteriol *176*, 5648-5653.

Kerner, M.J., Naylor, D.J., Ishihama, Y., Maier, T., Chang, H.C., Stines, A.P., Georgopoulos, C., Frishman, D., Hayer-Hartl, M., Mann, M.*, et al.* (2005). Proteome-wide analysis of chaperonin-dependent protein folding in Escherichia coli. Cell *122*, 209-220.

King, T., Ferenci, T., and Szabo, E.A. (2003). The effect of growth atmosphere on the ability of Listeria monocytogenes to survive exposure to acid, proteolytic enzymes and bile salts. International Journal of Food Microbiology *84*, 133-143.

Koebnik, R., Locher, K.P., and Van Gelder, P. (2000). Structure and function of bacterial outer membrane proteins: barrels in a nutshell. Mol Microbiol *37*, 239-253.

Koo, M.S., Lee, J.H., Rah, S.Y., Yeo, W.S., Lee, J.W., Lee, K.L., Koh, Y.S., Kang, S.O., and Roe, J.H. (2003). A reducing system of the superoxide sensor SoxR in Escherichia coli. EMBO J *22*, 2614-2622.

Kosolapov, A., and Deutsch, C. (2009). Tertiary interactions within the ribosomal exit tunnel. Nat Struct Mol Biol *16*, 405-411.

Kristoffersen, S.M., Ravnum, S., Tourasse, N.J., Okstad, O.A., Kolsto, A.B., and Davies, W. (2007). Low Concentrations of Bile Salts Induce Stress Responses and Reduce Motility in Bacillus cereus ATCC 14570. Journal of Bacteriology *189*, 5302-5313.

Kullik, I., Stevens, J., Toledano, M.B., and Storz, G. (1995). Mutational analysis of the redox-sensitive transcriptional regulator OxyR: regions important for DNA binding and multimerization. J Bacteriol *177*, 1285-1291.

Kwon, E., Kim, D.Y., Gross, C.A., Gross, J.D., and Kim, K.K. (2010). The crystal structure Escherichia coli Spy. Protein Sci *19*, 2252-2259.

Lanza, F. (1998). Clinical manifestation of myeloperoxidase deficiency. J Mol Med (Berl) *76*, 676-681.

Laskey, R.A., Honda, B.M., Mills, A.D., and Finch, J.T. (1978). Nucleosomes are assembled by an acidic protein which binds histones and transfers them to DNA. Nature *275*, 416-420.

Laskowska, E., Wawrzynow, A., and Taylor, A. (1996). IbpA and IbpB, the new heat-shock proteins, bind to endogenous Escherichia coli proteins aggregated intracellularly by heat shock. Biochimie *78*, 117-122.

Lee, G.J., Roseman, A.M., Saibil, H.R., and Vierling, E. (1997). A small heat shock protein stably binds heat-denatured model substrates and can maintain a substrate in a folding-competent state. EMBO J *16*, 659-671.

Leichert, L.I., Gehrke, F., Gudiseva, H.V., Blackwell, T., Ilbert, M., Walker, A.K., Strahler, J.R., Andrews, P.C., and Jakob, U. (2008a). Quantifying changes in the thiol redox proteome upon oxidative stress in vivo. Proc Natl Acad Sci U S A *105*, 8197-8202.

Leichert, L.I., Gehrke, F., Gudiseva, H.V., Blackwell, T., Ilbert, M., Walker, A.K., Strahler, J.R., Andrews, P.C., and Jakob, U. (2008b). Reactive Oxygen Species Special Feature: Quantifying changes in the thiol redox proteome upon oxidative stress in vivo. Proceedings of the National Academy of Sciences *105*, 8197-8202.

Leichert, L.I., and Jakob, U. (2004). Protein thiol modifications visualized in vivo. PLoS Biol *2*, e333.

Leverrier, P., Dimova, D., Pichereau, V., Auffray, Y., Boyaval, P., and Jan, G. (2003). Susceptibility and Adaptive Response to Bile Salts in Propionibacterium freudenreichii: Physiological and Proteomic Analysis. Applied and Environmental Microbiology *69*, 3809-3818.

Li, J., Qian, X., and Sha, B. (2003). The crystal structure of the yeast Hsp40 Ydj1 complexed with its peptide substrate. Structure *11*, 1475-1483.

Liberek, K., Marszalek, J., Ang, D., Georgopoulos, C., and Zylicz, M. (1991). Escherichia coli DnaJ and GrpE heat shock proteins jointly stimulate ATPase activity of DnaK. Proc Natl Acad Sci U S A *88*, 2874-2878.

Linke, K. (2003). The Roles of the Two Zinc Binding Sites in DnaJ. Journal of Biological Chemistry *278*, 44457-44466.

Lu, Z., and Cyr, D.M. (1998). The conserved carboxyl terminus and zinc finger-like domain of the co-chaperone Ydj1 assist Hsp70 in protein folding. J Biol Chem *273*, 5970-5978.

MacRitchie, D.M., Buelow, D.R., Price, N.L., and Raivio, T.L. (2008). Two-component signaling and gram negative envelope stress response systems. Adv Exp Med Biol *631*, 80-110.

Makishima, M., Okamoto, A.Y., Repa, J.J., Tu, H., Learned, R.M., Luk, A., Hull, M.V., Lustig, K.D., Mangelsdorf, D.J., and Shan, B. (1999). Identification of a nuclear receptor for bile acids. Science *284*, 1362-1365.

Malkin, L.I., and Rich, A. (1967). Partial resistance of nascent polypeptide chains to proteolytic digestion due to ribosomal shielding. J Mol Biol *26*, 329-346.

Martin, J.L. (1995). Thioredoxin--a fold for all reasons. Structure *3*, 245-250.

Martinez-Yamout, M., Legge, G.B., Zhang, O., Wright, P.E., and Dyson, H.J. (2000). Solution structure of the cysteine-rich domain of the Escherichia coli chaperone protein DnaJ. J Mol Biol *300*, 805-818.

Matuszewska, E., Kwiatkowska, J., Ratajczak, E., Kuczynska-Wisnik, D., and Laskowska, E. (2009). Role of Escherichia coli heat shock proteins IbpA and IbpB in protection of alcohol dehydrogenase AdhE against heat inactivation in the presence of oxygen. Acta Biochim Pol *56*, 55-61.

Maurizi, M.R., and Xia, D. (2004). Protein binding and disruption by Clp/Hsp100 chaperones. Structure *12*, 175-183.

Mayer, M.P., and Bukau, B. (2005). Hsp70 chaperones: Cellular functions and molecular mechanism. Cellular and Molecular Life Sciences *62*, 670-684.

Mayer, M.P., Rudiger, S., and Bukau, B. (2000). Molecular basis for interactions of the DnaK chaperone with substrates. Biol Chem *381*, 877-885.

Medicherla, B., and Goldberg, A.L. (2008). Heat shock and oxygen radicals stimulate ubiquitin-dependent degradation mainly of newly synthesized proteins. J Cell Biol *182*, 663-673.

Merritt, M.E., and Donaldson, J.R. (2009). Effect of bile salts on the DNA and membrane integrity of enteric bacteria. Journal of Medical Microbiology *58*, 1533-1541.

Merz, F., Boehringer, D., Schaffitzel, C., Preissler, S., Hoffmann, A., Maier, T., Rutkowska, A., Lozza, J., Ban, N., Bukau, B.*, et al.* (2008). Molecular mechanism and structure of Trigger Factor bound to the translating ribosome. EMBO J *27*, 1622-1632.

Messner, K.R., and Imlay, J.A. (1999). The identification of primary sites of superoxide and hydrogen peroxide formation in the aerobic respiratory chain and sulfite reductase complex of Escherichia coli. J Biol Chem *274*, 10119-10128.

Miller, R.A., and Britigan, B.E. (1997). Role of oxidants in microbial pathophysiology. Clin Microbiol Rev *10*, 1-18.

Missiakas, D., Schwager, F., and Raina, S. (1995). Identification and characterization of a new disulfide isomerase-like protein (DsbD) in Escherichia coli. EMBO J *14*, 3415-3424.

Mogk, A., Deuerling, E., Vorderwulbecke, S., Vierling, E., and Bukau, B. (2003a). Small heat shock proteins, ClpB and the DnaK system form a functional triade in reversing protein aggregation. Mol Microbiol *50*, 585-595.

Mogk, A., Schlieker, C., Friedrich, K.L., Schonfeld, H.J., Vierling, E., and Bukau, B. (2003b). Refolding of substrates bound to small Hsps relies on a disaggregation reaction mediated most efficiently by ClpB/DnaK. J Biol Chem *278*, 31033-31042.

Moreno, J.C., Bikker, H., Kempers, M.J., van Trotsenburg, A.S., Baas, F., de Vijlder, J.J., Vulsma, T., and Ris-Stalpers, C. (2002). Inactivating mutations in the gene for thyroid oxidase 2 (THOX2) and congenital hypothyroidism. N Engl J Med *347*, 95-102.

Morita, M., Kanemori, M., Yanagi, H., and Yura, T. (1999a). Heat-induced synthesis of sigma32 in Escherichia coli: structural and functional dissection of rpoH mRNA secondary structure. J Bacteriol *181*, 401-410.

Morita, M.T., Tanaka, Y., Kodama, T.S., Kyogoku, Y., Yanagi, H., and Yura, T. (1999b). Translational induction of heat shock transcription factor sigma32: evidence for a built-in RNA thermosensor. Genes Dev *13*, 655-665.

Narberhaus, F. (2002). Alpha-crystallin-type heat shock proteins: socializing minichaperones in the context of a multichaperone network. Microbiol Mol Biol Rev *66*, 64-93; table of contents.

Nonaka, G., Blankschien, M., Herman, C., Gross, C.A., and Rhodius, V.A. (2006). Regulon and promoter analysis of the E. coli heat-shock factor, sigma32, reveals a multifaceted cellular response to heat stress. Genes Dev *20*, 1776-1789.

Nunoshiba, T., deRojas-Walker, T., Wishnok, J.S., Tannenbaum, S.R., and Demple, B. (1993). Activation by nitric oxide of an oxidative-stress response that defends Escherichia coli against activated macrophages. Proc Natl Acad Sci U S A *90*, 9993-9997.

Nunoshiba, T., Hidalgo, E., Amabile Cuevas, C.F., and Demple, B. (1992). Two-stage control of an oxidative stress regulon: the Escherichia coli SoxR protein triggers redox-inducible expression of the soxS regulatory gene. J Bacteriol *174*, 6054-6060.

Onuchic, J.N., and Wolynes, P.G. (2004). Theory of protein folding. Curr Opin Struct Biol *14*, 70-75.

Packschies, L., Theyssen, H., Buchberger, A., Bukau, B., Goody, R.S., and Reinstein, J. (1997). GrpE accelerates nucleotide exchange of the molecular chaperone DnaK with an associative displacement mechanism. Biochemistry *36*, 3417-3422.

Palleros, D.R., Shi, L., Reid, K., and Fink, A. (1995). Hsp70-protein complexes: Their characterization by size-exclusion HPLC. Tech Prot Chem *6*, 467-474.

Palleros, D.R., Shi, L., Reid, K.L., and Fink, A.L. (1994). hsp70-protein complexes. Complex stability and conformation of bound substrate protein. J Biol Chem *269*, 13107-13114.

Pazzi, P., Puviani, A.C., Dalla Libera, M., Guerra, G., Ricci, D., Gullini, S., and Ottolenghi, C. (1997). Bile salt-induced cytotoxicity and ursodeoxycholate cytoprotection: in-vitro study in perifused rat hepatocytes. Eur J Gastroenterol Hepatol *9*, 703-709.

Pico, G.A., and Houssier, C. (1989). Bile salts-bovine serum albumin binding: spectroscopic and thermodynamic studies. Biochim Biophys Acta *999*, 128-134.

Popp, S., Packschies, L., Radzwill, N., Vogel, K.P., Steinhoff, H.J., and Reinstein, J. (2005). Structural dynamics of the DnaK-peptide complex. J Mol Biol *347*, 1039-1052.

Powell, A.A., LaRue, J.M., Batta, A.K., and Martinez, J.D. (2001). Bile acid hydrophobicity is correlated with induction of apoptosis and/or growth arrest in HCT116 cells. Biochem J *356*, 481-486.

Prieto, A.I., Ramos-Morales, F., and Casadesus, J. (2004). Bile-induced DNA damage in Salmonella enterica. Genetics *168*, 1787-1794.

Prieto, A.I., Ramos-Morales, F., and Casadesus, J. (2006). Repair of DNA Damage Induced by Bile Salts in Salmonella enterica. Genetics *174*, 575-584.

Prilusky, J., Felder, C.E., Zeev-Ben-Mordehai, T., Rydberg, E.H., Man, O., Beckmann, J.S., Silman, I., and Sussman, J.L. (2005). FoldIndex: a simple tool to predict whether a given protein sequence is intrinsically unfolded. Bioinformatics *21*, 3435-3438.

Prouty, A.M., Van Velkinburgh, J.C., and Gunn, J.S. (2002). Salmonella enterica serovar typhimurium resistance to bile: identification and characterization of the tolQRA cluster. J Bacteriol *184*, 1270-1276.

Quan, S., Koldewey, P., Tapley, T., Kirsch, N., Ruane, K.M., Pfizenmaier, J., Shi, R., Hofmann, S., Foit, L., Ren, G.*, et al.* (2011). Genetic selection designed to stabilize proteins uncovers a chaperone called Spy. Nature Structural & Molecular Biology *18*, 262-269.

Raffa, R.G., and Raivio, T.L. (2002). A third envelope stress signal transduction pathway in Escherichia coli. Mol Microbiol *45*, 1599-1611.

Raman, B., Siva Kumar, L.V., Ramakrishna, T., and Mohan Rao, C. (2001). Redox-regulated chaperone function and conformational changes of Escherichia coli Hsp33. FEBS Lett *489*, 19-24.

Rao, Y.P., Stravitz, R.T., Vlahcevic, Z.R., Gurley, E.C., Sando, J.J., and Hylemon, P.B. (1997). Activation of protein kinase C alpha and delta by bile acids: correlation with bile acid structure and diacylglycerol formation. J Lipid Res *38*, 2446-2454.

Ratajczak, E., Stróżecka, J., Matuszewska, M., Ziętkiewicz, S., Kuczyńska-Wiśnik, D., Laskowska, E., and Liberek, K. (2010). IbpA the small heat shock protein from Escherichia coli forms fibrils in the absence of its cochaperone IbpB. FEBS Letters *584*, 2253-2257.

Ray, M.C., Germon, P., Vianney, A., Portalier, R., and Lazzaroni, J.C. (2000). Identification by genetic suppression of Escherichia coli TolB residues important for TolB-Pal interaction. J Bacteriol *182*, 821-824.

Reed, D.J., Babson, J.R., Beatty, P.W., Brodie, A.E., Ellis, W.W., and Potter, D.W. (1980). High-performance liquid chromatography analysis of nanomole levels of glutathione, glutathione disulfide, and related thiols and disulfides. Anal Biochem *106*, 55-62.

Reichmann, D., Xu, Y., Cremers, Claudia M., Ilbert, M., Mittelman, R., Fitzgerald, Michael C., and Jakob, U. (2012). Order out of Disorder: Working Cycle of an Intrinsically Unfolded Chaperone. Cell *148*, 947-957.

Reis, S., Moutinho, C.G., Matos, C., de Castro, B., Gameiro, P., and Lima, J.L.F.C. (2004). Noninvasive methods to determine the critical micelle concentration of some bile acid salts. Analytical Biochemistry *334*, 117-126.

Richard, H.T., and Foster, J.W. (2003). Acid resistance in Escherichia coli. Adv Appl Microbiol *52*, 167-186.

Rietsch, A., and Beckwith, J. (1998). The genetics of disulfide bond metabolism. Annu Rev Genet *32*, 163-184.

Ritossa, F. (1962). New Puffing Pattern Induced by Temperature Shock and Dnp in Drosophila. Experientia *18*, 571-&.

Ritossa, F. (1996). Discovery of the heat shock response. Cell Stress Chaperon *1*, 97-98.

Ritz, D., and Beckwith, J. (2001). Roles of thiol-redox pathways in bacteria. Annu Rev Microbiol *55*, 21-48.

Robic, S., Linscott, K.B., Aseem, M., Humphreys, E.A., and McCartha, S.R. (2011). Bile acids as modulators of enzyme activity and stability. Protein J *30*, 539-545.

Rüdiger, S., Buchberger, A., and Bukau, B. (1997a). Interaction of Hsp70 chaperones with substrates. Nat Struct Biol *4*, 342-349.

Rüdiger, S., Germeroth, L., Schneider-Mergener, J., and Bukau, B. (1997b). Substrate specificity of the DnaK chaperone determined by screening cellulose-bound peptide libraries. EMBO J *16*, 1501-1507.

Ruiz, L., Coute, Y., Sanchez, B., de los Reyes-Gavilan, C.G., Sanchez, J.C., and Margolles, A. (2009). The cell-envelope proteome of Bifidobacterium longum in an in vitro bile environment. Microbiology *155*, 957-967.

Russell, D.W. (2003). The enzymes, regulation, and genetics of bile acid synthesis. Annu Rev Biochem *72*, 137-174.

Rutherford, B.J., Dahl, R.H., Price, R.E., Szmidt, H.L., Benke, P.I., Mukhopadhyay, A., and Keasling, J.D. (2010). Functional genomic study of exogenous n-butanol stress in Escherichia coli. Appl Environ Microbiol *76*, 1935-1945.

Rutkowska, A., Mayer, M.P., Hoffmann, A., Merz, F., Zachmann-Brand, B., Schaffitzel, C., Ban, N., Deuerling, E., and Bukau, B. (2008). Dynamics of trigger factor interaction with translating ribosomes. J Biol Chem *283*, 4124-4132.

Saito, H., Nakamura, Y., and Uchida, H. (1978). A transducing lambda phage carrying grpE, a bacterial gene necessary for lambda DNA replication, and two ribosomal protein genes, rpsP (S16) and rplS (L19). Mol Gen Genet *165*, 247-256.

Saito, H., and Uchida, H. (1977). Initiation of the DNA replication of bacteriophage lambda in Escherichia coli K12. J Mol Biol *113*, 1-25.

Sauer, R.T., Bolon, D.N., Burton, B.M., Burton, R.E., Flynn, J.M., Grant, R.A., Hersch, G.L., Joshi, S.A., Kenniston, J.A., Levchenko, I.*, et al.* (2004). Sculpting the proteome with AAA(+) proteases and disassembly machines. Cell *119*, 9-18.

Schildbach, J.F., Milla, M.E., Jeffrey, P.D., Raumann, B.E., and Sauer, R.T. (1995). Crystal structure, folding, and operator binding of the hyperstable Arc repressor mutant PL8. Biochemistry *34*, 1405-1412.

Schroder, H., Langer, T., Hartl, F.U., and Bukau, B. (1993). DnaK, DnaJ and GrpE form a cellular chaperone machinery capable of repairing heat-induced protein damage. EMBO J *12*, 4137-4144.

Schweitzer, B., Felippe, A.C., Dal Bó, A., Minatti, E., Zanette, D., and Lopes, A. (2006). Sodium dodecyl sulfate promoting a cooperative association process of sodium cholate with bovine serum albumin. Journal of Colloid and Interface Science *298*, 457-466.

Seidelt, B., Innis, C.A., Wilson, D.N., Gartmann, M., Armache, J.P., Villa, E., Trabuco, L.G., Becker, T., Mielke, T., Schulten, K.*, et al.* (2009). Structural Insight into Nascent Polypeptide Chain-Mediated Translational Stalling. Science *326*, 1412-1415.

Semsey, S., Krishna, S., Sneppen, K., and Adhya, S. (2007). Signal integration in the galactose network of Escherichia coli. Molecular Microbiology *65*, 465-476.

Sharma, S., Chakraborty, K., Muller, B.K., Astola, N., Tang, Y.C., Lamb, D.C., Hayer-Hartl, M., and Hartl, F.U. (2008). Monitoring protein conformation along the pathway of chaperonin-assisted folding. Cell *133*, 142-153.

Shearstone, J.R., and Baneyx, F. (1999). Biochemical characterization of the small heat shock protein IbpB from Escherichia coli. J Biol Chem *274*, 9937-9945.

Siegenthaler, R.K., and Christen, P. (2005). The importance of having thermosensor control in the DnaK chaperone system. J Biol Chem *280*, 14395-14401.

Siegenthaler, R.K., and Christen, P. (2006). Tuning of DnaK chaperone action by nonnative protein sensor DnaJ and thermosensor GrpE. J Biol Chem *281*, 34448-34456.

Slepenkov, S.V., and Witt, S.N. (1998). Kinetics of the reactions of the Escherichia coli molecular chaperone DnaK with ATP: evidence that a three-step reaction precedes ATP hydrolysis. Biochemistry *37*, 1015-1024.

Smock, R.G., Blackburn, M.E., and Gierasch, L.M. (2011). Conserved, Disordered C Terminus of DnaK Enhances Cellular Survival upon Stress and DnaK in Vitro Chaperone Activity. Journal of Biological Chemistry *286*, 31821-31829.

Sokol, R.J., Dahl, R., Devereaux, M.W., Yerushalmi, B., Kobak, G.E., and Gumpricht, E. (2005). Human hepatic mitochondria generate reactive oxygen species and undergo the permeability transition in response to hydrophobic bile acids. J Pediatr Gastroenterol Nutr *41*, 235-243.

Sokol, R.J., Devereaux, M., Khandwala, R., and O'Brien, K. (1993). Evidence for involvement of oxygen free radicals in bile acid toxicity to isolated rat hepatocytes. Hepatology *17*, 869-881.

Stadtman, E.R., and Levine, R.L. (2000). Protein oxidation. Ann N Y Acad Sci *899*, 191-208.

Stefani, M., and Dobson, C.M. (2003). Protein aggregation and aggregate toxicity: new insights into protein folding, misfolding diseases and biological evolution. Journal of Molecular Medicine *81*, 678-699.

Stevens, S.Y., Cai, S., Pellecchia, M., and Zuiderweg, E.R. (2003). The solution structure of the bacterial HSP70 chaperone protein domain DnaK(393-507) in complex with the peptide NRLLLTG. Protein Sci *12*, 2588-2596.

Storz, G., and Imlay, J.A. (1999). Oxidative stress. Curr Opin Microbiol *2*, 188-194.

Straus, D., Walter, W., and Gross, C.A. (1990). DnaK, DnaJ, and GrpE heat shock proteins negatively regulate heat shock gene expression by controlling the synthesis and stability of sigma 32. Genes Dev *4*, 2202-2209.

Sukhodolets, M.V., Cabrera, J.E., Zhi, H., and Jin, D.J. (2001). RapA, a bacterial homolog of SWI2/SNF2, stimulates RNA polymerase recycling in transcription. Genes Dev *15*, 3330-3341.

Sukhodolets, M.V., and Jin, D.J. (1998). RapA, a novel RNA polymerase-associated protein, is a bacterial homolog of SWI2/SNF2. J Biol Chem *273*, 7018-7023.

Sukhodolets, M.V., and Jin, D.J. (2000). Interaction between RNA polymerase and RapA, a bacterial homolog of the SWI/SNF protein family. J Biol Chem *275*, 22090-22097.

Sung, J.Y., Shaffer, E.A., and Costerton, J.W. (1993). Antibacterial activity of bile salts against common biliary pathogens. Effects of hydrophobicity of the molecule and in the presence of phospholipids. Dig Dis Sci *38*, 2104-2112.

Sunshine, M., Feiss, M., Stuart, J., and Yochem, J. (1977). New Host Gene (Gropc) Necessary for Lambda-DNA Replication. Molecular & General Genetics *151*, 27-34.

Szasz, C.S., Alexa, A., Toth, K., Rakacs, M., Langowski, J., and Tompa, P. (2011). Protein disorder prevails under crowded conditions. Biochemistry *50*, 5834-5844.

Tamarit, J., Cabiscol, E., and Ros, J. (1998). Identification of the major oxidatively damaged proteins in Escherichia coli cells exposed to oxidative stress. J Biol Chem *273*, 3027-3032.

Tang, Y.C., Chang, H.C., Roeben, A., Wischnewski, D., Wischnewski, N., Kerner, M.J., Hartl, F.U., and Hayer-Hartl, M. (2006). Structural features of the GroEL-GroES nano-cage required for rapid folding of encapsulated protein. Cell *125*, 903-914.

Tao, K. (1997). oxyR-dependent induction of Escherichia coli grx gene expression by peroxide stress. J Bacteriol *179*, 5967-5970.

Tao, K., Fujita, N., and Ishihama, A. (1993). Involvement of the RNA polymerase alpha subunit C-terminal region in co-operative interaction and transcriptional activation with OxyR protein. Mol Microbiol *7*, 859-864.

Tapley, T.L., Franzmann, T.M., Chakraborty, S., Jakob, U., and Bardwell, J.C.A. (2009a). Protein refolding by pH-triggered chaperone binding and release. Proceedings of the National Academy of Sciences *107*, 1071-1076.

Tapley, T.L., Korner, J.L., Barge, M.T., Hupfeld, J., Schauerte, J.A., Gafni, A., Jakob, U., and Bardwell, J.C.A. (2009b). Structural plasticity of an acid-activated chaperone allows promiscuous substrate binding. Proceedings of the National Academy of Sciences *106*, 5557-5562.

Thompson, A.D., Bernard, S.M., Skiniotis, G., and Gestwicki, J.E. (2012). Visualization and functional analysis of the oligomeric states of Escherichia coli heat shock protein 70 (Hsp70/DnaK). Cell Stress Chaperones *17*, 313-327.

Tofani, L., Feis, A., Snoke, R.E., Berti, D., Baglioni, P., and Smulevich, G. (2004). Spectroscopic and interfacial properties of myoglobin/surfactant complexes. Biophys J *87*, 1186-1195.

Tomoyasu, T., Gamer, J., Bukau, B., Kanemori, M., Mori, H., Rutman, A.J., Oppenheim, A.B., Yura, T., Yamanaka, K., Niki, H.*, et al.* (1995). Escherichia coli FtsH is a membrane-bound,

ATP-dependent protease which degrades the heat-shock transcription factor sigma 32. EMBO J *14*, 2551-2560.

Tomoyasu, T., Ogura, T., Tatsuta, T., and Bukau, B. (1998). Levels of DnaK and DnaJ provide tight control of heat shock gene expression and protein repair in Escherichia coli. Mol Microbiol *30*, 567-581.

Tompa, P. (2009). Structural disorder in amyloid fibrils: its implication in dynamic interactions of proteins. FEBS J *276*, 5406-5415.

Tompa, P., and Csermely, P. (2004). The role of structural disorder in the function of RNA and protein chaperones. FASEB J *18*, 1169-1175.

Tsalkova, T., Odom, O.W., Kramer, G., and Hardesty, B. (1998). Different conformations of nascent peptides on ribosomes. J Mol Biol *278*, 713-723.

Tsaneva, I.R., and Weiss, B. (1990). soxR, a locus governing a superoxide response regulon in Escherichia coli K-12. J Bacteriol *172*, 4197-4205.

Tuggle, C.K., and Fuchs, J.A. (1985). Glutathione reductase is not required for maintenance of reduced glutathione in Escherichia coli K-12. J Bacteriol *162*, 448-450.

Tyedmers, J., Mogk, A., and Bukau, B. (2010). Cellular strategies for controlling protein aggregation. Nat Rev Mol Cell Biol *11*, 777-788.

Uversky, V.N., Gillespie, J.R., and Fink, A.L. (2000). Why are "natively unfolded" proteins unstructured under physiologic conditions? Proteins *41*, 415-427.

Vabulas, R.M., and Hartl, F.U. (2005). Protein synthesis upon acute nutrient restriction relies on proteasome function. Science *310*, 1960-1963.

van Dalen, C.J., Whitehouse, M.W., Winterbourn, C.C., and Kettle, A.J. (1997). Thiocyanate and chloride as competing substrates for myeloperoxidase. Biochem J *327 (Pt 2)*, 487-492.

Vijayalakshmi, J., Mukhergee, M.K., Graumann, J., Jakob, U., and Saper, M.A. (2001). The 2.2 A crystal structure of Hsp33: a heat shock protein with redox-regulated chaperone activity. Structure *9*, 367-375.

Wang, H., Chen, J., Hollister, K., Sowers, L.C., and Forman, B.M. (1999). Endogenous bile acids are ligands for the nuclear receptor FXR/BAR. Mol Cell *3*, 543-553.

Wells, J.E., and Hylemon, P.B. (2000). Identification and characterization of a bile acid 7alpha-dehydroxylation operon in Clostridium sp. strain TO-931, a highly active 7alpha-dehydroxylating strain isolated from human feces. Appl Environ Microbiol *66*, 1107-1113.

Wholey, W.-Y., and Jakob, U. (2012). Hsp33 confers bleach resistance by protecting elongation factor Tu against oxidative degradation in Vibrio cholerae. Molecular Microbiology *83*, 981-991.

Williams, C.H., Jr. (1995). Mechanism and structure of thioredoxin reductase from Escherichia coli. FASEB J *9*, 1267-1276.

Winkler, J., Seybert, A., Konig, L., Pruggnaller, S., Haselmann, U., Sourjik, V., Weiss, M., Frangakis, A.S., Mogk, A., and Bukau, B. (2010). Quantitative and spatio-temporal features of protein aggregation in Escherichia coli and consequences on protein quality control and cellular ageing. EMBO J *29*, 910-923.

Winter, J., Ilbert, M., Graf, P.C.F., Özcelik, D., and Jakob, U. (2008). Bleach Activates a Redox-Regulated Chaperone by Oxidative Protein Unfolding. Cell *135*, 691-701.

Winter, J., and Jakob, U. (2004). Beyond transcription--new mechanisms for the regulation of molecular chaperones. Crit Rev Biochem Mol Biol *39*, 297-317.

Winter, J., Linke, K., Jatzek, A., and Jakob, U. (2005). Severe oxidative stress causes inactivation of DnaK and activation of the redox-regulated chaperone Hsp33. Mol Cell *17*, 381-392.

Winterbourn, C.C., Hampton, M.B., Livesey, J.H., and Kettle, A.J. (2006). Modeling the reactions of superoxide and myeloperoxidase in the neutrophil phagosome - Implications for microbial killing. Journal of Biological Chemistry *281*, 39860-39869.

Wong, C., Sridhara, S., Bardwell, J.C., and Jakob, U. (2000). Heating greatly speeds Coomassie blue staining and destaining. Biotechniques *28*, 426-428, 430, 432.

Wu, J., and Weiss, B. (1991). Two divergently transcribed genes, soxR and soxS, control a superoxide response regulon of Escherichia coli. J Bacteriol *173*, 2864-2871.

Wu, Y., Li, J., Jin, Z., Fu, Z., and Sha, B. (2005). The crystal structure of the C-terminal fragment of yeast Hsp40 Ydj1 reveals novel dimerization motif for Hsp40. J Mol Biol *346*, 1005-1011.

Wu, Y.E., Hong, W., Liu, C., Zhang, L., and Chang, Z. (2008). Conserved amphiphilic feature is essential for periplasmic chaperone HdeA to support acid resistance in enteric bacteria. Biochem J *412*, 389-397.

Xia, T.H., Bushweller, J.H., Sodano, P., Billeter, M., Bjornberg, O., Holmgren, A., and Wuthrich, K. (1992). NMR structure of oxidized Escherichia coli glutaredoxin: comparison with reduced E. coli glutaredoxin and functionally related proteins. Protein Sci *1*, 310-321.

Xu, Z., Horwich, A.L., and Sigler, P.B. (1997). The crystal structure of the asymmetric GroEL-GroES-(ADP)7 chaperonin complex. Nature *388*, 741-750.

Yamamoto, K., and Ishihama, A. (2005). Transcriptional response of Escherichia coli to external copper. Mol Microbiol *56*, 215-227.

Yamamoto, K., Ogasawara, H., and Ishihama, A. (2008). Involvement of multiple transcription factors for metal-induced spy gene expression in Escherichia coli. J Biotechnol *133*, 196-200.

Yan, L.-J. (2009). Protein carbonylation detection Current Protocols in Protein Science *56*.

Yang, F., Gustafson, K.R., Boyd, M.R., and Wlodawer, A. (1998). Crystal structure of Escherichia coli HdeA. Nat Struct Biol *5*, 763-764.

Yang, H., Huang, S., Dai, H., Gong, Y., Zheng, C., and Chang, Z. (1999). The Mycobacterium tuberculosis small heat shock protein Hsp16.3 exposes hydrophobic surfaces at mild conditions: conformational flexibility and molecular chaperone activity. Protein Sci *8*, 174-179.

Young, J.C., Agashe, V.R., Siegers, K., and Hartl, F.U. (2004). Pathways of chaperone-mediated protein folding in the cytosol. Nat Rev Mol Cell Biol *5*, 781-791.

Yura, T., Nagai, H., and Mori, H. (1993). Regulation of the heat-shock response in bacteria. Annu Rev Microbiol *47*, 321-350.

Yura, T., and Nakahigashi, K. (1999). Regulation of the heat-shock response. Curr Opin Microbiol *2*, 153-158.

Zhang, A., Altuvia, S., Tiwari, A., Argaman, L., Hengge-Aronis, R., and Storz, G. (1998). The OxyS regulatory RNA represses rpoS translation and binds the Hfq (HF-I) protein. EMBO J *17*, 6061-6068.

Zheng, D., Constantinidou, C., Hobman, J.L., and Minchin, S.D. (2004). Identification of the CRP regulon using in vitro and in vivo transcriptional profiling. Nucleic Acids Res *32*, 5874-5893.

Zheng, M., Aslund, F., and Storz, G. (1998). Activation of the OxyR transcription factor by reversible disulfide bond formation. Science *279*, 1718-1721.

Zhu, X., Zhao, X., Burkholder, W.F., Gragerov, A., Ogata, C.M., Gottesman, M.E., and Hendrickson, W.A. (1996). Structural analysis of substrate binding by the molecular chaperone DnaK. Science *272*, 1606-1614.

Zoetendal, E.G., Smith, A.H., Sundset, M.A., and Mackie, R.I. (2008). The BaeSR two-component regulatory system mediates resistance to condensed tannins in Escherichia coli. Appl Environ Microbiol *74*, 535-539.